US Army Corps of Engineers

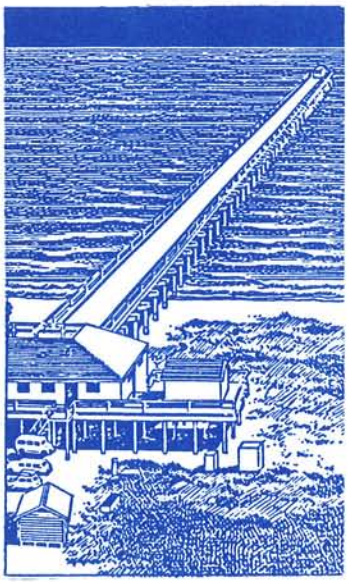

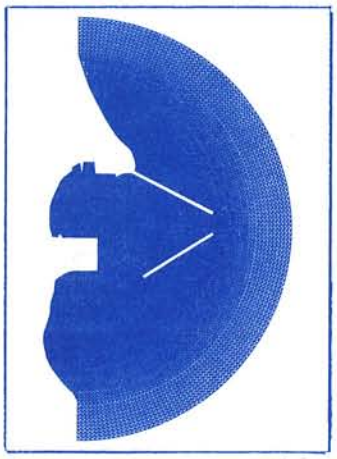

COASTAL ENGINEERING RESEARCH CENTER

MISCELLANEOUS PAPER CERC-88-11

COMPARISON OF NUMERICAL AND PHYSICAL MODELS OF WAVE RESPONSE IN A HARBOR

by

Peter L. Crawford, H. S. Chen

Coastal Engineering Research Center

DEPARTMENT OF THE ARMY
Waterways Experiment Station, Corps of Engineers
PO Box 631, Vicksburg, Mississippi 39180-0631

U.S. ARMY ENGINEER WATERWAYS EXPERIMENT STATION

August 1988
Final Report

Prepared for DEPARTMENT OF THE ARMY
US Army Corps of Engineers
Washington, DC 20314-1000
Under Waves at Entrances Work Unit 31673

Destroy this report when no longer needed. Do not return it to the originator.

The findings in this report are not to be construed as an official Department of the Army position unless so designated by other authorized documents.

The contents of this report are not to be used for advertising, publication, or promotional purposes. Citation of trade names does not constitute an official endorsement or approval of the use of such commercial products.

REPORT DOCUMENTATION PAGE

Form Approved
OMB No 0704-0188
Exp. Date Jun 30, 1986

1a. REPORT SECURITY CLASSIFICATION
Unclassified

1b. RESTRICTIVE MARKINGS

2a. SECURITY CLASSIFICATION AUTHORITY

2b. DECLASSIFICATION / DOWNGRADING SCHEDULE

3. DISTRIBUTION / AVAILABILITY OF REPORT
Approved for public release; distribution unlimited.

4. PERFORMING ORGANIZATION REPORT NUMBER(S)
Miscellaneous Paper CERC-88-11

5. MONITORING ORGANIZATION REPORT NUMBER(S)

6a. NAME OF PERFORMING ORGANIZATION
USAEWES, Coastal Engineering Research Center

6b. OFFICE SYMBOL (*If applicable*)

7a. NAME OF MONITORING ORGANIZATION

6c. ADDRESS (*City, State, and ZIP Code*)
PO Box 631
Vicksburg, MS 39180-0631

7b. ADDRESS (*City, State, and ZIP Code*)

8a. NAME OF FUNDING / SPONSORING ORGANIZATION
US Army Corps of Engineers

8b. OFFICE SYMBOL (*If applicable*)

9. PROCUREMENT INSTRUMENT IDENTIFICATION NUMBER

8c. ADDRESS (*City, State, and ZIP Code*)
Washington, DC 20314-1000

10. SOURCE OF FUNDING NUMBERS

PROGRAM ELEMENT NO.	PROJECT NO.	TASK NO.	WORK UNIT ACCESSION NO
			31673

11. TITLE (*Include Security Classification*)
Comparison of Numerical and Physical Models of Wave Response in a Harbor

12. PERSONAL AUTHOR(S)
Crawford, Peter L.; Chen, H. S.

13a. TYPE OF REPORT	13b. TIME COVERED	14. DATE OF REPORT (*Year, Month, Day*)	15. PAGE COUNT
Final report	FROM _____ TO _____	August 1988	78

16. SUPPLEMENTARY NOTATION
Available from National Technical Information Service, 5285 Port Royal Road, Springfield, VA 22161.

17. COSATI CODES		
FIELD	GROUP	SUB-GROUP

18. SUBJECT TERMS (*Continue on reverse if necessary and identify by block number*)
Finite element method
Harbor
Hybrid element method
Numerical modeling
Physical modeling
Water waves

19. ABSTRACT (*Continue on reverse if necessary and identify by block number*)

Results of a numerical and a physical model study of wave response of the small-boat harbor at Barcelona, New York, are presented and compared. The numerical model used was HARBD, a monochromatic linear wave model. Both monochromatic and irregular waves were considered, and wave superposition was used to investigate harbor response to irregular waves.

Wave records from the physical model tests matched the intended wave forcing conditions near the wave generator. Wave records in and around the harbor, however, usually showed the effects of nonlinearity and in some instances exhibited wave grouping and the effects of breaking and overtopping. Hence, even for the monochromatic tests, the water surface oscillations at each gage in the harbor were characterized by a distribution of wave heights. Procedures were developed for displaying information about the irregularity of physical model wave records. These procedures provide a rational means for comparing

(Continued)

20. DISTRIBUTION / AVAILABILITY OF ABSTRACT
☒ UNCLASSIFIED/UNLIMITED ☐ SAME AS RPT ☐ DTIC USERS

21. ABSTRACT SECURITY CLASSIFICATION
Unclassified

22a. NAME OF RESPONSIBLE INDIVIDUAL

22b. TELEPHONE (*Include Area Code*)

22c. OFFICE SYMBOL

19. ABSTRACT (Continued).

numerical and physical model results. Using them, engineering judgement can be used to assess the nature of irregular waves in the physical model and to assess, for a given application, the appropriateness of the linear theory assumption of the numerical model.

PREFACE

This study was authorized as part of the Civil Works Research and Development Program of the Office, Chief of Engineers (OCE), US Army Corps of Engineers. Work was performed at the Coastal Engineering Research Center (CERC) of the US Army Engineer Waterways Experiment Station (WES) as a part of the Harbor Entrances and Coastal Channels Program under Waves at Entrances Work Unit 31673. Messrs. John H. Lockhart, Jr., and John G. Housley were OCE Technical Monitors, and Dr. Charles L. Vincent was the CERC Program Manager during preparation and publication of this report.

The study was conducted by personnel of the Coastal Oceanography Branch (CR-O), Research Division (CR), CERC. Work was performed under direct supervision of Dr. Edward F. Thompson, Chief, CR-O, and Mr. H. Lee Butler, Chief, CR; and under general supervision of Dr. James R. Houston, Chief, CERC, and Mr. Charles C. Calhoun, Jr., Assistant Chief, CERC. This report was prepared by Mr. Peter L. Crawford and Dr. H. S. Chen (CR-O). Mrs. Linda L. Lillycrop (CR-O) assisted in processing the model data. Mr. Ernest R. Smith, Wave Processes Branch (CW-P), Wave Dynamics Division (CW), CERC, supplied the data from the physical model. Dr. Thompson, Mr. Butler, Mr. C. E. Chatham, Chief, CW, and Mr. D. G. Outlaw, Chief, CW-P, assisted in the review of this report. Adaptation of the HARBD computer code for enhanced execution on the CDC Cyber 205 was provided by Mr. Christopher N. Moran of Control Data Corporation. This report was edited by Ms. Shirley A. J. Hanshaw, Information Technology Laboratory, Information Products Division, WES.

During report publication, COL Dwayne G. Lee, EN, was Commander and Director of WES. Dr. Robert W. Whalin was Technical Director.

CONTENTS

CONVERSION FACTORS, NON-SI TO SI (METRIC)
UNITS OF MEASUREMENT

Non-SI units of measurement in this report can be converted to SI units as follows:

Multiply	By	To Obtain
feet	0.3048	metres
inches	0.0254	metres
square feet per Hertz	0.092903	square metres per Hertz

COMPARISON OF NUMERICAL AND PHYSICAL MODELS OF WAVE RESPONSE IN A HARBOR

PART I: INTRODUCTION

Wave Conditions In Harbors

1. Water waves in harbors are primarily excited by waves penetrating through the harbor entrance or opening. In engineering practice, waves of principal concern for harbor tranquility have periods in the range of about 5 sec to 4 min. In small-boat harbors, 5- to 20-sec waves are the primary concern.

2. The principal adverse effects of excessive wave action in harbors are associated with navigation and mooring. Excessive wave action is caused by resonance or insufficient shelter by the protection breakwaters. Resonance in harbors occurs when the natural period of the harbor is equal or close to an incident wave period. Resonant oscillation of a moored vessel occurs when the natural period of the dynamic response of the moored vessel is equal or close to an incident wave period. The severe wave chop, and possibly strong currents associated with excessive wave action in harbors, can cause navigational difficulty, unacceptable motion of moored vessels, and undesired shoaling or erosion within the harbor.

3. Effects of water waves in harbors can be estimated from field measurements, physical model studies, or mathematical/numerical model studies. All three sources of information are accompanied by assumptions and simplifications. Nevertheless, it is accepted that useful estimates of waves in an existing harbor can be obtained from field measurements used in conjunction with physical and/or mathematical models. Unfortunately, wave measurements in a harbor are difficult and expensive to collect, and very limited field data are available. For a proposed harbor, field measurements can only provide incident wave climate; hence, physical and/or mathematical models must be used to predict wave conditions in the harbor. The models are most useful for engineering studies when they provide a reasonable representation of the prototype.

4. Corps of Engineers harbor projects are designed with consideration of the wave conditions that can be expected inside the harbor. Occasionally,

existing harbor projects also need structural modification for reasons which may include overly severe wave conditions inside the harbor. Since costs associated with harbor construction and modification are generally high, project engineers need accurate and efficient models--physical and/or mathematical--which can be used to test the performance of alternative designs before construction.

Investigation of Waves In Harbors

5. Historically, both physical and mathematical models have been used at the US Army Corps of Engineers Waterways Experiment Station (WES) to investigate waves in harbors. For example, Bottin (1984) used a physical model to investigate the effects of proposed harbor improvements on wave action in the small-boat harbor at Barcelona, New York. Houston (1976) used a numerical model to investigate the effects of proposed improvements on the response of Long Beach Harbor to long-period waves. Many other studies of waves in harbors have been conducted at WES. The majority of these studies used physical models because WES has excellent laboratory facilities for physical model studies and because numerical models are relatively new as practical engineering tools. The advent of modern computer hardware and computational methods has led to a dramatic world-wide increase in the use of numerical models in all fields of engineering. Because of the time and cost efficiency of numerical models for some studies, their use is increasing within the Corps of Engineers.

6. A variety of numerical models has been used to investigate waves in harbors (Lee 1969; Chen and Mei 1974; Yue, Chen, and Mei 1976; Berkhoff 1976; Houston 1981; Lepelletier 1981; Ganaba, Welford, and Lee 1982; Behrendt and Jonsson 1984; Skovgaard, Behrendt, and Jonsson 1984; Yoshida, Ijima, and Okuzono 1984; Matsoukis 1985; and Chen 1986). These authors used various numerical techniques, including the ray method, Green's function method, eigenfunction method, finite difference method, finite element method, and hybrid element method. Recently, WES's Coastal Engineering Research Center (CERC) developed and implemented the HARBS and HARBD computer codes to model waves in harbors. These numerical models use a hybrid element method to determine the wave response of a harbor to a simple time-harmonic incident wave train. HARBS is used for shallow-water harbors; HARBD is used for

arbitrary-depth harbors. The models have been tested against some laboratory data (Chen 1984 and 1986) and have been used to predict wave response in several prototype harbors (Farrar and Chen 1987 and Mathiesen 1987).

7. The Shore Protection Manual (SPM) (1984) presents diffraction diagrams and methods of implementing them which can be used to study wave propagation into a harbor if the problem description meets a variety of restrictive criteria. The methods are useful only for the simplest problems. It was realized that diffraction diagrams were not strictly applicable to the problem of determining wave conditions in Barcelona Harbor. Nevertheless, it was deemed worthwhile to determine wave conditions inside the harbor by using diffraction diagrams and then to compare the results with results from the physical and numerical models. The method, results, and comparisons are presented in Appendix A.

Purpose of Study

8. The purpose of the study herein is to determine the wave response at Barcelona Harbor, New York, using the HARBD numerical model and then to compare the numerical model results with data from the physical model study described by Bottin (1984). This study is intended to provide technical information which will help establish preliminary engineering guidelines for conducting harbor wave studies; it is not intended to provide information concerning the time and cost requirements of the two modeling approaches.

PART II: PHYSICAL AND NUMERICAL MODEL STUDIES OF BARCELONA HARBOR, NEW YORK

Physical Model Study

9. At the request of US Army Engineer District, Buffalo (NCB), a physical model study of wave conditions in Barcelona Harbor, New York, was conducted at WES during late 1983 and early 1984. The effects of a variety of proposed harbor improvements on wave action in the harbor were investigated.

10. The model study is described in detail by Bottin (1984). A brief description of relevant aspects of the study is given here. The model was a 1:60-scale undistorted model. A time scale of 1:7.75 was required by the Froude model law. Figure 1 shows the model layout. Model tests were performed for 60 different harbor configurations, three of which were considered as part of the numerical model study described in paragraphs 28 through 38. Only waves with periods between 4.9 and 10.1 sec were considered.

11. Model tests were conducted for monochromatic and irregular waves. During development and selection of an optimum plan, monochromatic model tests were made for each harbor configuration using a variety of water levels and incident waves with different heights, directions, and periods. Irregular wave tests were made only for the optimal proposed plan (Plan 58 in Bottin's (1984) report). The irregular wave tests represented CERC's initial development of the capability to generate irregular wave conditions in a three-dimensional model. (The capability to conduct irregular wave tests in wave flumes had previously been developed.) For each test, wave records were taken at 14 gages within or near the harbor. The locations of Gages 3 through 14 were the same for all harbor configurations. The locations of Gages 1 and 2 varied slightly for different harbor configurations, but they were always near the harbor entrance. The locations of the gages are shown in Figures 2 through 4.

12. For the monochromatic tests, most wave records had some variation of individual wave heights and periods. For each test, a crest-to-trough wave height analysis technique (Turner and Durham 1984) was used to calculate $H_{1/3}$, the average of the one-third highest waves in the record, at each gage. The technique closely duplicates analysis techniques used for monochromatic

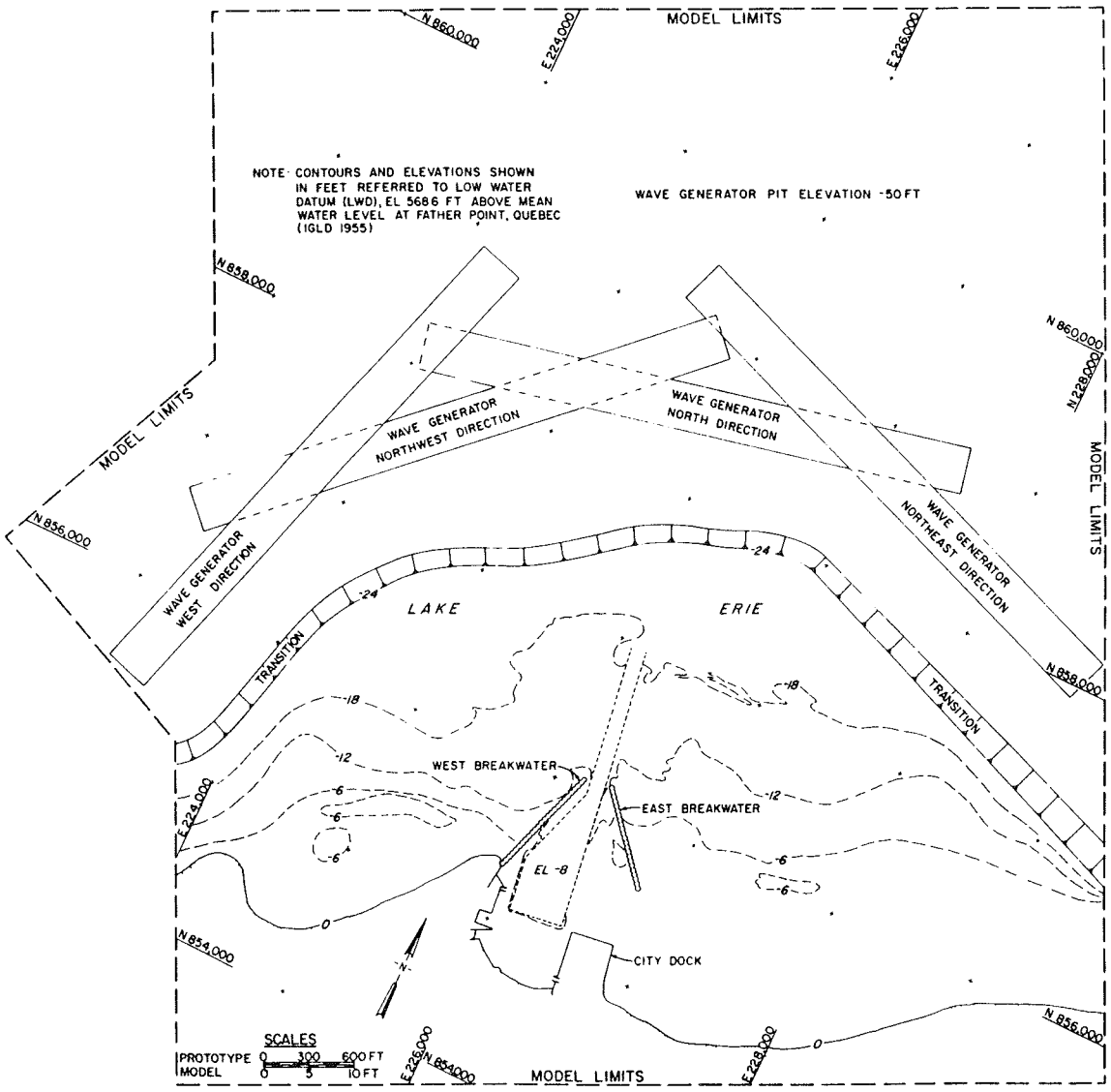

Figure 1. Layout of the hydraulic model

wave tests prior to implementation of an automated data acquisition and analysis system at CERC. The technique differs from a zero-crossing analysis in that small oscillations in the wave record between a crest and trough are ignored. Keulegan's* equation was then used to further adjust the $H_{1/3}$ values to compensate for excess (as compared to the prototype) wave height

---

* G. H. Keulegan, 1950, "The Gradual Damping of a Progressive Oscillatory Wave with Distance in a Prismatic Rectangular Channel" (unpublished data), National Bureau of Standards, Washington, DC; prepared at the request of the Director, US Army Engineer Waterways Experiment Station, Vicksburg, MS, by letter of 2 May 1950.

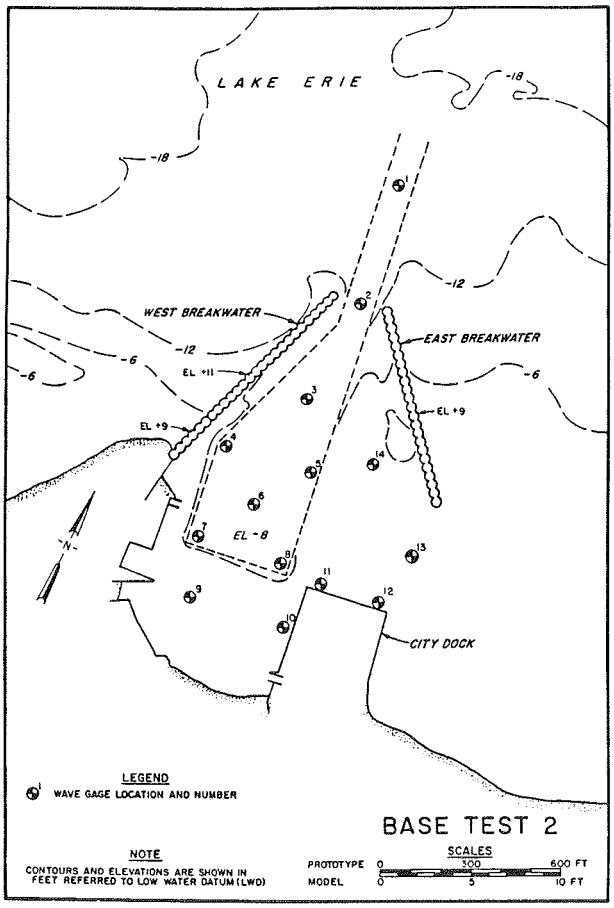

Figure 2. Harbor configuration for base Test 2

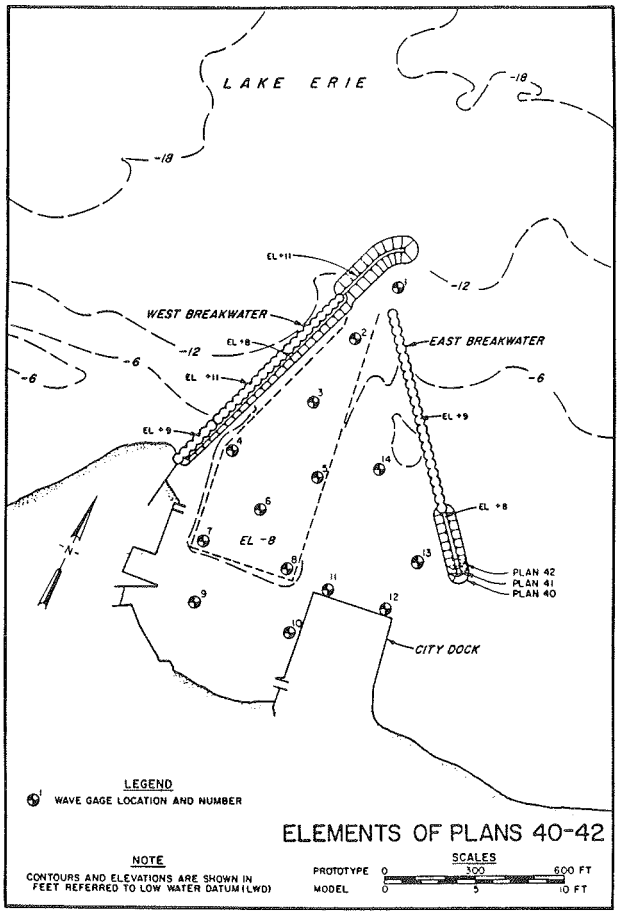

Figure 3. Harbor configuration for Plan 42

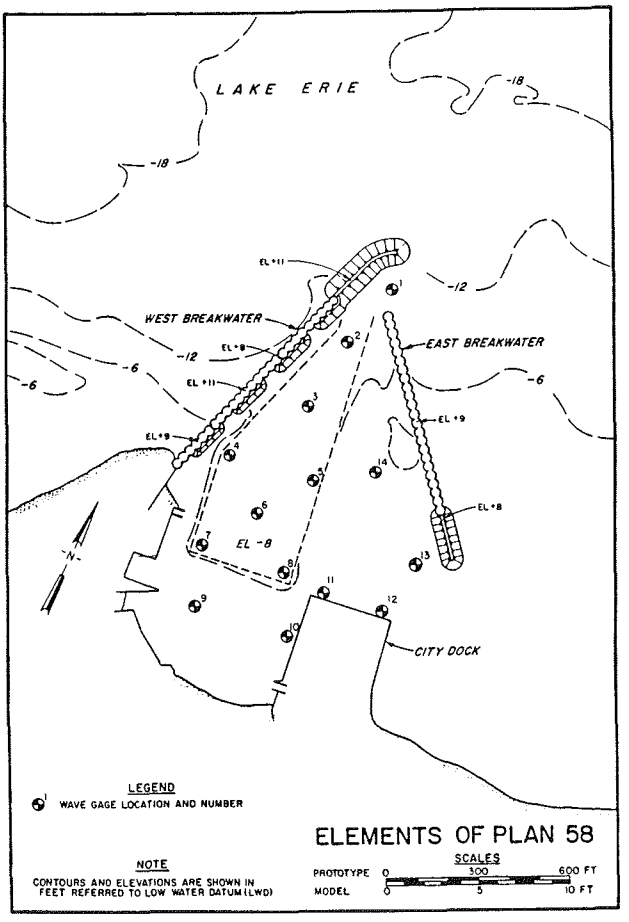

Figure 4. Harbor configuration for Plan 58

attenuation caused by viscous bottom friction in the model. The adjustment, which is a function of temperature, is estimated to be in the range of 4 to 19 percent. Values of the adjusted $H_{1/3}$ are used to characterize the wave conditions at each gage (Bottin 1984). The use of the adjusted $H_{1/3}$ to represent the wave height at a gage in the physical model study is regarded as a good estimate for engineering purposes such as plan evaluation. However, the adjusted $H_{1/3}$ does not fully characterize the model data. (See paragraphs 19 through 27.)

13. Scale effects (Hudson et al. 1979) in a small-scale physical model are not limited to viscous energy dissipation at the bottom. Other scale effects are related to transmission through and reflection from breakwaters, reflection from the sloped transition section between the generator pit and the modeled bathymetry, and reflections from the wave generator and model basin boundaries. Physical models are carefully designed to minimize these scale effects. Operationally, monochromatic wave test data are acquired and analyzed

prior to the time at which waves reflected from the model boundary or wave generator return to the harbor area.

14. Wave generator characteristics also affect monochromatic and irregular wave generation. In practice, as the stroke of the wave generator increases, wave generators designed to produce monochromatic waves usually tend to generate energy at harmonics of the fundamental frequency. The wave record from a gage located near the center and 10 ft* in front of the wave generator for a 6.7-sec (prototype) wave is shown in Figure 5a. A 0.2-in. (model) stroke was used to generate this wave. The $H_{1/3}$ of this wave is 1.66 ft (prototype), and the mean amplitude is 1.64 ft (prototype). The corresponding energy spectrum, shown in Figure 5b, indicates very little wave energy at harmonic frequencies. A taper function was applied to the data during the frequency analysis, but smoothing techniques were not used. The wave record from the same gage for a larger amplitude wave having a period of 5.3 sec (prototype) is shown in Figure 6a. A 0.5-in. (model) stroke was used to generate this wave. The $H_{1/3}$ for this wave is 6.74 ft (prototype), and the mean wave height is 6.67 ft (prototype). Generation of a small amount of energy at the first harmonic is evident in the corresponding energy spectrum shown in Figure 6b. Spectral analysis results also indicate wave energy at frequencies adjacent to the fundamental frequency. The amount of energy at adjacent frequencies is relatively small. However, the presence of even a relatively small amount of wave energy away from the intended frequency can significantly affect wave propagation and transformation. It should also be noted that energy transfer to harmonics may occur in shallow water in both the physical model and prototype.

15. If paddle wave generators are used for irregular wave tests, incorrect boundary conditions may cause spurious long waves (Jensen and Warren 1986). Depending on the test conditions, the total long-period wave energy in a model may be increased or decreased. Long-period wave energy associated with wave setdown under wave groups will occur and should be expected during irregular wave tests. As noted by Jensen and Warren, long-period waves will be reflected and re-reflected from nondissipating boundaries such as the wave generator and basin boundaries, but limited comparisons with prototype data

---

* A table of factors for converting non-SI units of measurement to SI (metric) units is presented on page 3.

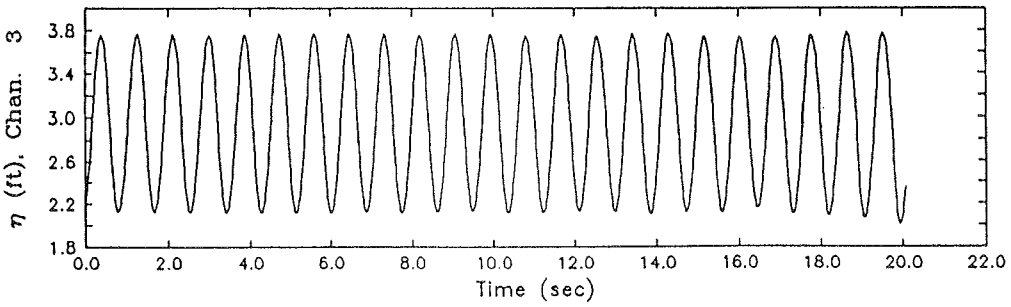

a. Wave record

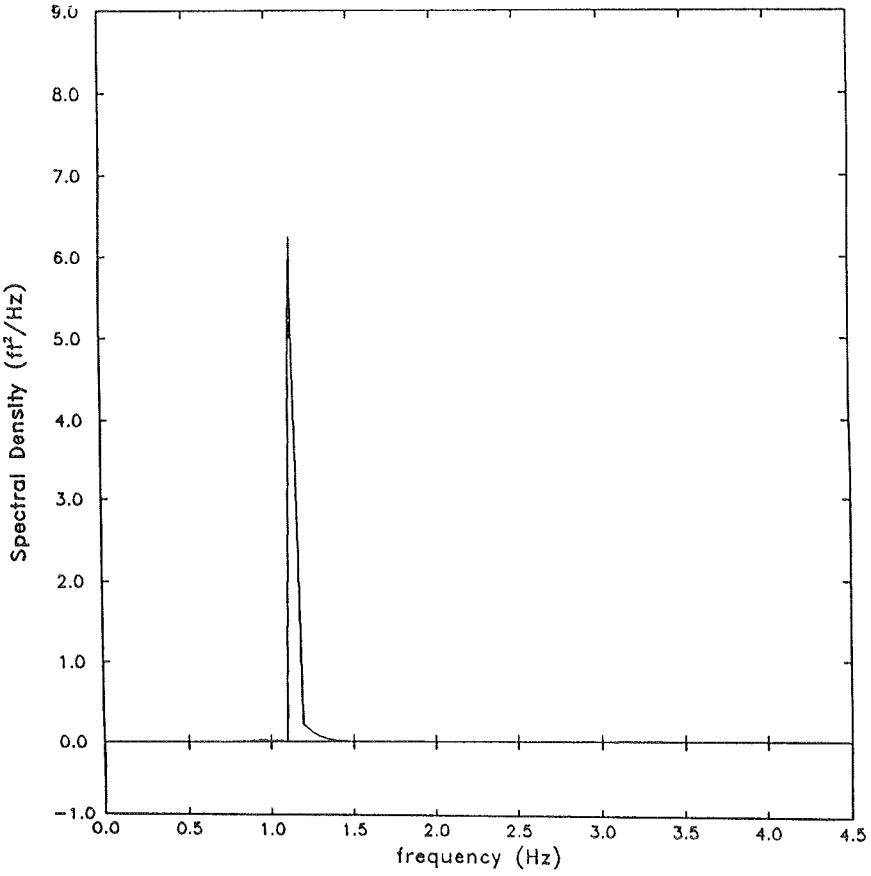

b. Energy spectrum

Figure 5. Wave record and energy spectrum for a 6.7-sec wave recorded near the wave generator

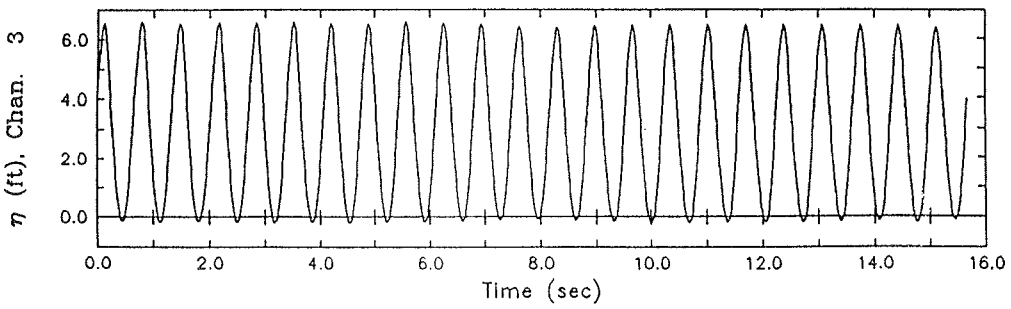

a. Wave record

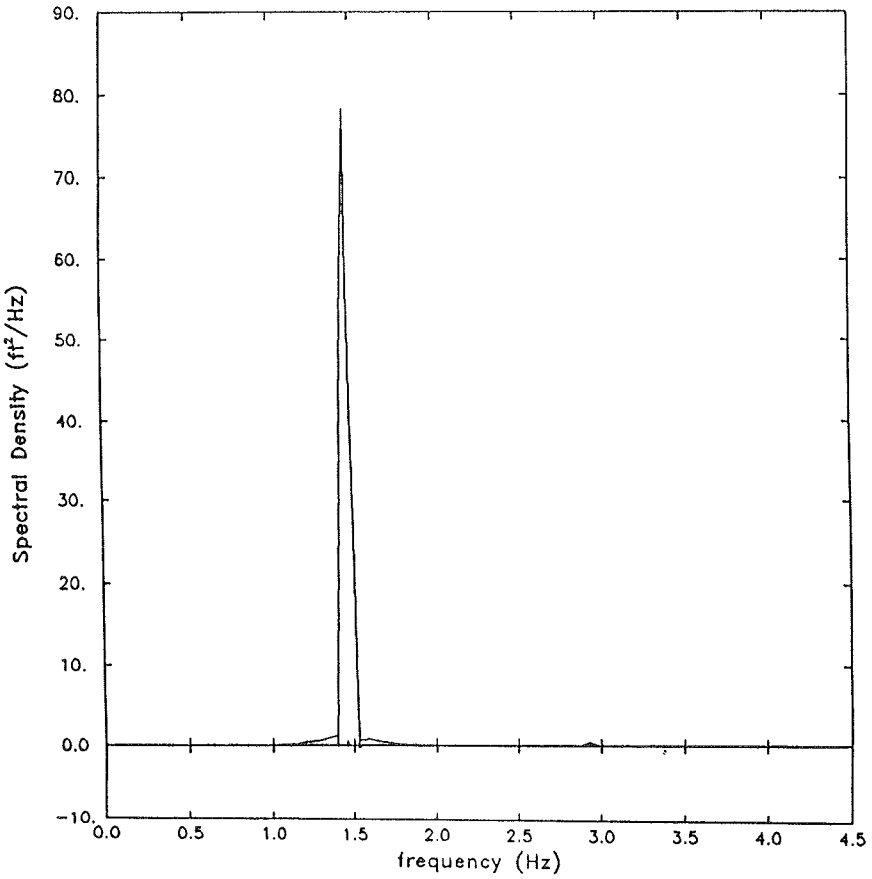

b. Energy spectrum

Figure 6. Wave record and energy spectrum for a 5.3-sec wave recorded near the wave generator

seem to indicate long-wave energy in physical models can be simulated in a realistic way. Additional studies are needed in this area. Theoretical results to date consider piston/paddle wave generators and not the plunger generator used for the Barcelona Harbor study.

16. Most of the wave records in the vicinity of the harbor from the monochromatic model tests are not as regular as the records from deeper water near the wave generator. Instead, they show the effects of nonlinearity and exhibit some degree of wave grouping. Some wave records also contain small-amplitude, high-frequency, random oscillations which result from wave breaking and overtopping of the breakwaters. The $H_{1/3}$ determined from the analysis described in Paragraph 12 does not fully characterize these wave records and was not, by itself, adequate for the purpose of making comparisons between physical and numerical model results.

17. In Bottin's report only $H_{1/3}$ values were presented. For this study the physical model data were reanalyzed using a slightly different procedure which permitted investigation of the full distribution of wave heights. Wave heights were determined by performing a simple upcrossing analysis: two consecutive upcrossings delineate a wave, the height of which is equal to the difference in the maximum and minimum water surface elevations between the upcrossings. From the resulting wave height distributions, the maximum wave height H_{max}, the minimum wave height H_{min}, the wave height with an exceedance probability of 50 percent $H_{0.50}$, and the average of the one-third highest waves $H_{1/3}$ were determined. These parameters were used to characterize the oscillations at each wave gage. Because of the limitation of time and resources, no effort was made to conduct further statistical analyses of the wave data.

18. The resulting $H_{1/3}$ values (presented later in this report) are generally lower than those presented by Bottin (1984) because the simple upcrossing analysis used for this study sometimes classified small-amplitude oscillations between crest and trough as individual waves. Furthermore, the physical model wave heights presented in this report have not been adjusted using Keulegan's equation. For comparison purposes, the adjustment was not necessary because bottom friction coefficients used in the numerical model were chosen which were appropriate for the scale of the physical model. In general, $H_{1/3}$ from Bottin (1984) lies between the H_{max} and $H_{1/3}$ determined for this study. This result is a matter of convention and is not

important relative to the comparisons of physical and numerical model results presented in Part III.

19. Typical wave records from inside the harbor are shown in Figures 7(a) through 10(a). For comparison, Figure 11a is a typical wave record from deeper water near the wave generator for a relatively low amplitude wave. The corresponding cumulative probability distributions (CPD's) of wave heights, derived from the results of simple upcrossing analyses, are shown in Figures 7b through 11b. The variation of wave heights is easily seen in the CPD's.

20. For each run, the values of H_{max}, H_{min}, $H_{0.50}$, and $H_{1/3}$, were normalized by the value of the generated wave height of the run, as listed in Table 1. The results are plotted along vertical bars in Figures 7c through 11c. Hereafter, references to H_{max}, H_{min}, $H_{0.50}$, and $H_{1/3}$ are to their normalized values. Essentially, the vertical bar plots are simple, graphical representations of the CPD's; they provide a convenient, concise means of reporting wave height data from the monochromatic physical model tests. Similar plots are used in Part III to make comparisons between the results of monochromatic physical model tests and the numerical model.

21. The positions of the four wave heights on the vertical bar plots depend on the nature of the corresponding wave records. For a wave record which is a simple sinusoid, the CPD is a step function; and H_{max}, H_{min}, $H_{0.50}$, and $H_{1/3}$ plot at exactly the same point on the vertical bar plot. However, none of the wave records considered in this report plot as simple sinusoids. Deviations from the simple sinusoid can generally be explained in terms of wave grouping, nonlinearity, and the small-amplitude, high-frequency, random oscillations caused by wave breaking and overtopping.

22. Wave records in and near the harbor from the monochromatic physical model tests can be roughly sorted into the four cases typified by Figures 7 through 10; however, Figures 8 and 9 typify the majority of wave records. In paragraphs 23 through 26 the four cases are discussed. Attention is given to the manner in which nonlinearity, wave grouping, breaking, and overtopping manifest themselves in the CPD's and the vertical bar plots. The discussion is given to provide background information which will allow the reader to more easily understand the comparisons between the physical and numerical model results which are presented in Part III.

23. The wave record in Figure 7 is not quite a simple sinusoid.

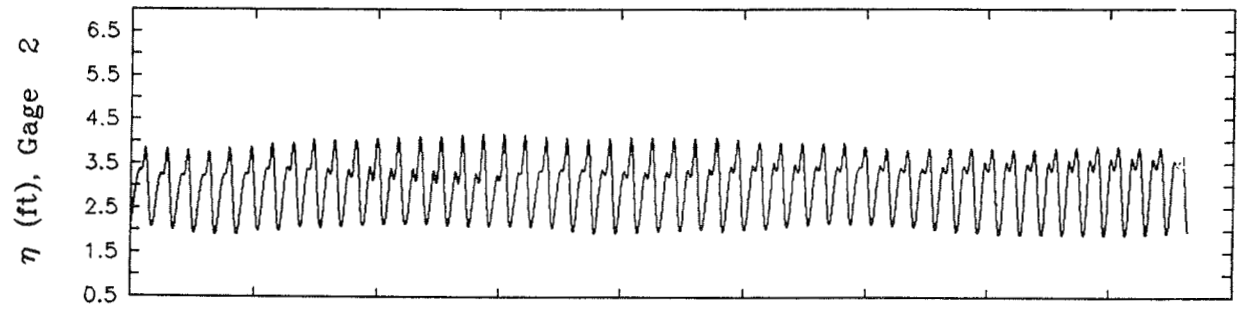

a. Wave record

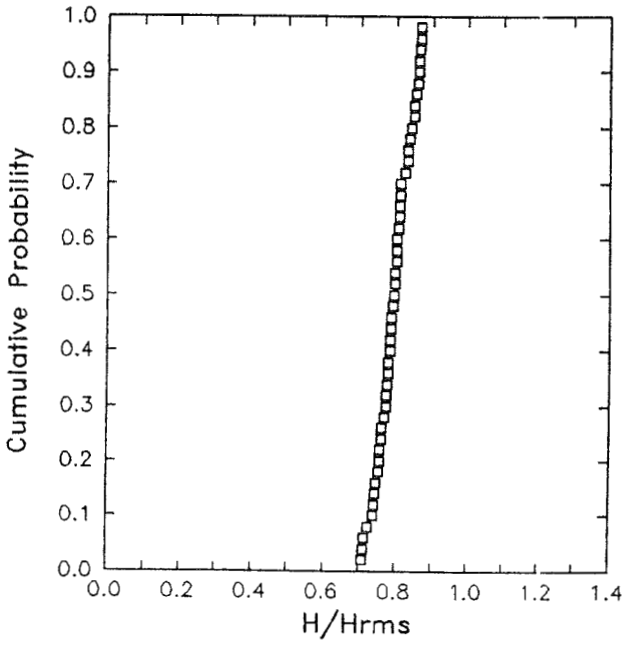

b. Cumulative probability distribution

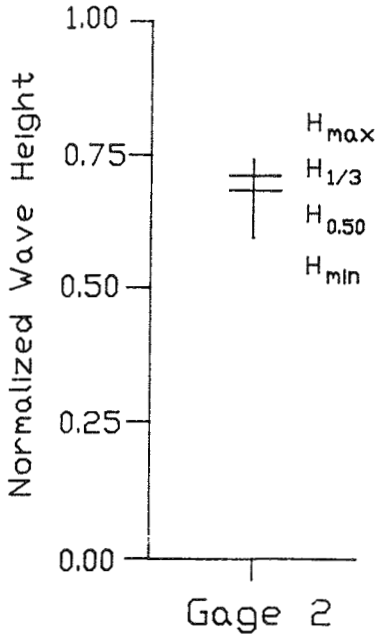

c. Vertical bar plot

Figure 7. Wave record from the physical model, cumulative probability distribution, and vertical bar plot at Gage 2 for Run 11

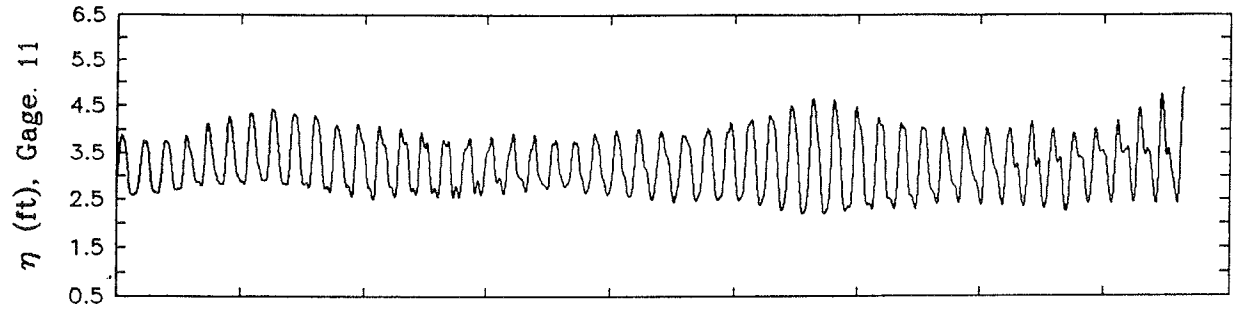

a. Wave record

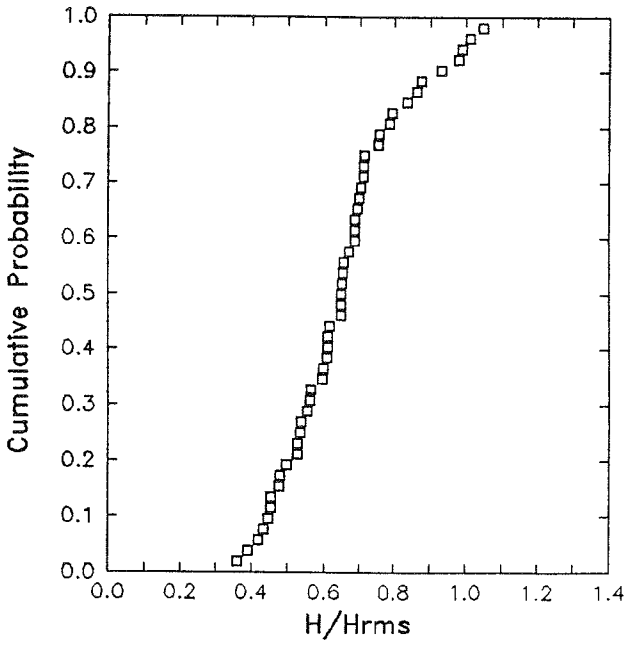

b. Cumulative probability distribution

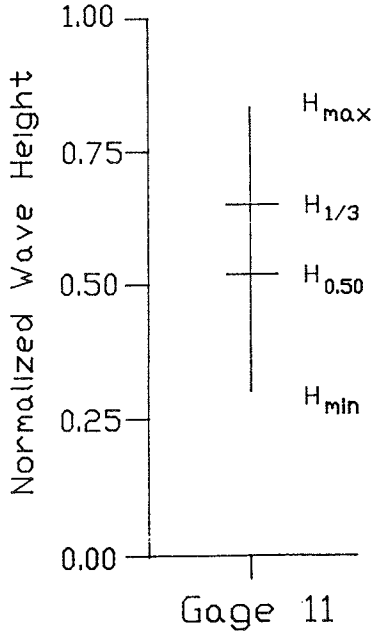

c. Vertical bar plot

Figure 8. Wave record from the physical model, cumulative probability distribution, and vertical bar plot at Gage 11 for Run 5

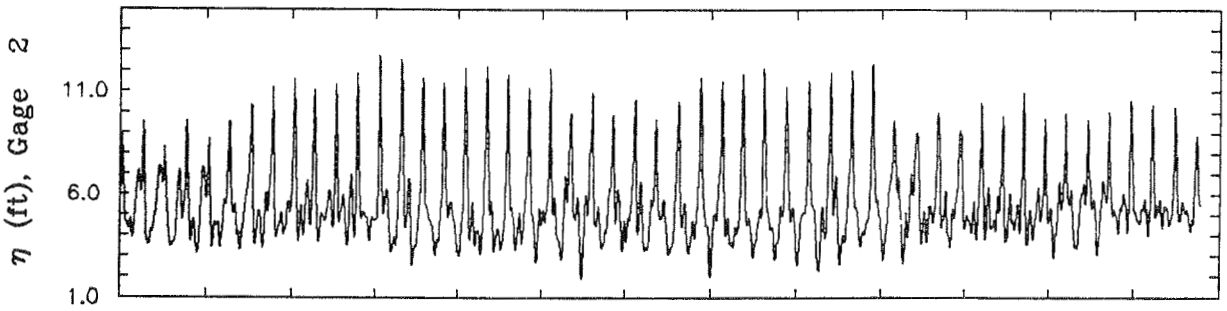

a. Wave record

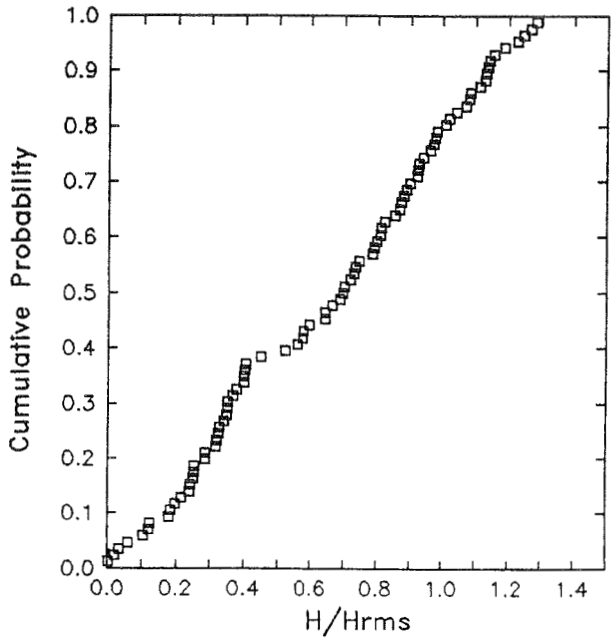

b. Cumulative probability distribution

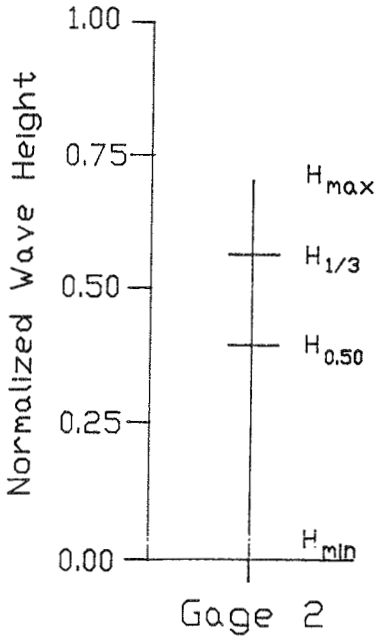

c. Vertical bar plot

Figure 9. Wave record from the physical model, cumulative probability distribution, and vertical bar plot at Gage 2 for Run 2

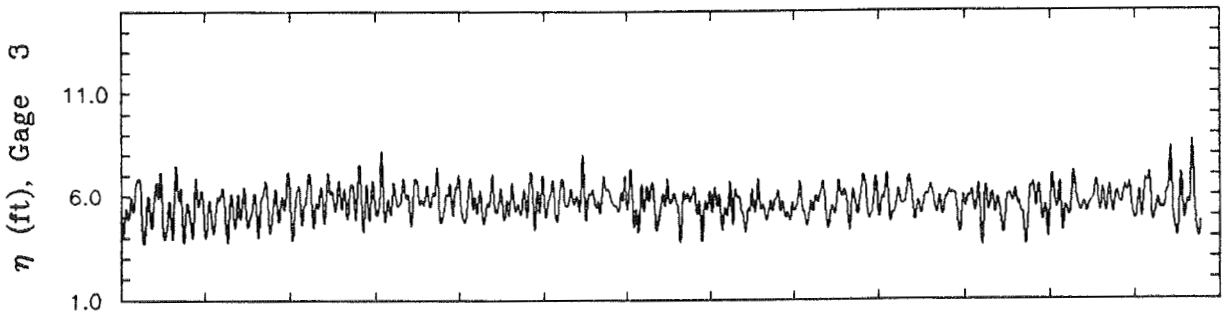

a. Wave record

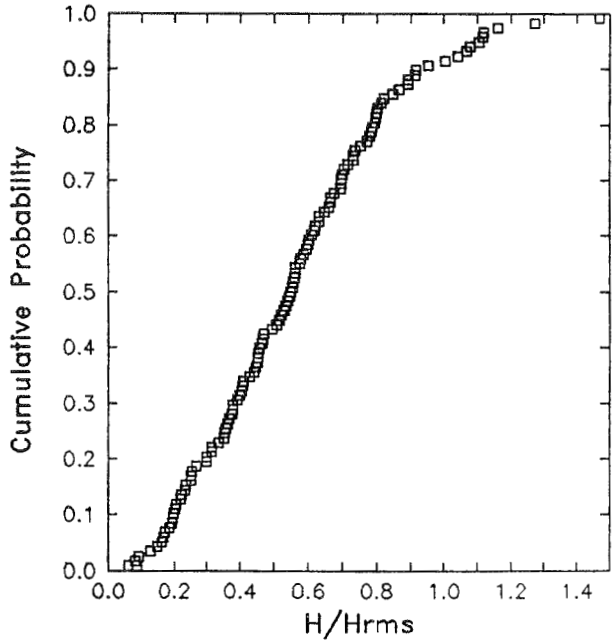

b. Cumulative probability distribution

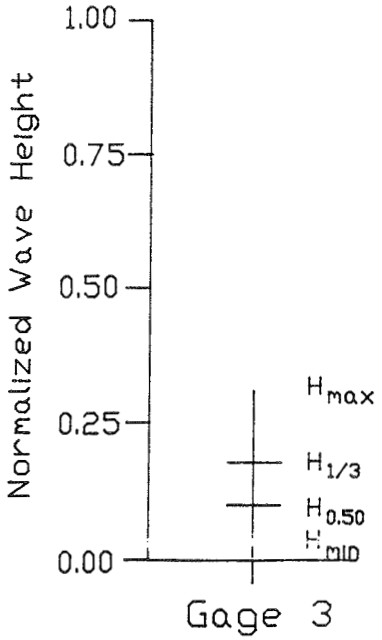

c. Vertical bar plot

Figure 10. Wave record from the physical model, cumulative probability distribution, and vertical bar plot at Gage 3 for Run 2

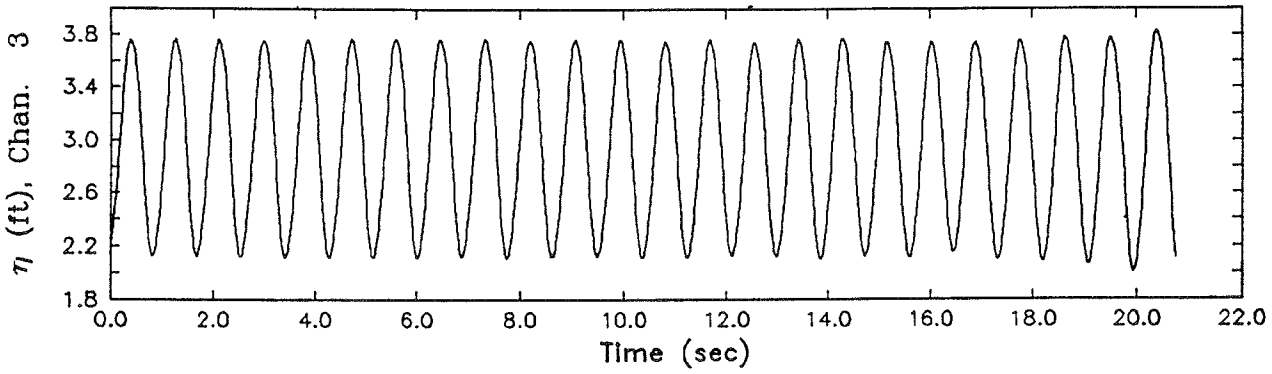

a. Wave record

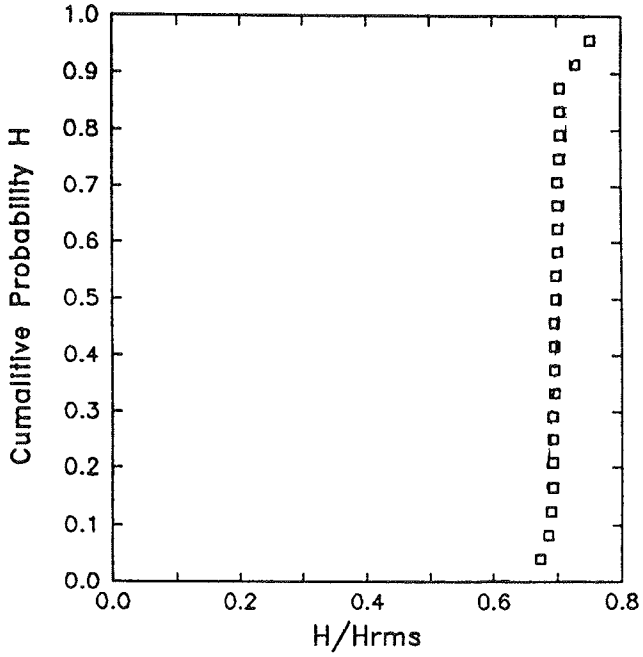

b. Cumulative probability distribution

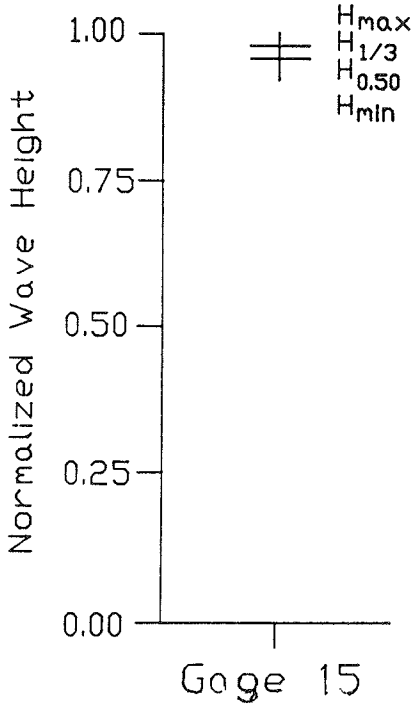

c. Vertical bar plot

Figure 11. Wave record from the physical model, cumulative probability distribution, and vertical bar plot at a gage near the wave generator during model calibration

Table 1

Characteristics of 15 Monochromatic Runs*

Run No.	Harbor Configuration	Wave Direction	Water Level ft	Wave Period sec	Wave Height ft	Photo No. in Bottin's (1984) Report
1	Base Test 2	West	+5.5	9.9	6.2	NA
2					13.9	26
3		North	+4.0	7.5	4.5	NA
4					9.6	38
5		Northeast	+3.0	6.7	2.9	NA
6					5.7	44
7	Plan 42	West	+5.5	9.9	6.2	NA
8					13.9	96
9		North	+4.0	7.5	4.5	NA
10					9.6	102
11		Northeast	+3.0	6.7	2.9	NA
12					5.7	105
13	Plan 58	West	+6.5	7.7	7.9	131
14		North	+4.0	7.5	9.6	132
15		Northeast	+3.0	6.7	5.7	133

* Wave characteristics are values for the prototype waves.

Instead, it exhibits the effects of nonlinearity (as indicated by the steep peaks and by the small perturbations near the mean water level) and shows a slight degree of wave grouping. The CPD is very steep, and the four wave heights are closely spaced on the vertical bar plot. In this example, though not for all cases, the upcrossing analysis has not identified any of the small perturbations as a wave. Every wave identified by the upcrossing analysis has a period which is essentially equal to the period of the incident wave. The apparent grouping causes the CPD to deviate slightly from a step function and the vertical bar not to collapse to a single point. If the upcrossing analysis had identified one of the small perturbations as an individual wave, then H_{min} would have plotted much lower on the vertical bar plot.

24. The wave record in Figure 8 is similar to the one in Figure 7 but

exhibits a more pronounced beat pattern. As a result the CPD is less steep, and the four wave heights on the vertical bar plot are more widely spaced.

25. The wave record in Figure 9 is similar to the one in Figure 8 but is more sharply peaked, having some small-amplitude high-frequency random oscillations. The CPD is much less steep and shows two significant segments, one below $H/H_{rms} = 0.5$ and the other above. (H_{rms} is the root mean square wave height.) Wave heights below $H/H_{rms} = 0.5$ primarily represent the small-amplitude high-frequency random oscillations. The variation of wave heights above $H/H_{rms} = 0.5$ results from the beat pattern. On the vertical bar plot, H_{max}, $H_{1/3}$, and $H_{0.5}$ are near one another; and their separation gives a measure of the degree of development of the beat pattern. H_{min}, which represents the small-amplitude oscillations, is much lower.

26. In the wave records shown in Figures 7a through 9a, waves with frequencies equal to the generated wave frequency are apparent. Also apparent is that the majority of the wave energy is associated with the frequency of the generated wave. The wave record in Figure 10, however, appears to be dominated by small-amplitude, high-frequency, random oscillations. The CPD shows the large number of small-amplitude high-frequency random oscillations picked up by the upcrossing analysis. The four wave heights on the vertical bar plot are widely and evenly spaced indicating the irregular nature of the wave record.

27. Energy spectra for each of the four wave records in Figures 7a through 10a are shown in Figures 12 through 15, respectively. Results for the first three wave records show that the wave energy is concentrated at the frequency of the incident wave with much less energy at harmonics. Analysis for the wave record in Figure 10 shows a similar trend, though some energy is scattered throughout the spectrum. Hence, even when breaking and overtopping are pronounced, much of the energy remains at the frequency of the generated wave. Spectral analyses show the transfer of energy to harmonic frequencies and the complexity of wave patterns which resulted even when the generated wave was very nearly monochromatic.

Numerical Model Study

28. The computer code HARBD was used to model the wave response of Barcelona Harbor to a variety of incident wave conditions. HARBD is a hybrid

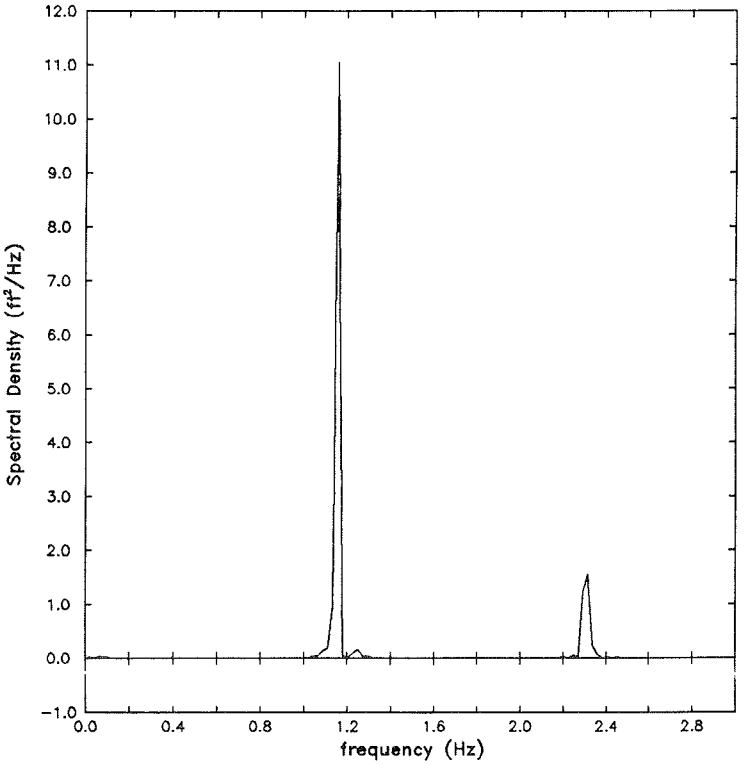

Figure 12. Energy spectrum for the wave record in Figure 7

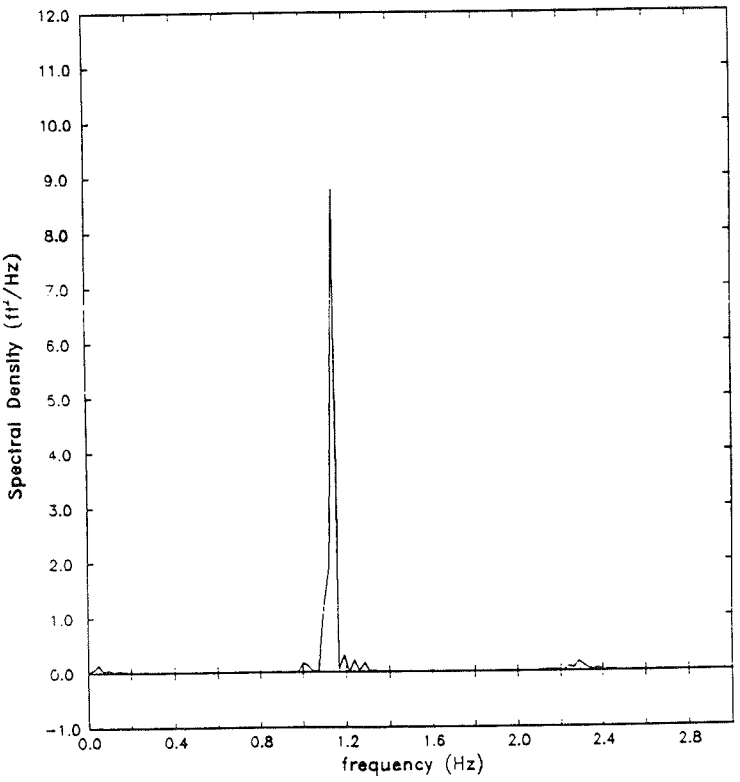

Figure 13. Energy spectrum for the wave record in Figure 8

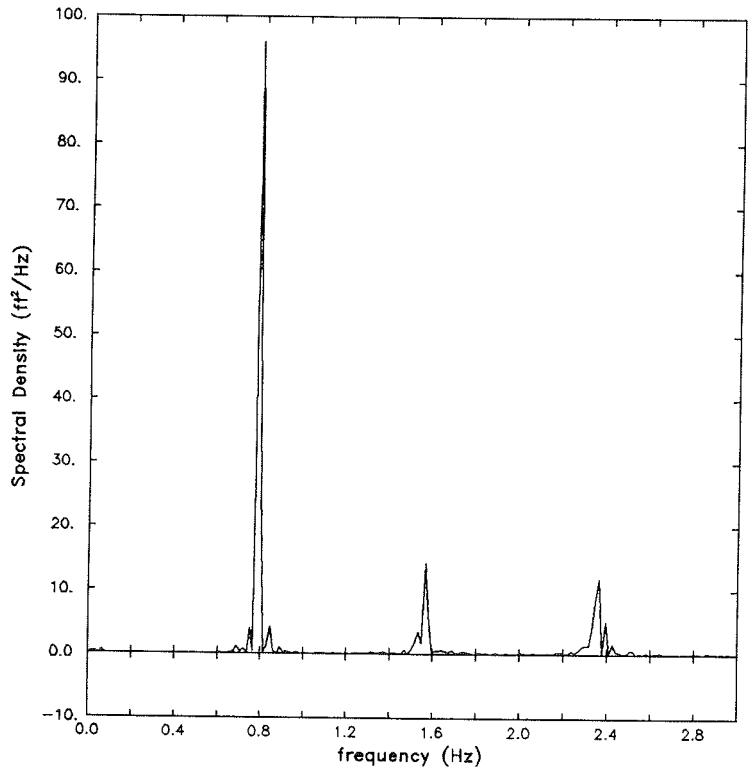

Figure 14. Energy spectrum for the wave record in Figure 9

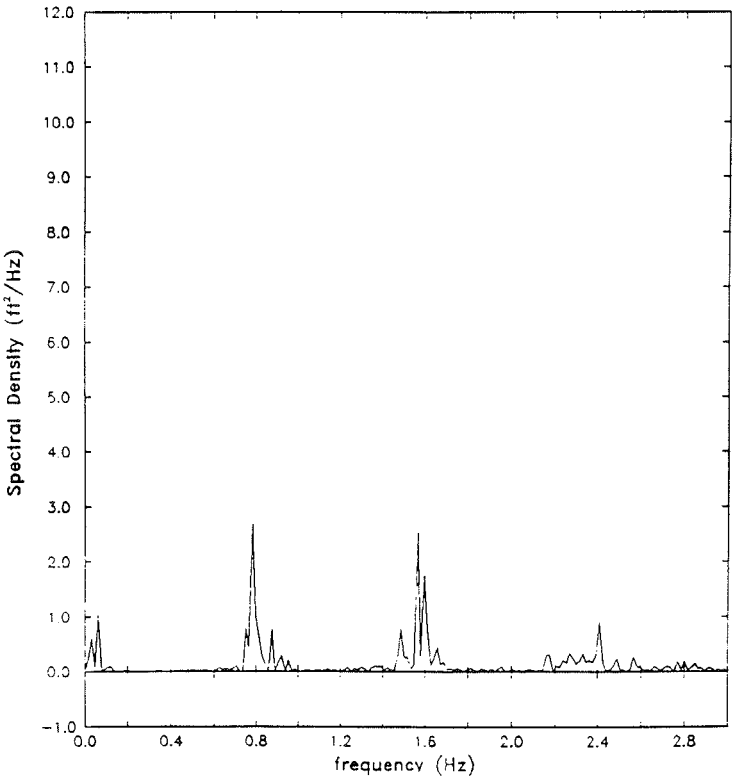

Figure 15. Energy spectrum for the wave record in Figure 10

element model for calculating time-harmonic linear wave oscillations in and near coastal harbors of arbitrary water depth. The model includes the effects of bottom friction and boundary absorption. The bottom friction is assumed to be proportional to flow velocity with a phase difference. The boundary absorption is formulated similar to the impedance condition in acoustics and is expressed in terms of wave number and reflection coefficient of the boundary. In the model the entire water domain is divided into near and far regions by an artificial semicircular boundary. The near region encompasses the harbor and the concerned marine structure and bathymetry. The far region is assumed to have a straight coastline and constant water depth. A variational principle with a proper functional is established to ensure the matching conditions are satisfied along the artificial semicircular boundary. A conventional finite element approximation is used for the solution in the near region, and an analytical solution is used in the far region.

29. HARBD, and similar models using the same numerical technique, have been tested against analytical solutions and laboratory data (Chen and Mei 1974 and Chen 1986). The results are excellent, but all the comparisons were made for simple bathymetry and within the regime of linear wave theory. As an engineering tool, the model has been used to predict wave response in several harbors (Bottin, Sargent, and Mize 1985, Farrar and Chen 1987, and Mathiesen 1987). The predictions are reasonable, but no prototype data are available for comparisons.

30. The HARBD model is intended to model harbor waves which can be reasonably presumed to be governed by the mild slope equation. Therefore, as the waves become increasingly nonlinear and/or gradients in the bathymetry become very steep, the accuracy of the model is expected to decrease. Fortunately, many harbor wave response problems are included in the class of problems for which HARBD is applicable.

31. Another limitation of the HARBD model is that the near-region finite element grid can only cover a finite extent of the open water surrounding the harbor. This situation is analogous to that of the finite basin size limitation of physical models. The limitation results because the prototype bathymetry and shoreline configuration cannot be modelled exactly in the far region (see paragraph 27). Furthermore, some preliminary HARBD model runs indicated that wave heights inside the harbor were slightly sensitive to the location of the artificial semicircular boundary. Theoretically, the

limitation could be removed by placing the artificial semicircular boundary so that it encloses all important bathymetry and shoreline, thus increasing the number of grid cells in the near region. The limitation imposes itself only when the capacity of the available computer is insufficient and/or the cost of data management and computations is too great. Grid size and spacing can be chosen which will allow accurate and economical solutions for many problems.

32. A possible difficulty in using HARBD is that bottom friction and reflection coefficients must be specified. Presumably reasonable choices for reflection coefficients can be made based on information in the SPM (1984) or based on experience. The sensitivity of the model's accuracy to the choice of bottom friction and reflection coefficients depends on the application. For example, solutions for wind waves in relatively deep water are extremely insensitive to the bottom friction coefficients, whereas solutions for the amplifications of the resonant modes of a harbor are at least slightly sensitive to the bottom friction coefficients.

33. To obtain a reasonable variety of tests using the HARBD model, fifteen monochromatic runs and one irregular wave run were made. Wave characteristics and harbor configurations were chosen from the total set of runs made during the physical model study. The three harbor configurations considered (Base Test 2, Plan 42, and Plan 58 in Bottin's (1984) report) are shown in Figures 2 through 4, respectively. Table 1 lists the harbor configuration, water level, and incident wave period, height, and direction of each of the 15 monochromatic runs. Tabulated water levels are referred to the same lwd used in the physical model study.

34. Finite element grids representing each harbor configuration are shown in Figures 16 through 18. The location of the artificial semicircular boundary is the same for all three finite element grids and is shown superposed on the model layout in Figure 19. Notably, the finite element grid does not cover the entire modeled bathymetry of the physical model because wave transformation--principally refraction and shoaling--which occurs before the waves reach the finite element grid was not simulated by the numerical model. Ideally, the grid would have included the entire bathymetry of the physical model. Unfortunately, at the time of the study, the cost of data management and computing for a larger grid exceeded the resources of the study. This problem has been discussed for general applications of HARBD (paragraph 30). To account for shoaling, shoaling coefficients were calculated for each wave

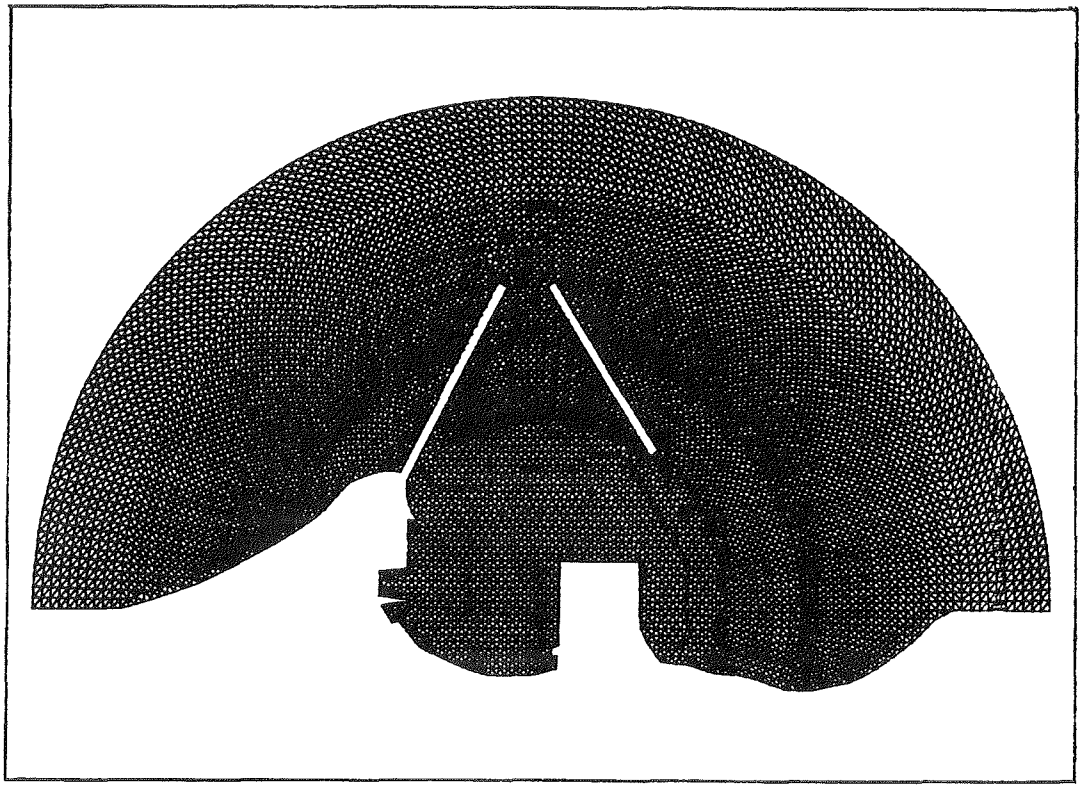

Figure 16. Finite element grid for base Test 2 harbor configuration

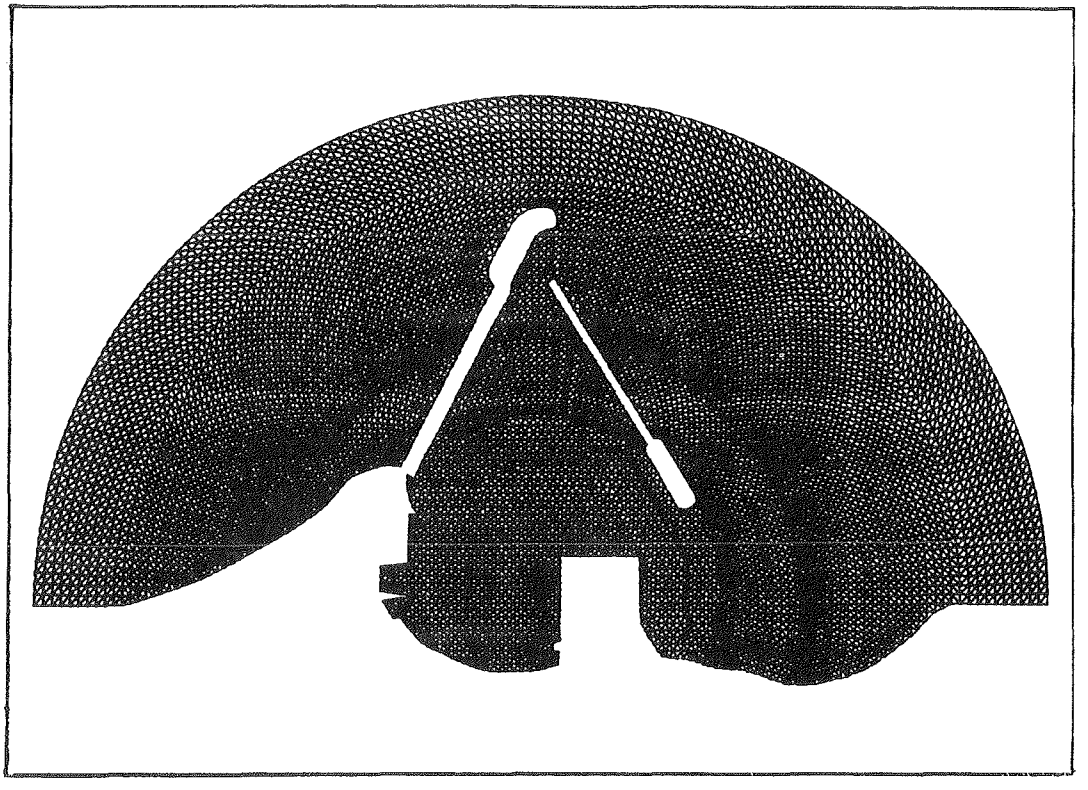

Figure 17. Finite element grid for Plan 42 harbor configuration

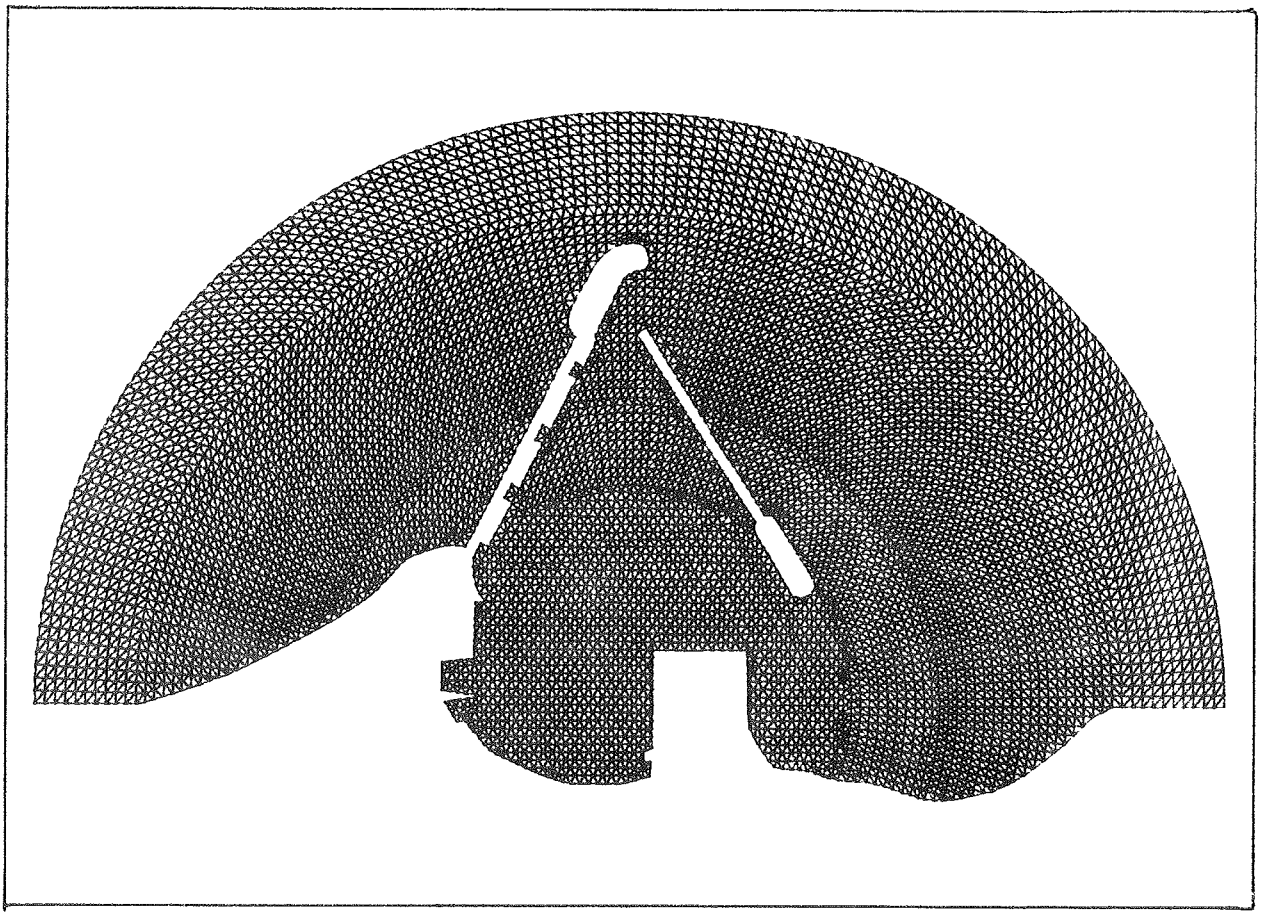

Figure 18. Finite element grid for Plan 58 harbor configuration

period based on the change in depth from the wave generator pit to the edge of the finite element grid. Shoaling coefficients for the 9.9-sec, 7.5-sec, and 6.7-sec waves were 1.14, 1.07, and 1.03, respectively. Wave heights calculated by HARBD based on the incident wave heights in Table 1 were adjusted by multiplying by the appropriate shoaling coefficient. No attempt was made to account for refraction between the generator pit and the edge of the grid; hence, wave transformation between the generator pit and edge of the finite element grid is a cause of discrepancies between the physical and numerical model results.

35. The total numbers of nodes and elements for each harbor configuration are 6,786 and 13,108, 6,693 and 12,872, and 6,704 and 12,888, for Base Test 2, Plan 42, and Plan 58, respectively. The grids provided a resolution of approximately 5 grid cells per wavelength for the shortest-period (6.7-sec) wave considered. The approximate resolution for the 7.5-sec and 9.9-sec waves was 6 and 8 grid cells per wavelength, respectively. As discussed in Part IV,

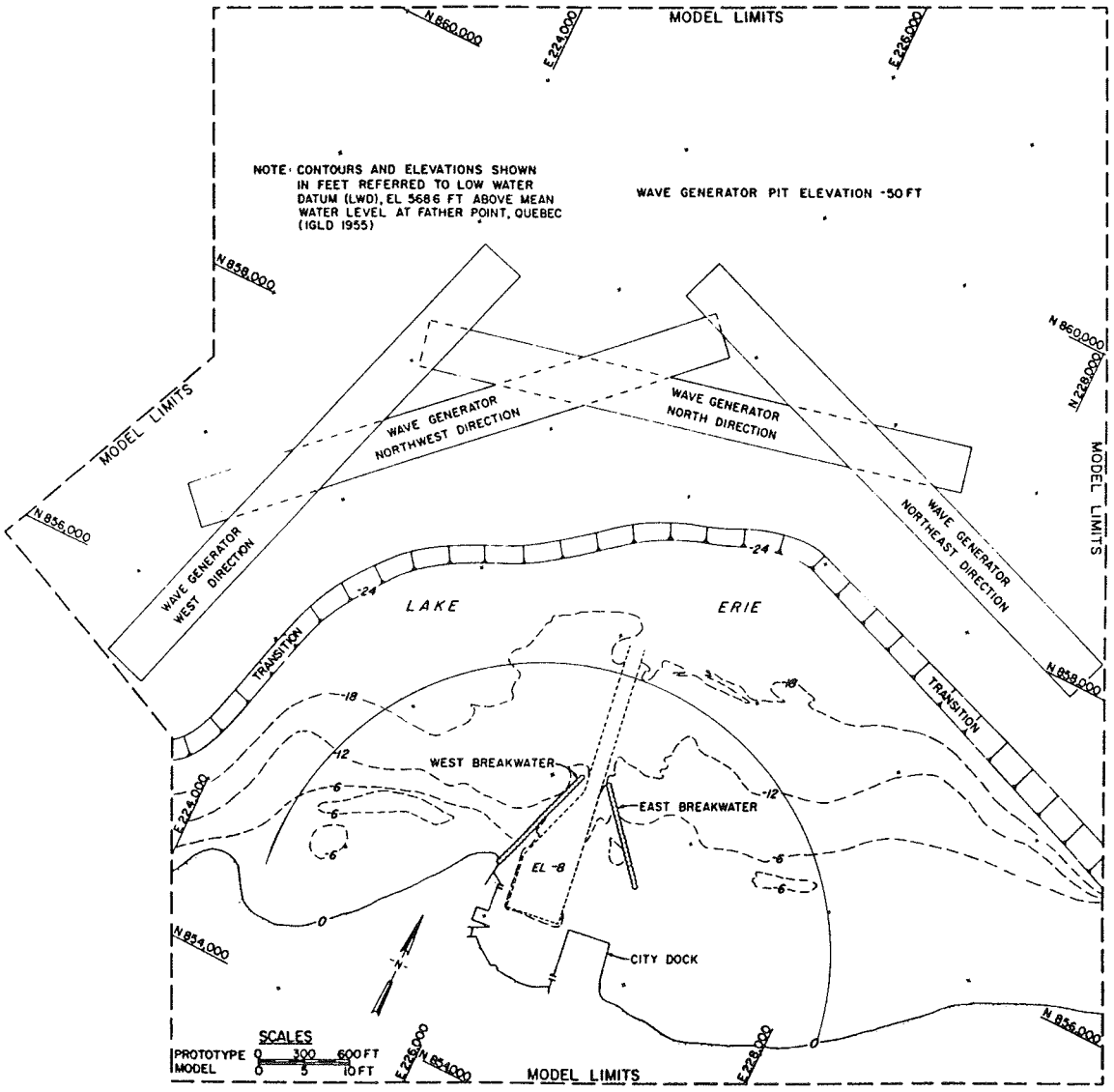

Figure 19. Physical model layout showing the location of the semicircular boundary of the HARBD finite element grid

the results of this study suggest a minimum resolution of 7 grid cells per wavelength to obtain the best results from HARBD.

36. The bathymetry was obtained from the same hydrographic surveys used to design the physical model. The elevation of the lake floor specified for the far region was -15 ft. The seawall around the city dock, along the improved western area of the harbor, and along the original breakwaters was assigned a reflection coefficient of 0.95. The rubble-mound breakwater extensions and wave absorbers were assigned a reflection coefficient of 0.40. Elsewhere, along the unimproved shore, a reflection coefficient of 0.0 was assigned because waves are essentially broken and absorbed there. The bottom

friction coefficient defined by Chen and Houston (1987) was assigned to be 0.1. The values of the reflection and bottom friction coefficients are typical of prototype situations and are thought to be reasonable choices for the present study. However, the sensitivity of the solutions to changes in these coefficients has not been investigated.

37. This study is the first adaptation of HARBD to spectral modeling. One irregular wave run was made. The Plan 58 harbor configuration was used. Wave approach was from the northwest, and the still-water level was at an el of +5.0 ft. The energy density spectrum generated by the wave generator during physical model testing was used as input to the HARBD numerical model. The spectrum is shown in Figure 20. To simulate this run using HARBD, the spectrum was divided into 5 frequency bands centered at 0.116 Hz, 0.138 Hz, 0.161 Hz, 0.187 Hz, and 0.211 Hz, as shown in Figure 20. Higher frequencies were not included because they are less significant in most engineering practice and because the finite element grids shown in Figures 16 through 18 were

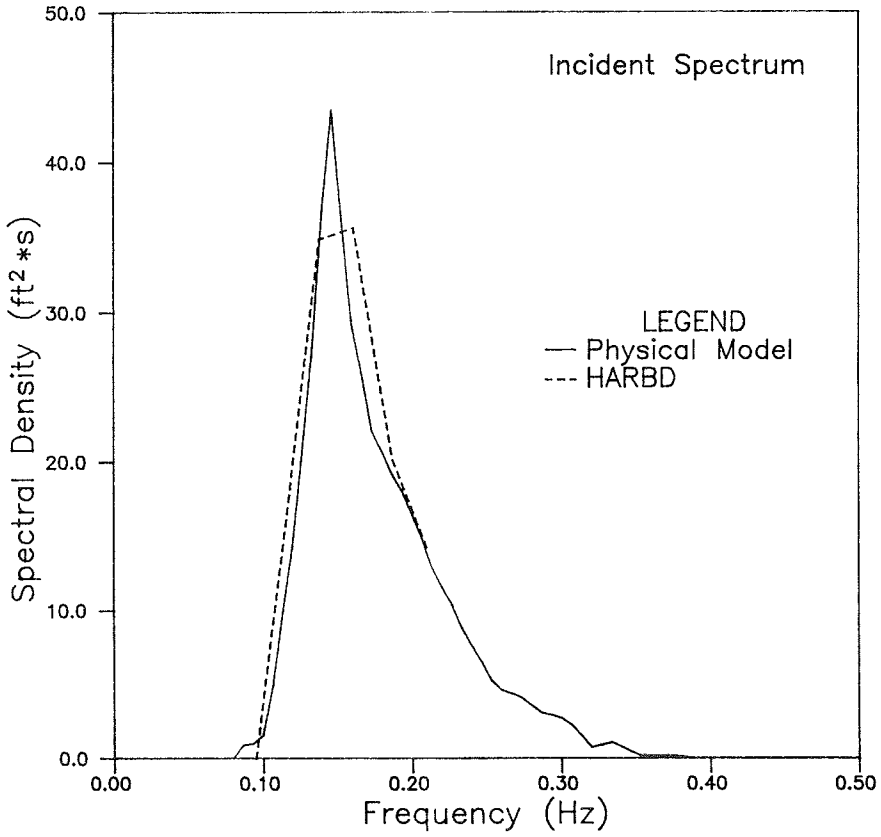

Figure 20. Incident wave energy spectral density

prepared for wave frequencies up to about 0.211 Hz; they could not provide the requisite resolution for investigating higher frequencies. Indeed, resolution of the two highest frequencies is less than that suggested by results of this study (see Part IV). The decision to use 5 frequency bands and the choice of frequencies was completely arbitrary. The rationale was that the 5 selected frequencies provide a reasonable representation of the range of frequencies in which significant energy is present. HARBD was run for each of the five frequencies, and the wave amplitudes at each gage were determined. At each gage, the energy density corresponding to each of the five frequencies was calculated as the energy density of the generated spectrum at that frequency times the square of the amplification factor for the gage. The amplification factor at a gage is defined as the ratio of the wave height at the gage to the incident wave height.

38. HARBD was run on a CDC Cyber Model 205 series 501 computer. The central processing unit (CPU) time for each monochromatic run was about 2 min. Each run required approximately 700 system billing units (SBU) which, at the time of the study, translated to a cost per run of $63.70, assuming a P2 (i.e. overnight) job priority. This information is given only to provide a rough indication of the cost of a single HARBD model run. No inferences concerning the total cost of a study can be made based solely on this information. The total cost of a study depends on the nature of the study and includes the cost of preparing the finite element grid(s), debugging and managing the input and output data, and managing the study as a whole. The cost of grid generation and data management depends on the efficiency of the preprocessing and post-processing software which are areas of active development at the present time.

PART III: RESULTS AND COMPARISONS

39. The fifteen monochromatic wave runs listed in Table 1 and one irregular wave run were made using the HARBD numerical model. Wave response, which includes the amplification factor and phase at each node on the finite element grid, was computed. In this Part, the HARBD results are presented and compared with the results of the physical model.

Monochromatic Waves

40. In a qualitative sense, the major features of the wave response in and around the harbor were similarly predicted by the physical and numerical models for most runs, even when breaking and overtopping in the physical model were pronounced. A typical example is shown in Figure 21 which represents a

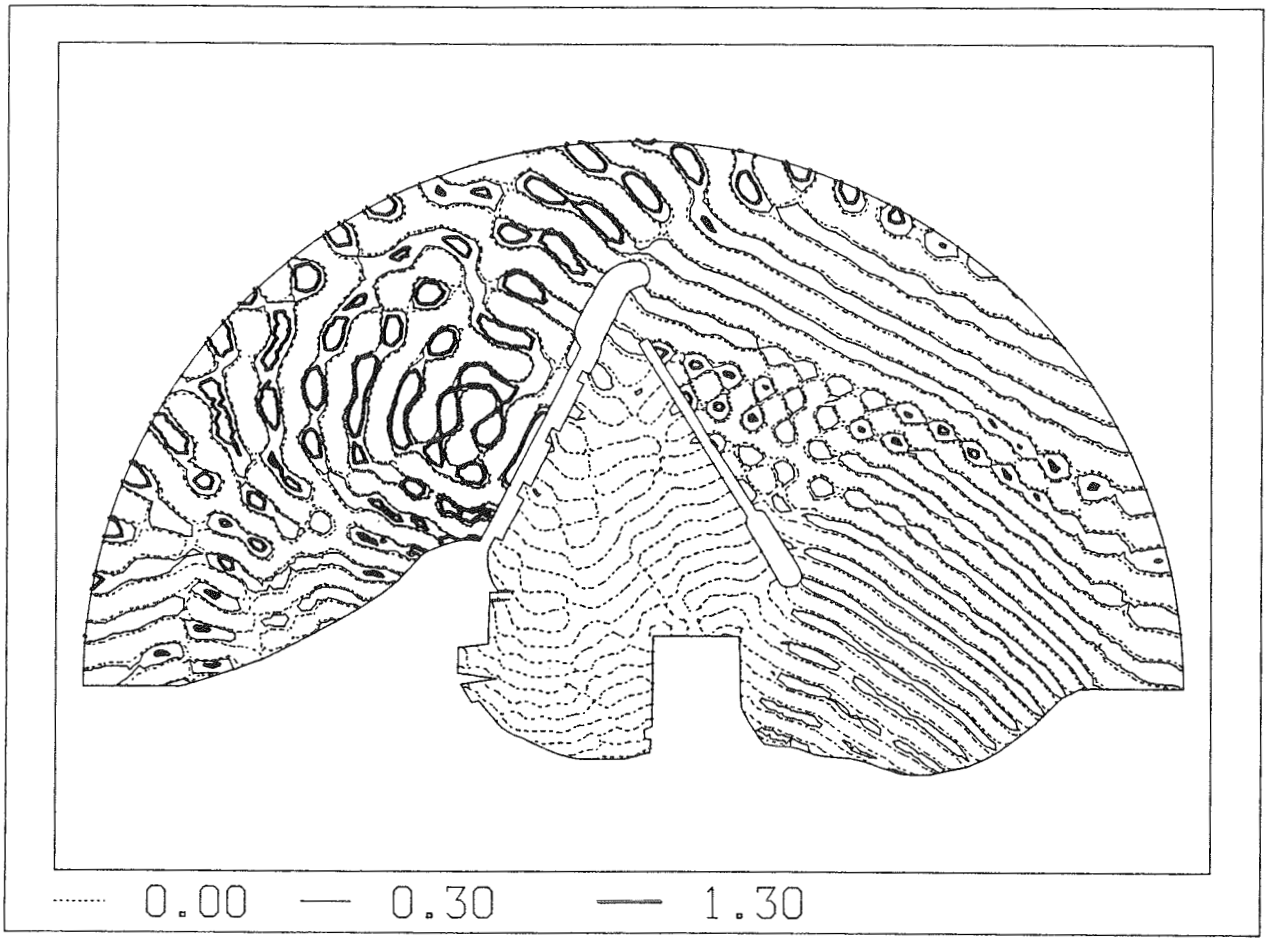

Figure 21. Snapshot of the water surface contour for Run 15

snapshot of the water surface elevation at time $t = 0$ for Run 15. This example corresponds to Photo 1 (Photo 133, Bottin (1984)). In the plot, the isopleths are lines of equal water surface elevation. The values given are the water surface elevation above the still-water level divided by the amplitude of the generated wave. Both the numerical and physical models indicate that waves outside the harbor are generally high and that there is a complex interference pattern near the breakwaters. At the harbor entrance, wave heights are about one-third as high as outside the harbor. Wave heights inside the harbor are significantly less than outside, and the harbor is relatively calm.

41. Strictly speaking, straightforward quantitative comparisons could not be made because of the irregularity of the physical model wave records. Still it was possible to make meaningful comparisons at each gage for each run. The comparisons are presented in Plates 1 through 15. In each plate, the vertical bar connecting H_{max}, $H_{1/3}$, $H_{0.50}$, and H_{min} represents the physical model results, and the circular symbol represents the numerical model result. In each case, actual wave heights have been normalized by the height of the generated wave, as listed in Table 1. The vertical bar plots are interpreted in Part II. Amplification factors from the numerical model were rounded to the nearest 0.05 unit of the incident wave height before multiplying by the appropriate shoaling coefficient. Most of the comparisons agree reasonably well. Surprisingly, even in cases such as Runs 2, 4, 8, 10, and 14 (corresponding to Photos 26, 38, 96, 102, and 105, respectively, in Bottin's (1984) report) where wave breaking and overtopping occur, the comparisons are good for many gages though they are poor for some. These poor comparisons probably result from the effects of wave breaking and overtopping not being strong enough in these cases to significantly alter major features of the harbor's response.

42. Most of the numerical model wave heights are between H_{max} and $H_{0.5}$ from the physical model. However, the numerical model underpredicted wave height for the shortest-period waves (6.7-sec waves from the northeast in Runs 5, 6, 11, 12, and 15). The underpredictions are partly caused by the fact that the finite element grid spacing did not provide adequate resolution for the shortest-period wave; however, for the 7.5-sec waves from the North (Runs 3, 4, 9, 10 and 14) the comparisons are much better despite the fact that the resolution was only slightly better. The most severe

underpredictions were for Runs 5 and 6, which were made using the base Test 2 harbor configuration. For this harbor configuration, waves from the northeast can easily propagate through the navigation entrance and through the opening between the east breakwater and the city dock. Hence, for base Test 2, differences in the direction and/or height of waves incident to the harbor in the physical and numerical models can result in very different harbor responses. For Plan 42 and Plan 58 differences in the incident waves of the physical and numerical models are not as important because the harbor breakwaters allow very little energy into the harbor. Wave transformation which takes place over the bathymetry of the physical model between the wave generator and the edge of the finite element grid is not simulated by the numerical model (paragraph 33). This fact may partly explain the poor comparison for Runs 5 and 6. It also indicates that the finite element grid should be constructed to include as much of the important bathymetry as possible.

Irregular Waves

43. For the irregular wave run, the incident wave spectrum shown in Figure 20 was used as input to the numerical model. The input spectrum was divided into 5 frequency bands centered at 0.116, 0.138, 0.161, 0.187, and 0.211 Hz. At each gage, the spectral density at these five frequencies was predicted by the numerical model. The spectral density was set to zero at frequencies below 0.09 Hz because the incident wave spectral density was zero at lower frequencies, whence the HARBD model (which is based on the linear theory) must yield zero spectral density below 0.09 Hz. The numerical model study did not consider frequencies greater than 0.211 Hz because very poor resolution was expected using the finite element grids shown in Figures 16 through 18.

44. For each gage, the energy spectra yielded by the physical and numerical models are compared in Plates 16 through 29. Notably, the scales are not the same for each spectrum. The comparisons generally agree well for the range of frequencies considered by the numerical model. For Gage 1 near the harbor entrance, spectra from the physical and numerical models are very similar in shape. The spectral density peaks are about the same value of 4.5 ft^2 sec. For Gages 2 through 14 inside the harbor, results from both models indicate that spectral densities are all small and less than 0.5 ft^2 sec for

frequencies greater than 0.09 Hz. This occurrence indicates that only a very small portion of the energy of the incident wave train reaches inside the harbor.

45. Differences in the spectra occur at frequencies less than 0.09 Hz. Below this frequency the numerical model spectra must predict zero spectral density at each gage because spectral density of the input spectrum was zero below 0.09 Hz (paragraph 43). However, the physical model spectra show significant spectral density below 0.09 Hz, particularly in the very low frequency end. In the harbor, the wave energy at lower frequencies may be associated with excitation by wave groups, nonlinear wave energy transfer, and breaking and overtopping.

PART IV: CONCLUSION

46. Most of the wave records from the physical model tests exhibited the effects of nonlinearity and some degree of wave grouping. In several tests wave breaking and overtopping occurred which, in turn, generated low-amplitude, high-frequency, random oscillations. The spread of the wave height distribution at many gages was fairly wide. It has, therefore, been useful and convenient to characterize wave height at each gage by the vertical bar plot of H_{max}, H_{min}, $H_{1/3}$, and $H_{0.50}$, rather than by a single value such as $H_{1/3}$. For the monochromatic tests, the vertical bar plots were used to compare results from the physical and numerical models.

47. The HARBD numerical model used in this study is based on linear wave theory which, in a rigorously theoretical sense, is not intended to model the wave conditions of the physical model tests. (Some of the physical model tests include nonlinear wave transformation and extensive breaking and overtopping.) Nevertheless, results of the two models are reasonably consistent in that they yield comparable harbor responses for most cases even though the magnitude of the response at various locations in the harbor was very different in a few instances. These differences are important because they may materially affect the ultimate design of the harbor. It must be emphasized that the comparisons were not straightforward because the physical model results are characterized by a distribution of wave heights, whereas the HARBD model result is simply the height of a monochromatic wave.

48. For the monochromatic wave comparisons, the HARBD numerical model yielded wave heights which, in most cases, were between H_{max} and $H_{0.50}$ from the physical model. However, for the shortest-period waves--6.7 sec in Runs 5, 6, 11, and 15--the wave heights from the numerical model were less than those from the physical model. This is mainly because the grid spacing, which was approximately one-fifth of the incident wave length for these waves, was too coarse to provide adequate resolution. A grid spacing less than one-seventh of the incident wave length is recommended to obtain the best results for most engineering practice. The worst predictions were for Runs 5 and 6. The large discrepancies between wave heights from the physical and numerical models for these runs may be partly due to wave transformation between the wave generator pit and the edge of the finite element grid.

49. For irregular wave comparisons the HARBD model yielded spectra

which, for frequencies greater than about 0.09 Hz, agreed reasonably well with those from the physical model. However, there was a great difference for the portion of the spectra below 0.09 Hz. The physical model showed a significant amount of spectral density; whereas the numerical model predicted no spectral density since there was zero spectral density below 0.09 Hz in the incident spectrum. The significant amount of spectral density at low frequencies may be due to excitation by wave groups, nonlinear wave energy transfer, and wave breaking and overtopping. The HARBD numerical model is incapable of simulating these phenomena.

50. Both models have limitations related to their ability to accurately simulate the prototype. For the physical model these are primarily related the scale effects, limited basin size, performance of the wave generator, and determination of reflective properties of the shore and harbor structures. The negative effects of these limitations always are minimized to the extent possible as was the case during the physical model study of Barcelona Harbor. The main limitation on the HARBD model is that it is based on linear wave theory with mild bottom slope approximation. Accuracy of the HARBD model decreases as nonlinearity of the wave increases. HARBD is not intended to model certain phenomena such as wave breaking and overtopping. Nevertheless, the study indicates that if these phenomena are not dominant, HARBD is able to predict wave heights inside the harbor fairly accurately. For engineering purposes, HARBD can be used somewhat beyond the limits of its theoretical range of applicability. For some problems the accuracy of the solution is adversely affected if the finite element grid is not extended sufficiently far seaward to cover the entire area of important bathymetry. The error is not inherent to the HARBD model; rather, it results when resources available to the study limit the size of the finite element grid which can be constructed. This problem is analogous to the finite basin size limitation of physical models.

51. HARBD represents a significant improvement over previous numerical models because it is able to simulate bottom friction and boundary absorption. HARBD can predict wave response inside a harbor more accurately than previous numerical models, particularly at or near the resonant modes of the harbor.

52. Since no prototype data were available, inferences cannot be made concerning the ability of either model to predict wave response in the prototype. To more rigorously assess the models, prototype data are indispensable.

Furthermore, conceiving and conducting this study after the physical model study had been completed presented several problems. The principal problem was that physical model results were not ideally suited for the purpose of making comparisons with results from the HARBD numerical model. For example, some waves considered in the physical model study had heights and periods which indicated they might not be well described by the linear theory. An intercomparison study similar to the one described in this report, but with the physical and numerical models studies planned and conducted simultaneously, would be useful. Ideally, prototype data would also be available for such a study.

53. Even though the physical model results were not ideally suited for making comparisons with the linear HARBD model, some differences in the results of the two models stand out. Much of the difference in the monochromatic tests can be attributed to the long-period beats seen in the physical model wave records. Most of the difference in the irregular wave tests is seen at the extreme low frequency end of the spectrum, below the low-frequency cutoff of the generated spectrum. It is not known whether these are nonlinear phenomena which also occur in the prototype. If they are spurious, the procedure for conducting physical model studies should be reassessed. If they are not spurious, then an even greater emphasis should be placed on developing a nonlinear numerical model.

54. The SPM (1984) wave diffraction method requires great simplification of most harbor wave problems. In the case of Barcelona Harbor it exhibited serious limitations, particularly in neglecting wave reflections from interior harbor boundaries. Since interior reflections were the primary source of problems in the prototype harbor, the SPM method is considered unsuitable for this study.

55. In a practical engineering project study, the modeling approach must be carefully selected. The nature of the important hydrodynamic processes (e.g. wave reflection, breaking, overtopping, and resonance) and the scale and characteristics of the harbor area are critical in model selection. Other important considerations are the number and types of alternatives to be investigated, the importance of tangible demonstrations for co-sponsors and the public, and the available time and funding. The primary driving force behind the choice of an appropriate modeling approach should be the required accuracy and completeness of the predictions. Physical models can yield

information concerning the effects of wave grouping, nonlinearity, wave breaking, and overtopping which are not available from numerical models. They can also provide information on wave-induced currents and shoaling patterns. For some studies, numerical models have advantages in terms of time, cost and flexibility. SPM (1984) methodologies are useful for rough estimates and for very quick studies of simple harbors but have serious limitations for most actual project studies. This report focuses on the accuracy of the various modeling approaches. It does not provide detailed information on the time and cost requirements of physical and numerical models.

REFERENCES

Behrendt, L., and Jonsson, I. G. 1984. "The Physical Basis of the Mild-Slope Equation," Proceedings of the 19th International Conference on Coastal Engineering, American Society of Civil Engineers, pp 941-954.

Berkhoff, J. C. W. 1976. "Mathematical Models for Simple Harmonic Linear Water Waves," Delft Hydraulics Laboratory, Report No. 163, Delft, The Netherlands.

Bottin, Jr., R. R. 1984. "Barcelona Harbor, New York; Design for Harbor Improvements," Technical Report CERC-84-3, US Army Engineer Waterways Experiment Station, Vicksburg, MS.

Bottin, Jr., R. R., Sargent, F. E., and Mize, M. G. 1985. "Fisherman's Wharf Area, San Francisco Bay, California, Design for Wave Protection," Technical Report CERC-85-7, US Army Engineer Waterways Experiment Station, Vicksburg, MS.

Chen, H. S. 1984. "Hybrid Element Modeling of Harbor Resonance," Proceedings of the 4th International Conference on Applied Numerical Modeling, pp 312-316.

_____. 1986. "Effects of Bottom Friction and Boundary Absorption on Water Wave Scattering," Applied Ocean Research, Vol 8, No. 2, pp 99-104.

Chen, H. S. and Houston, J. R. 1987. "Calculation of Water Oscillation in Coastal Harbors; HARBS and HARBD User's Manual," Technical Report CERC-87-2, US Army Engineer Waterways Experiment Station, Vicksburg, MS.

Chen, H. S. and Mei, C. C. 1974. "Oscillations and Wave Forces in an Offshore Harbor," Report No. 190, Department of Civil Engineering, Massachusetts Institute of Technology, Cambridge, MA.

Farrar, P., and Chen, H. S. 1987. "Wave Response of the Proposed Harbor at Agat, Guam; Numerical Model Investigation," Technical Report CERC-87-4, US Army Engineer Waterways Experiment Station, Vicksburg, MS.

Ganaba, M. B., Welford, C., and Lee, J. J. 1982. "Dissipative Finite Element Models for Harbor Resonance Problems" in Kawai, T. (ed.), Finite Element Flow Analysis, University of Tokyo Press, Japan.

Houston, J. R. 1976 (Sep). "Long Beach Harbor Numerical Analysis of Harbor Oscillations," Reports 1, 2, and 3, Miscellaneous Paper H-76-20, Hydraulics Laboratory, US Army Engineer Waterways Experiment Station, Vicksburg, MS.

_____. 1981. "Combined Refraction and Diffraction of Short Waves Using the Finite Element Method," Applied Ocean Research, Vol 3, No. 4, pp 163-170.

Hudson, R. Y., et al. 1979. "Coastal Hydraulic Models," CERC SR-5, US Army Engineer Waterways Experiment Station, Vicksburg, MS.

Jensen, O. J., and Warren, I. R. 1986. "Modeling of Waves in Harbors - Review of Physical and Numerical Methods," The Dock and Harbor Authority, Vol 67, No. 783, pp 123-129.

Lee, J. J. 1969. "Wave Induced Oscillations in Harbors of Arbitrary Shape," Report No. KH-R-20, W. M. Keck Laboratory of Hydraulics and Water Resources, Division of Engineering and Applied Sciences, California Institute of Technology, Pasadena, CA.

Lepelletier, T. G. 1981. "Tsunamis - Harbor Oscillations Induced by Non-linear Transient Long Waves," Report No. KH-R-41, W. M. Keck Laboratory of Hydraulics and Water Resources, Division of Engineering and Applied Sciences, California Institute of Technology, Pasadena, CA.

Matsoukis, P. F. 1985. "Numerical Modelling of Long Waves in Harbours," International Conference on Numerical and Hydraulic Modelling of Ports and Harbours, pp 257-261.

Mathiesen, M. 1987. "Sklinna-Langperiodiske Bolger," STF60 F87035, Norwegian Hydrotechnical Laboratory, Norway.

Shore Protection Manual. 1984. 4th ed., 2 vols, US Army Engineer Waterways Experiment Station, Coastal Engineering Research Center, US Government Printing Office, Washington, DC.

Skovgaard, O., Behrendt, L., and Jonsson, I. G. 1984. "A Finite Element Model for Wind Wave Diffraction," Proceedings of the 19th International Conference on Coastal Engineering, pp 1090-1102.

Turner, K. A. and Durham, D. L. 1984. "Documentation of Wave Height and Tidal Analysis Programs for Automated Data Acquisition Systems," Miscellaneous Paper HL-84-2, US Army Engineer Waterways Experiment Station, Vicksburg, MS.

Yoshida, A., Ijima, T., and Okuzono, H. 1984. "Wave-Induced Oscillations in Harbors with Wave-Absorbing Quay," Proceedings of the 19th International Conference on Coastal Engineering, Vol 1, pp 929-940.

Yue, D. K. P., Chen, H. S., and Mei, C. C. 1976. "A Hybrid Element Method for Calculating Three-Dimensional Water Wave Scattering," Report No. 225, Department of Civil Engineering, Massachusetts Institute of Technology, Cambridge, MA.

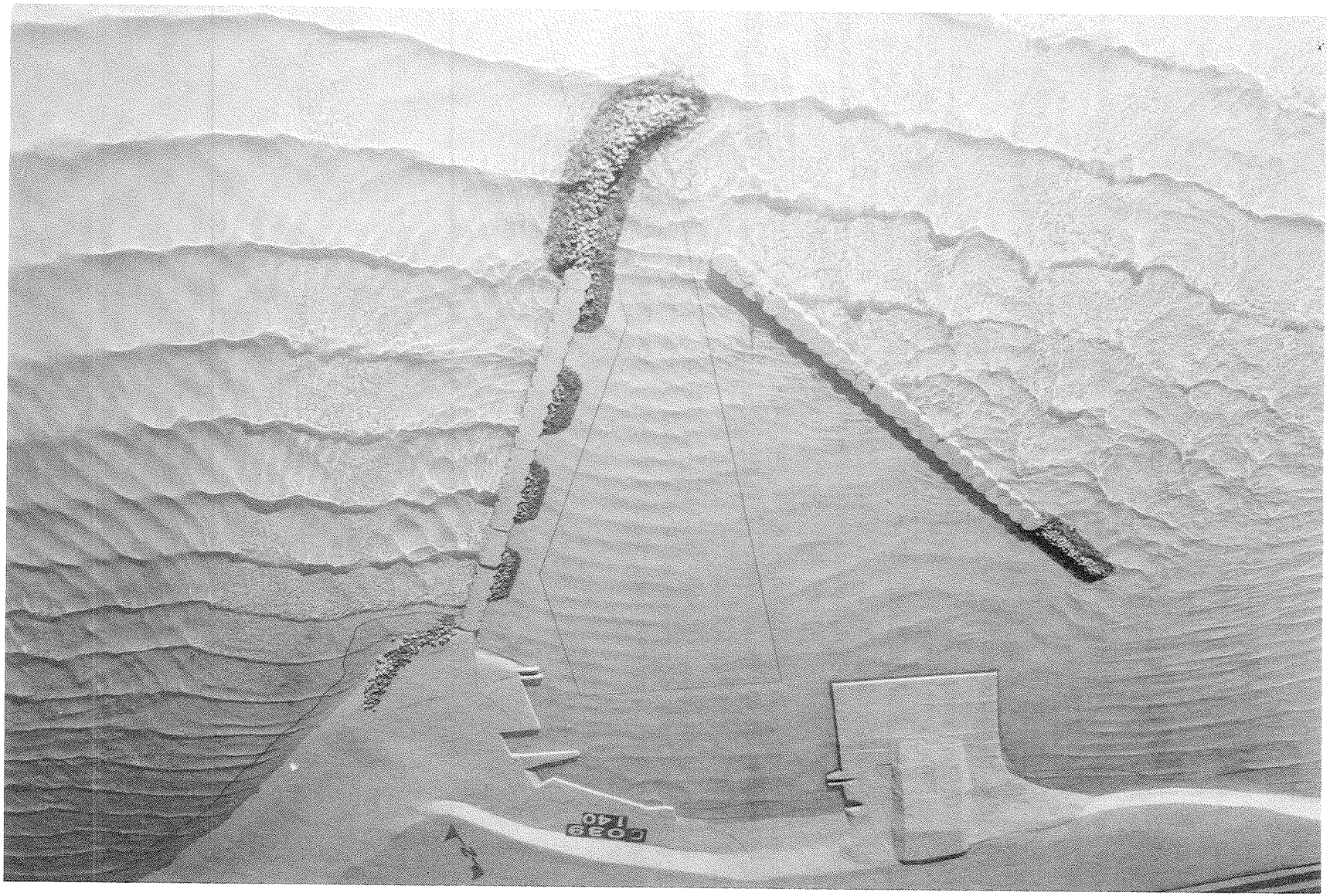

Photo 1. Water surface elevation at time t = 0 (Photo 133 in Bottin's report)

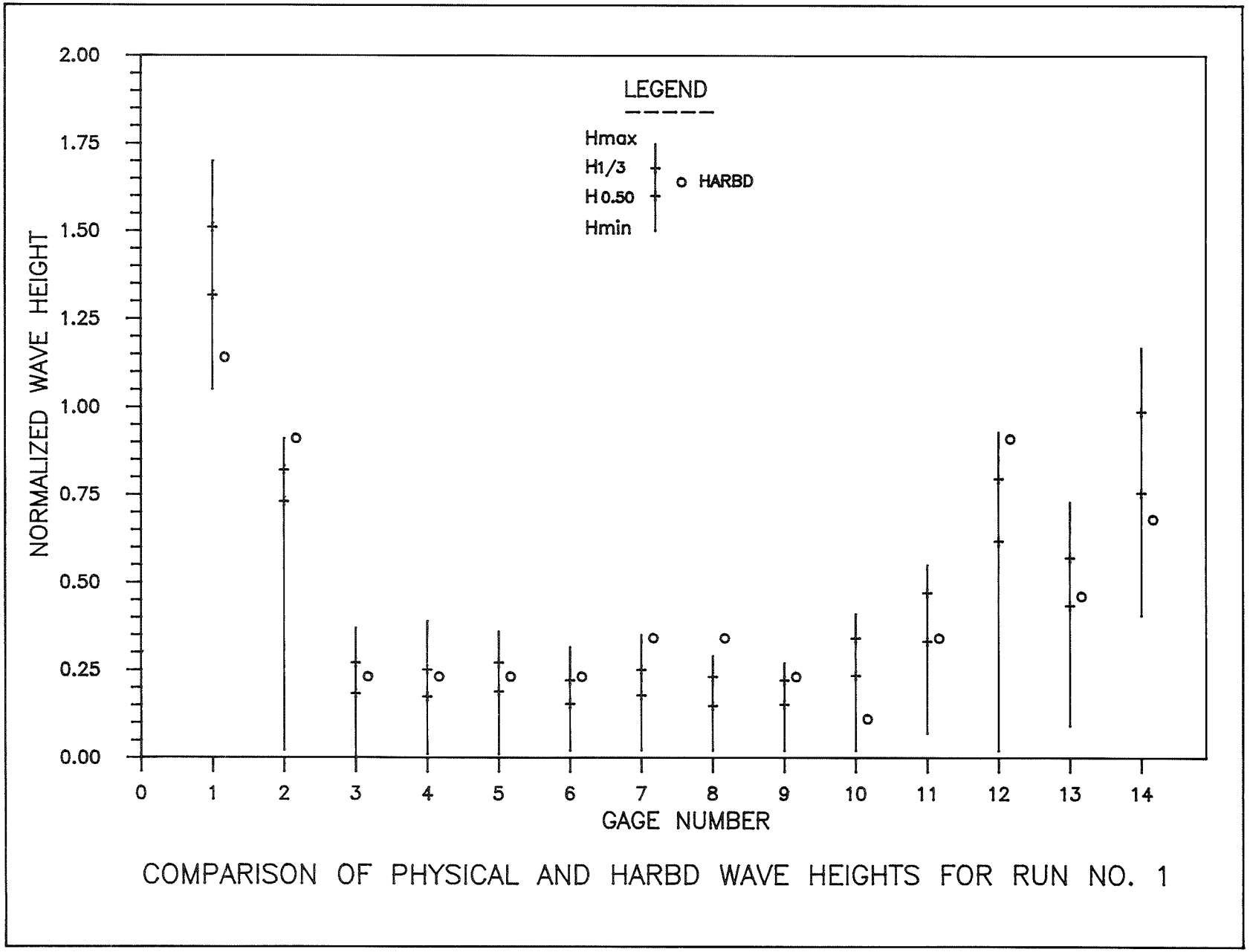

COMPARISON OF PHYSICAL AND HARBD WAVE HEIGHTS FOR RUN NO. 1

PLATE 1

PLATE 2

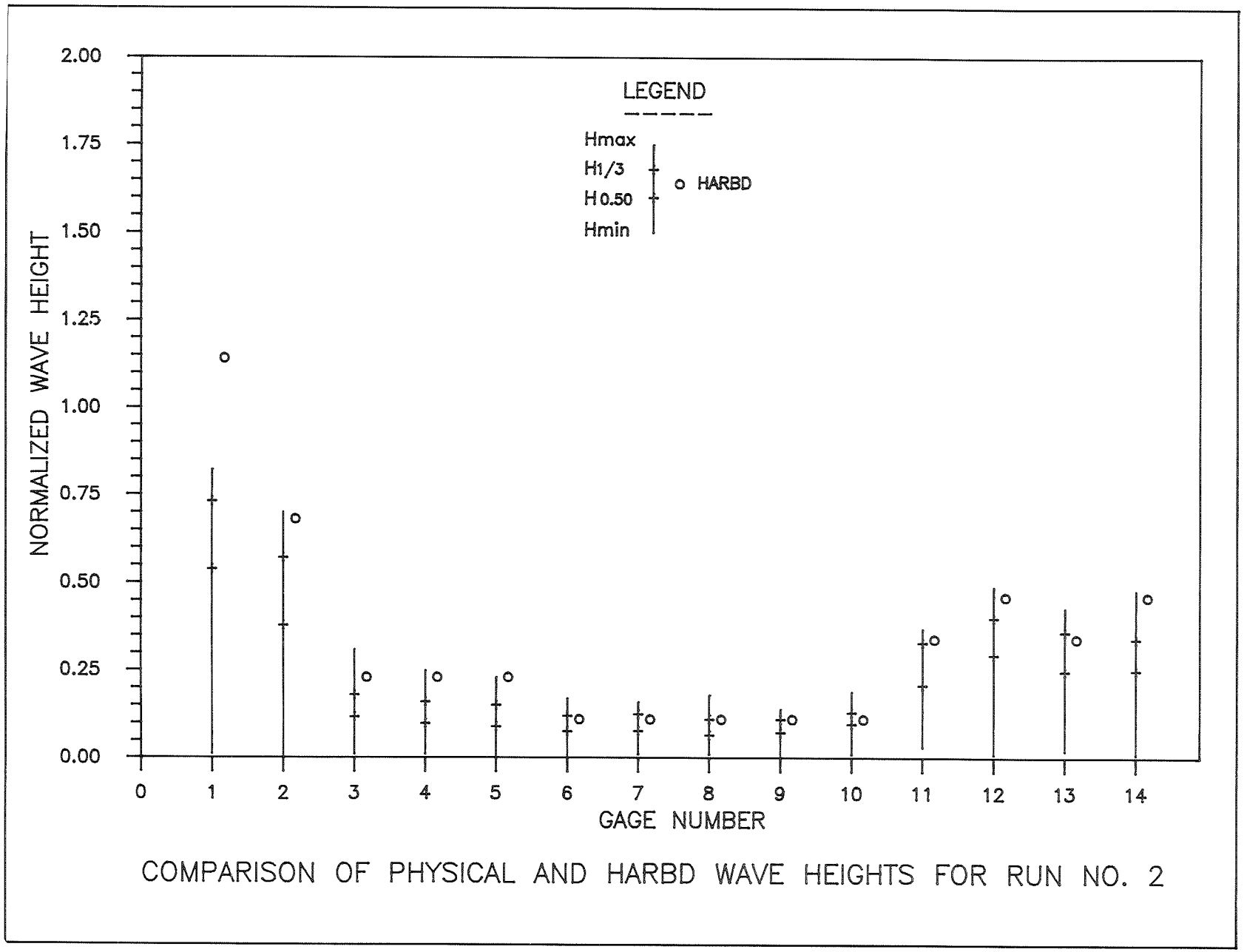

COMPARISON OF PHYSICAL AND HARBD WAVE HEIGHTS FOR RUN NO. 2

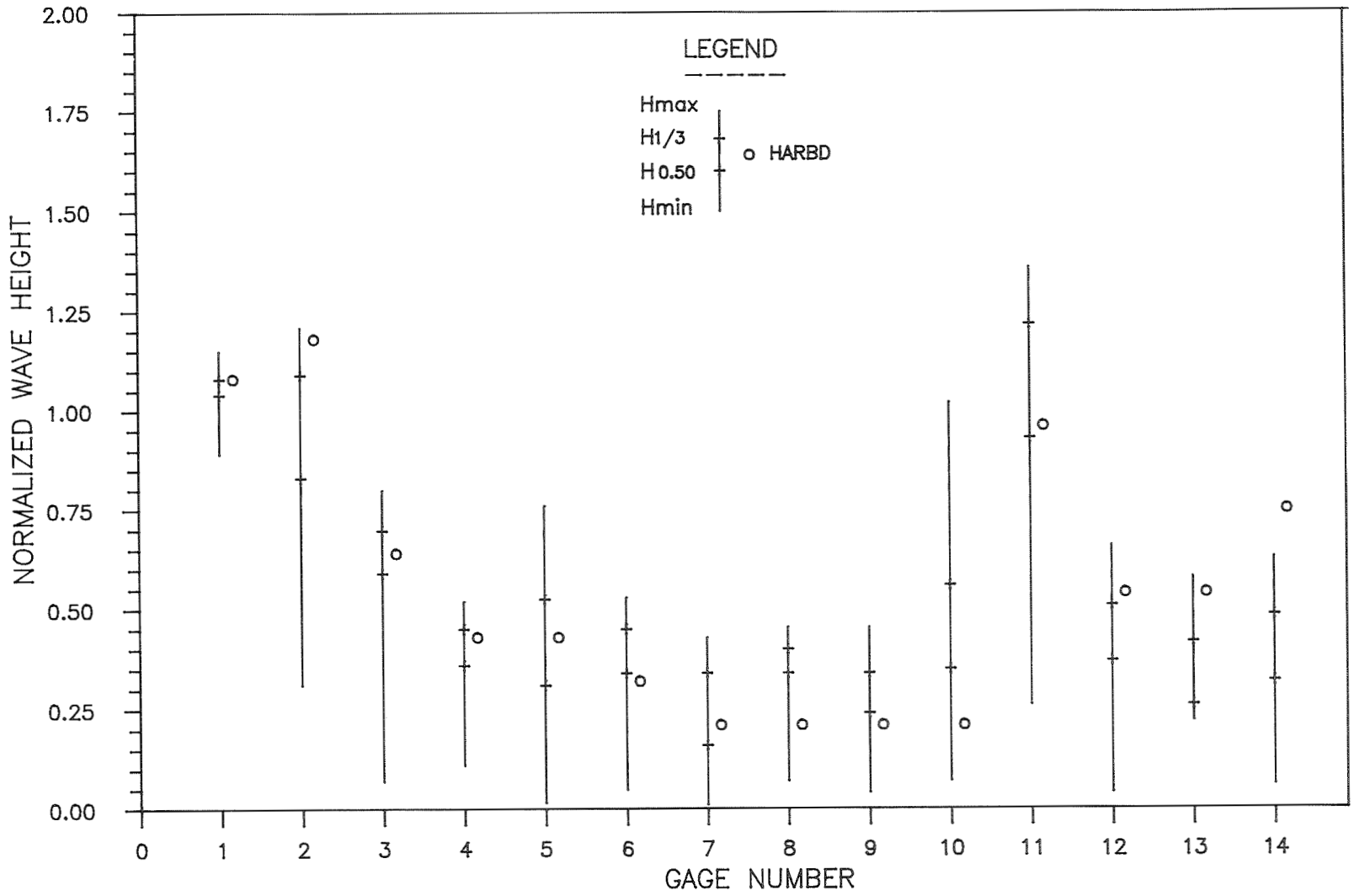

COMPARISON OF HYDRAULIC AND HARBD WAVE HEIGHTS FOR RUN NO. 3

PLATE 3

PLATE 4

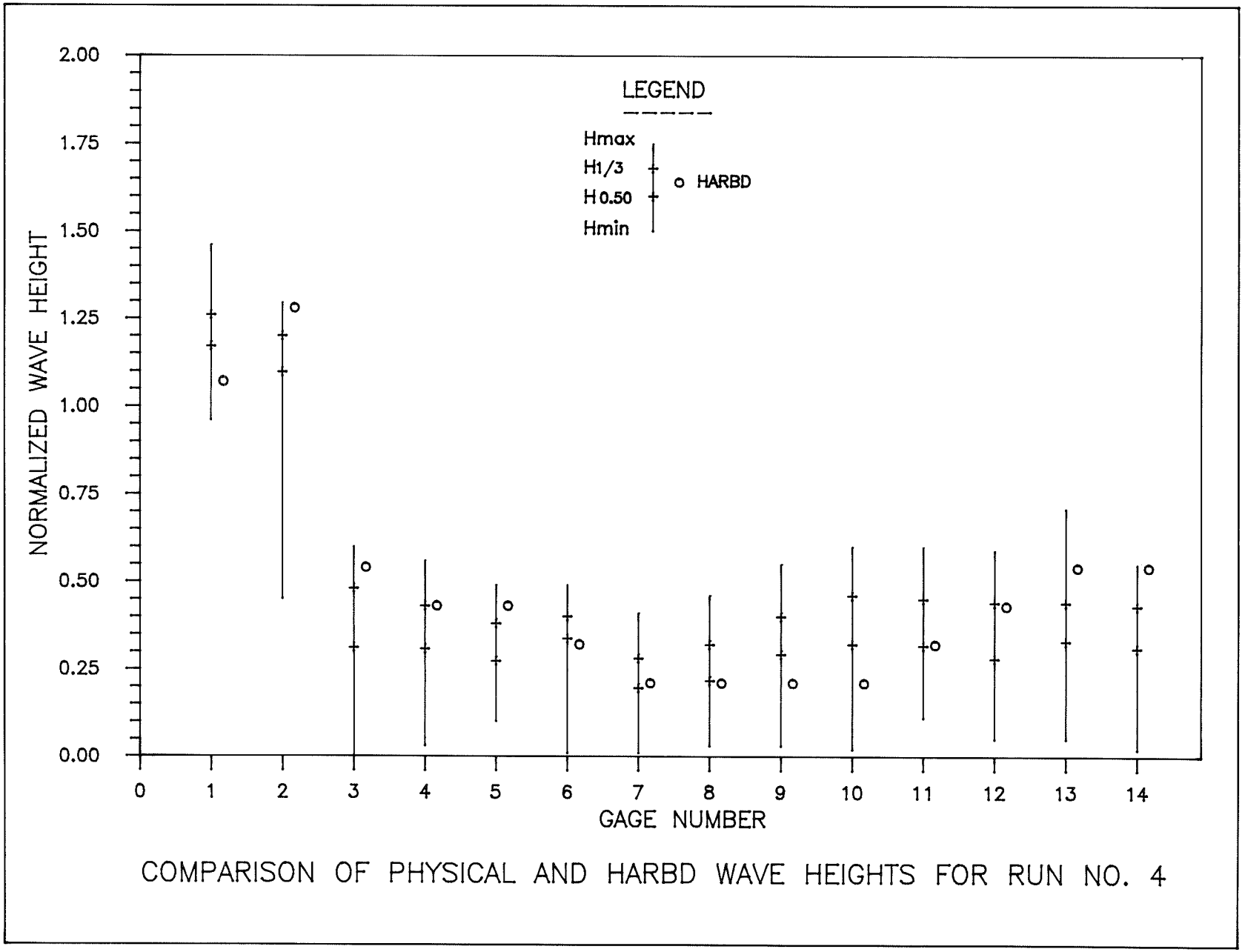

COMPARISON OF PHYSICAL AND HARBD WAVE HEIGHTS FOR RUN NO. 4

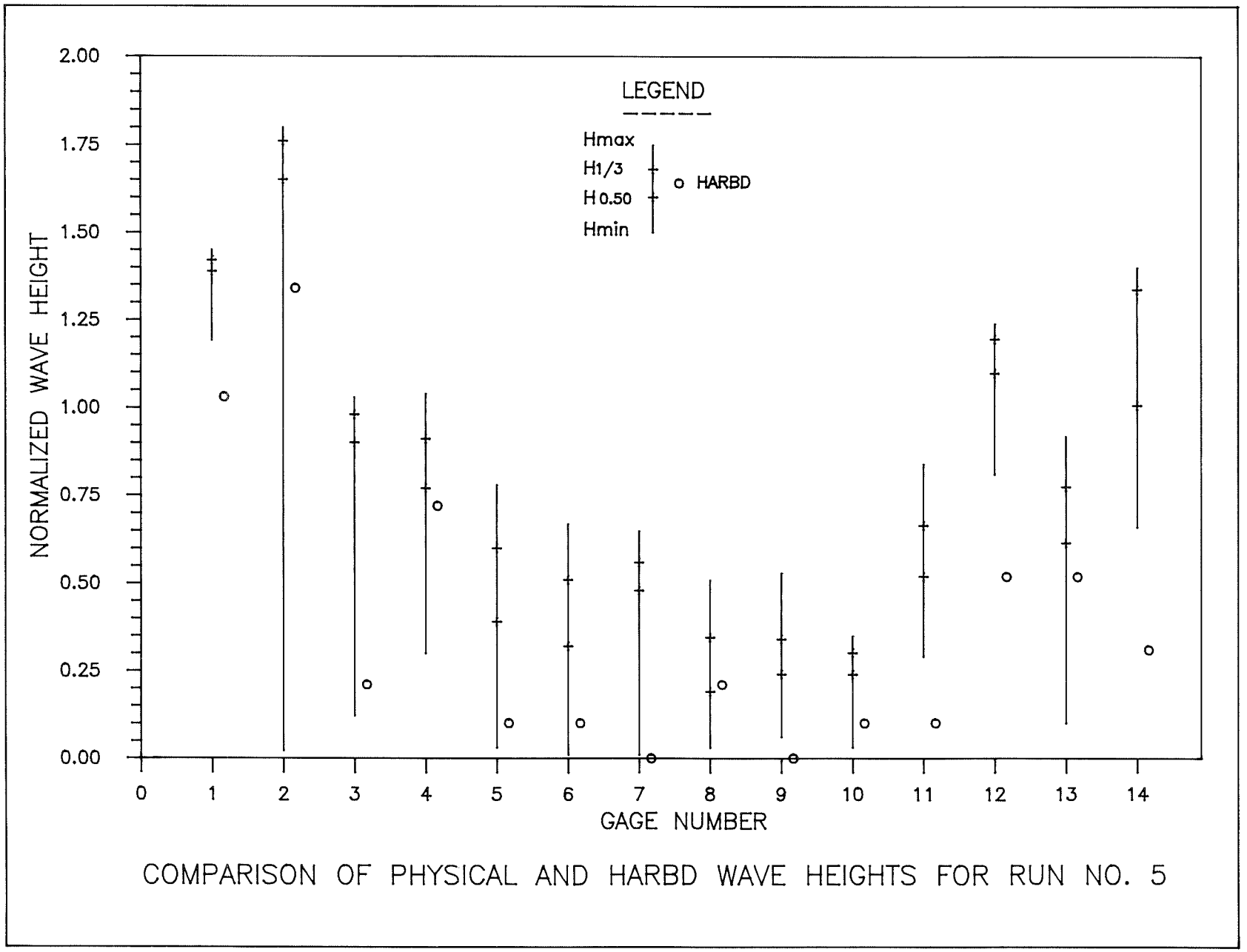

COMPARISON OF PHYSICAL AND HARBD WAVE HEIGHTS FOR RUN NO. 5

PLATE 5

PLATE 6

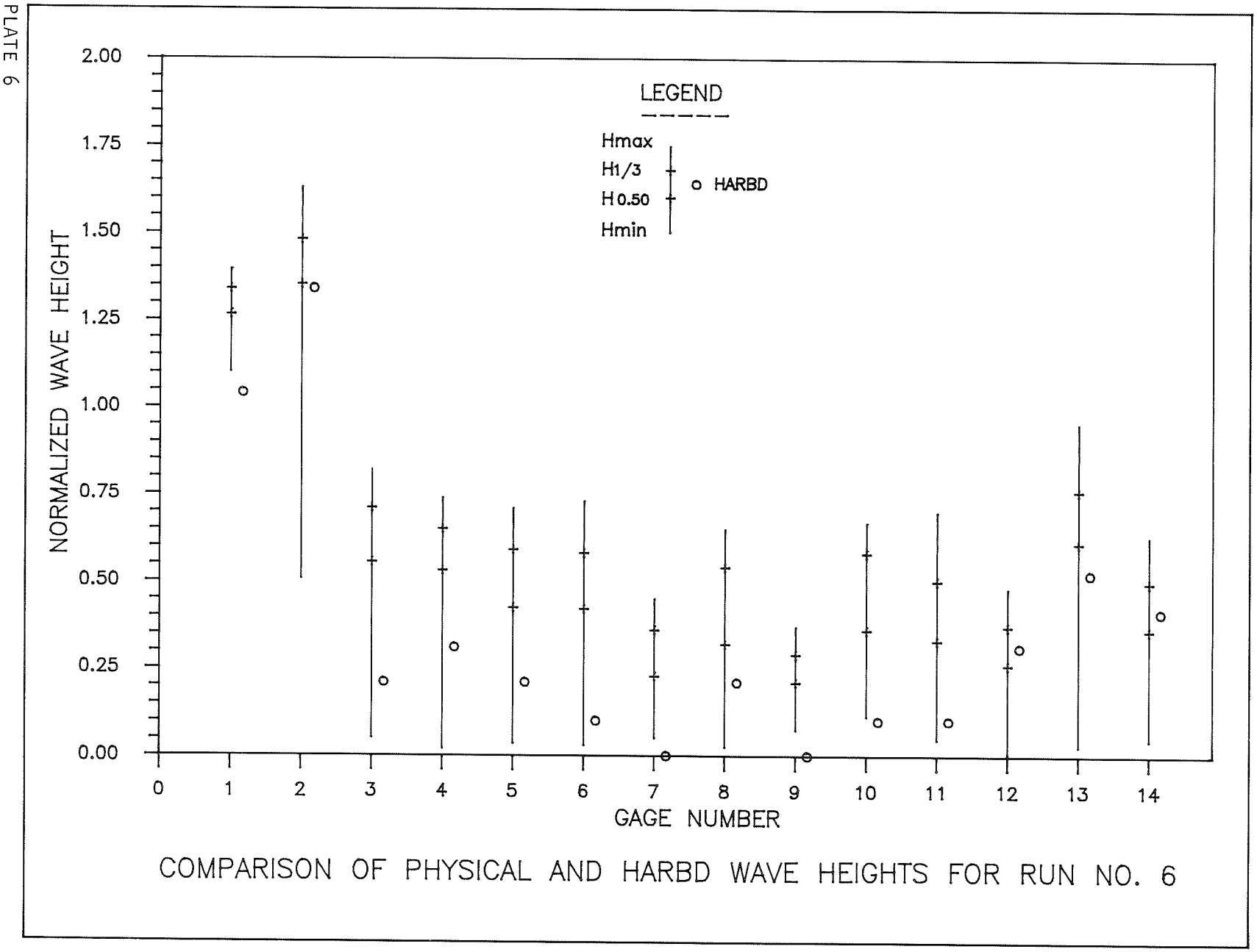

COMPARISON OF PHYSICAL AND HARBD WAVE HEIGHTS FOR RUN NO. 6

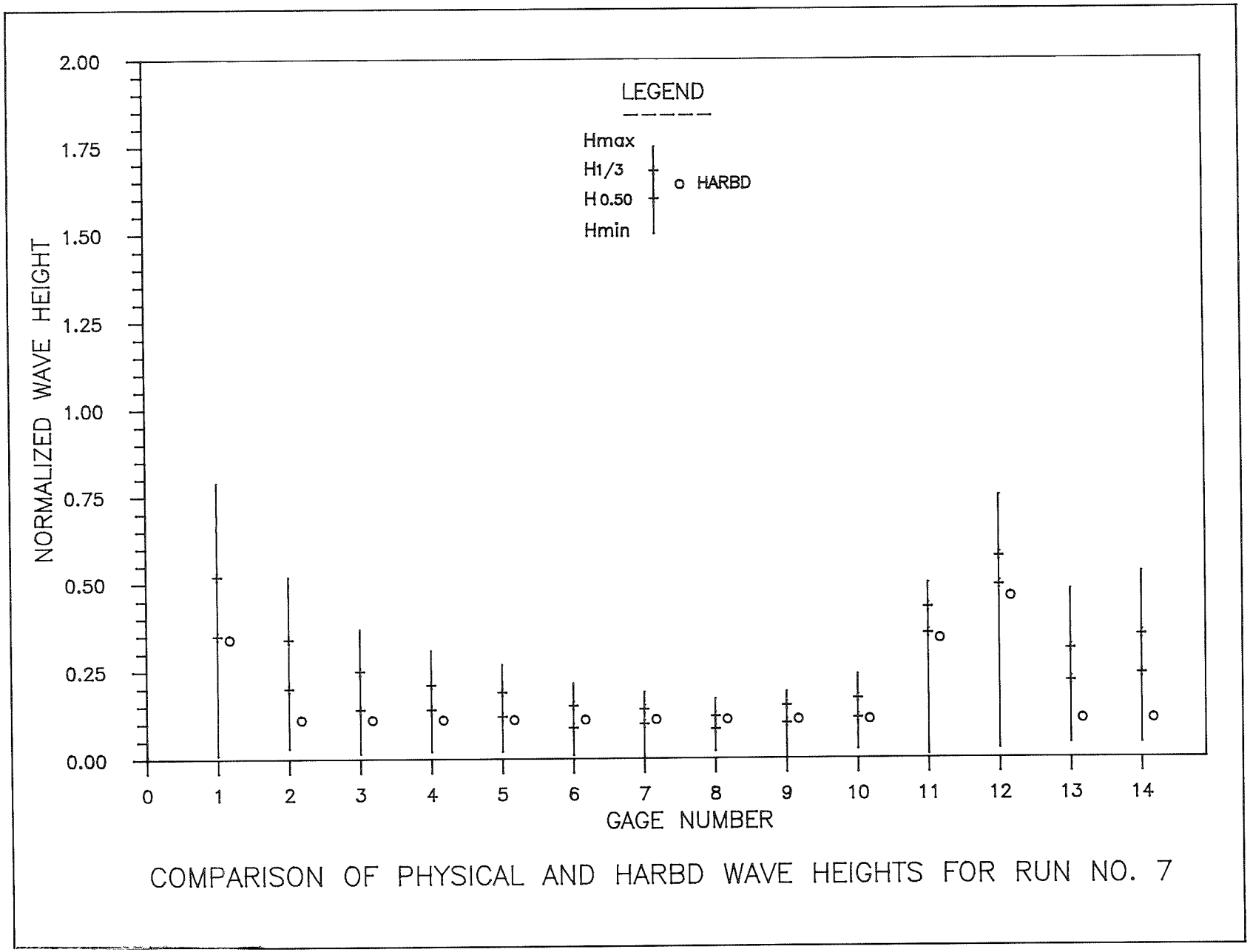

COMPARISON OF PHYSICAL AND HARBD WAVE HEIGHTS FOR RUN NO. 7

PLATE 7

PLATE 8

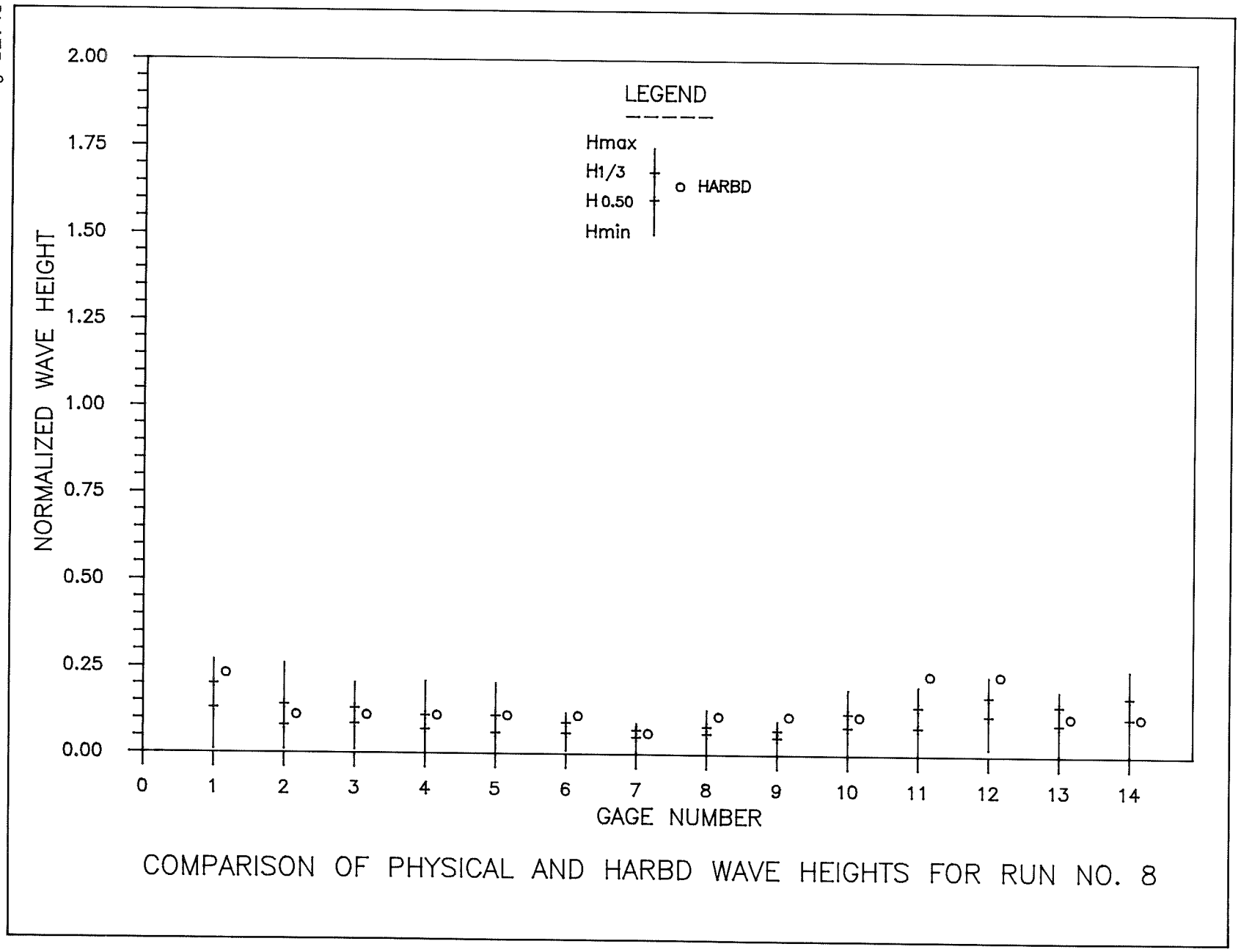

COMPARISON OF PHYSICAL AND HARBD WAVE HEIGHTS FOR RUN NO. 8

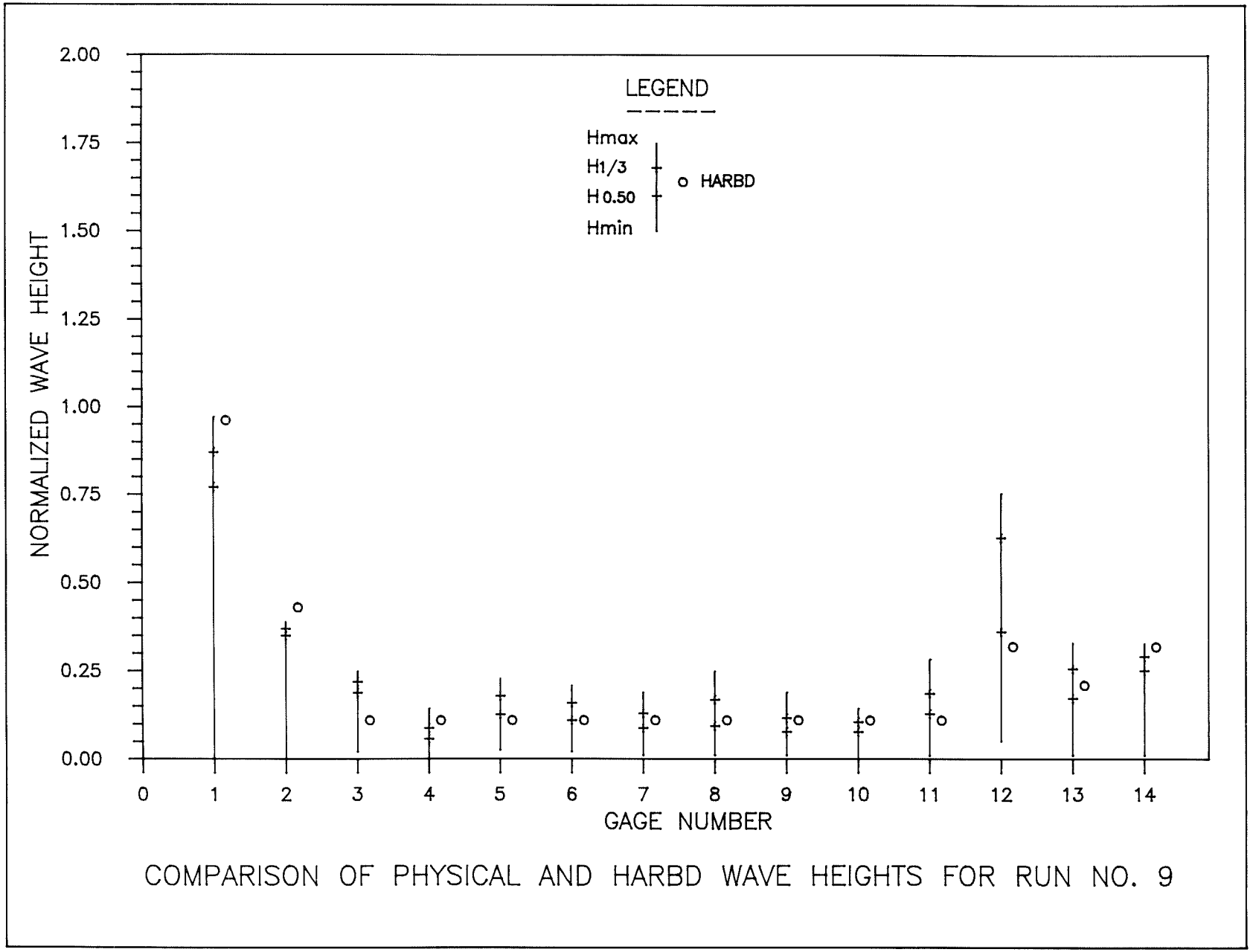

COMPARISON OF PHYSICAL AND HARBD WAVE HEIGHTS FOR RUN NO. 9

PLATE 9

PLATE 10

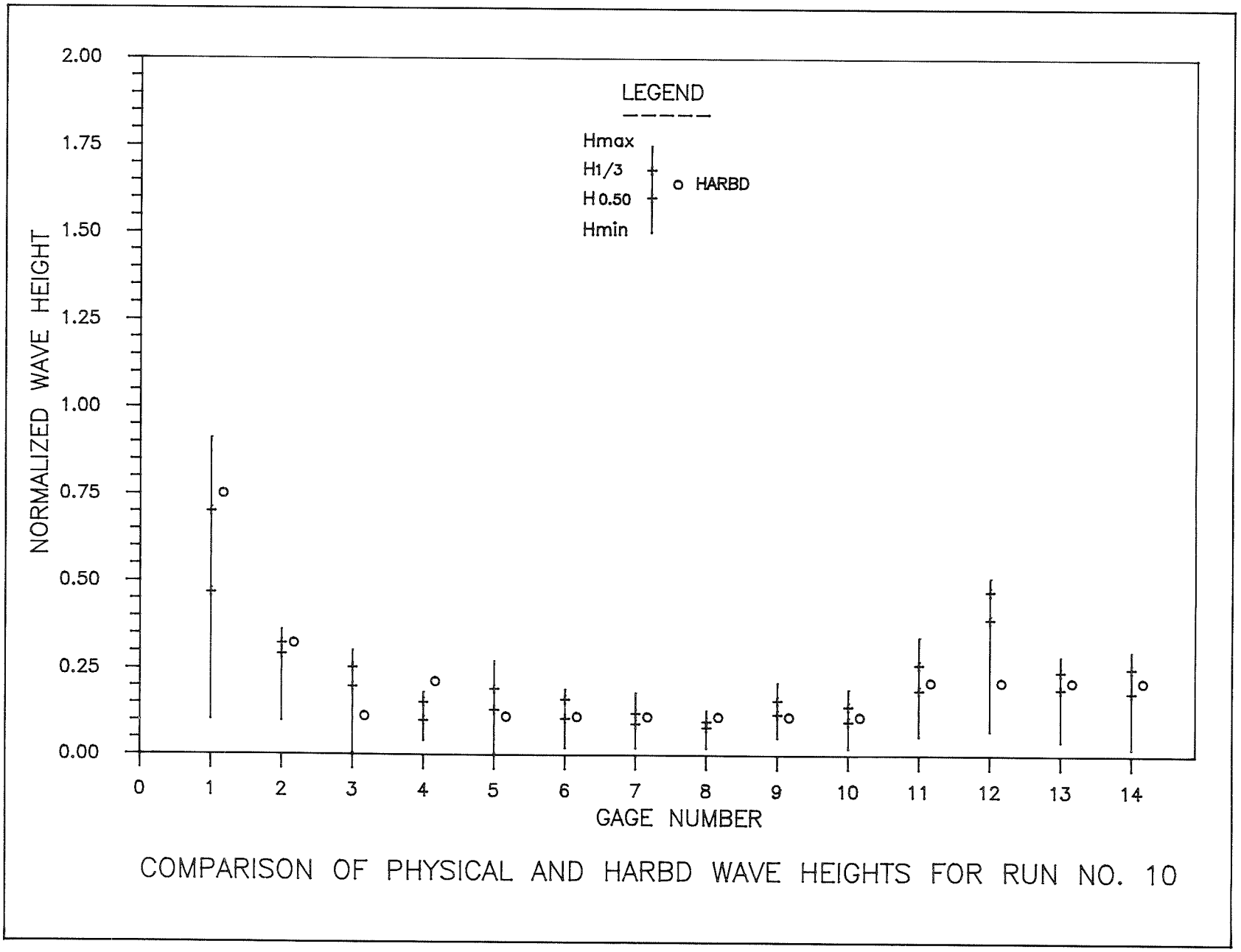

COMPARISON OF PHYSICAL AND HARBD WAVE HEIGHTS FOR RUN NO. 10

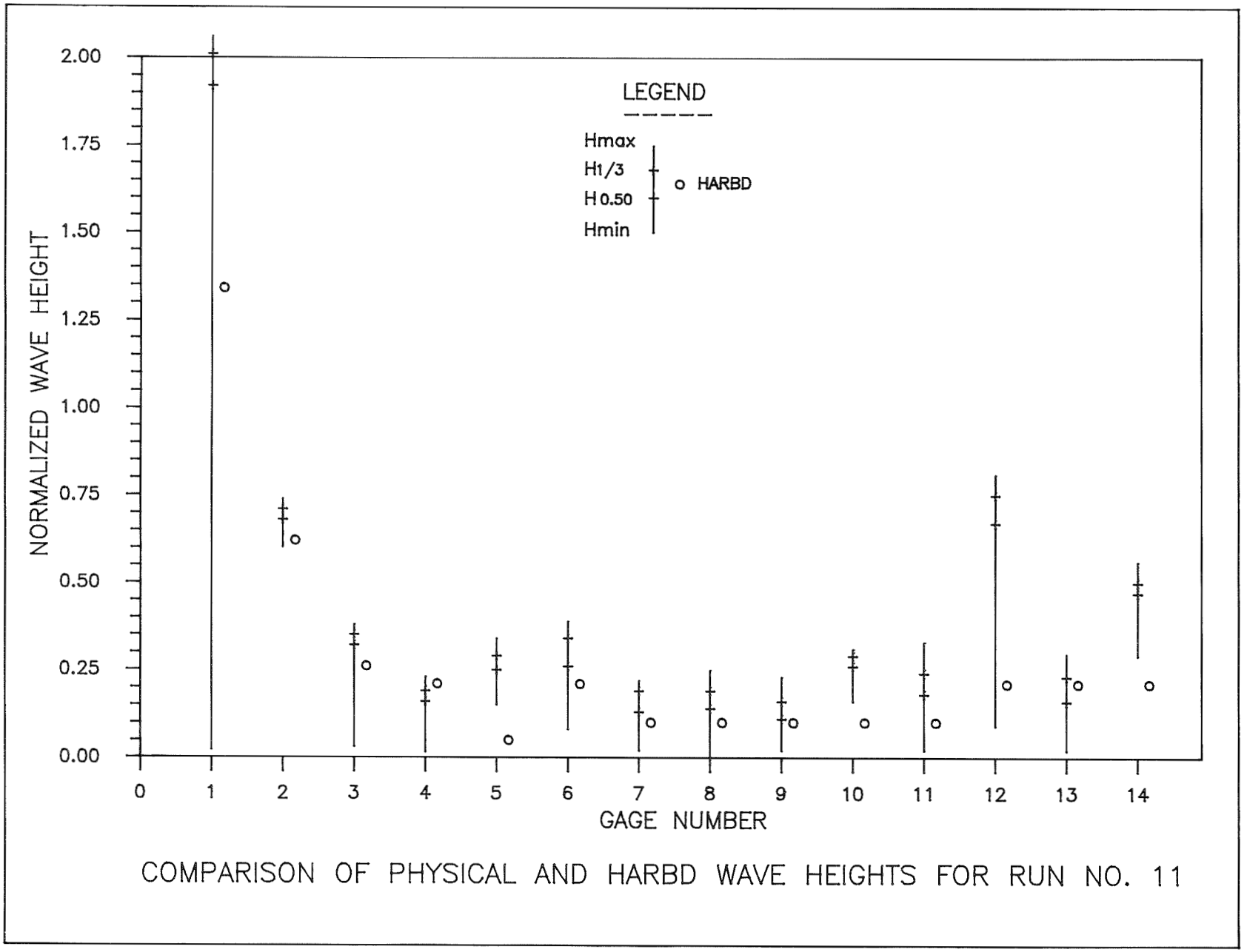

COMPARISON OF PHYSICAL AND HARBD WAVE HEIGHTS FOR RUN NO. 11

PLATE 11

PLATE 12

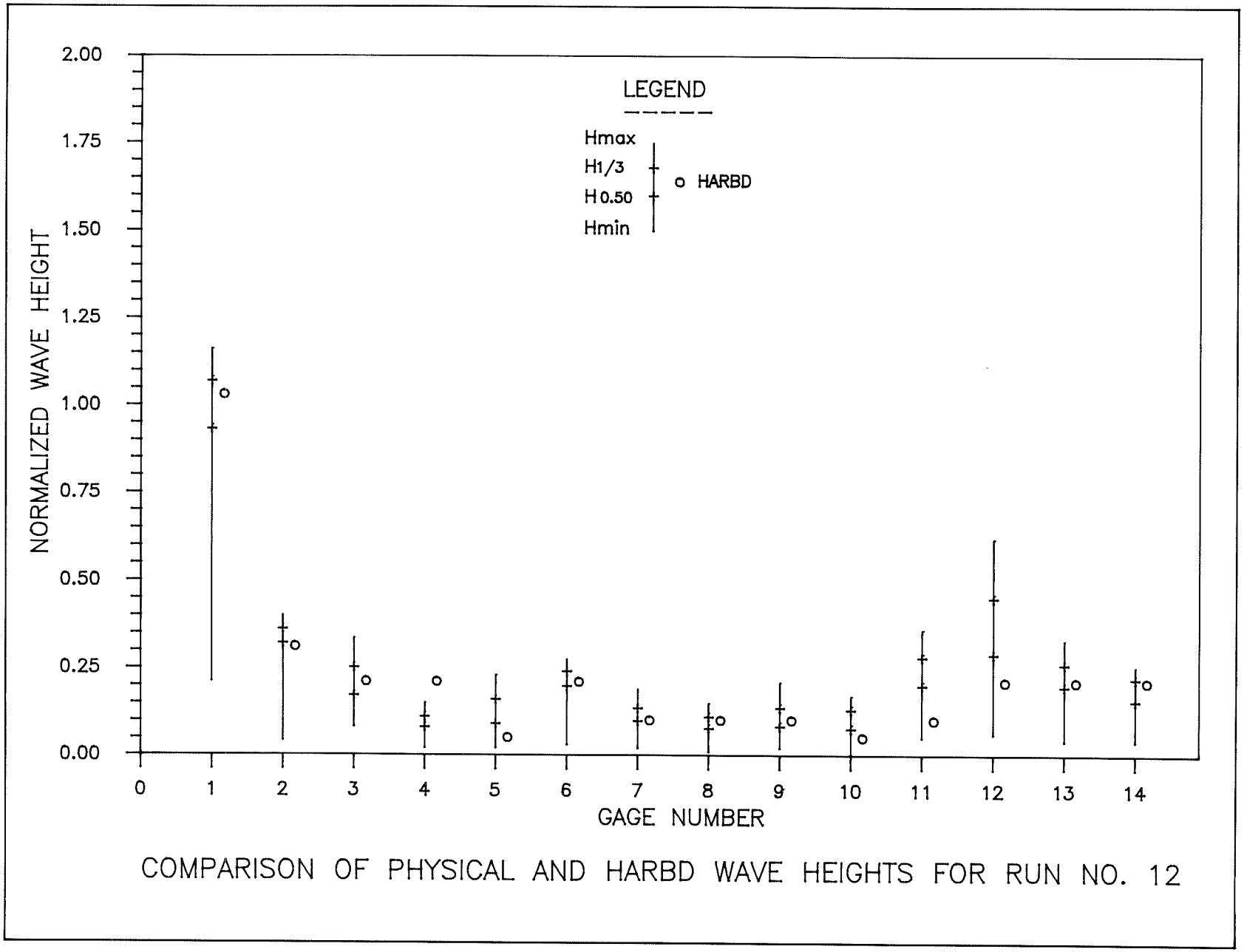

COMPARISON OF PHYSICAL AND HARBD WAVE HEIGHTS FOR RUN NO. 12

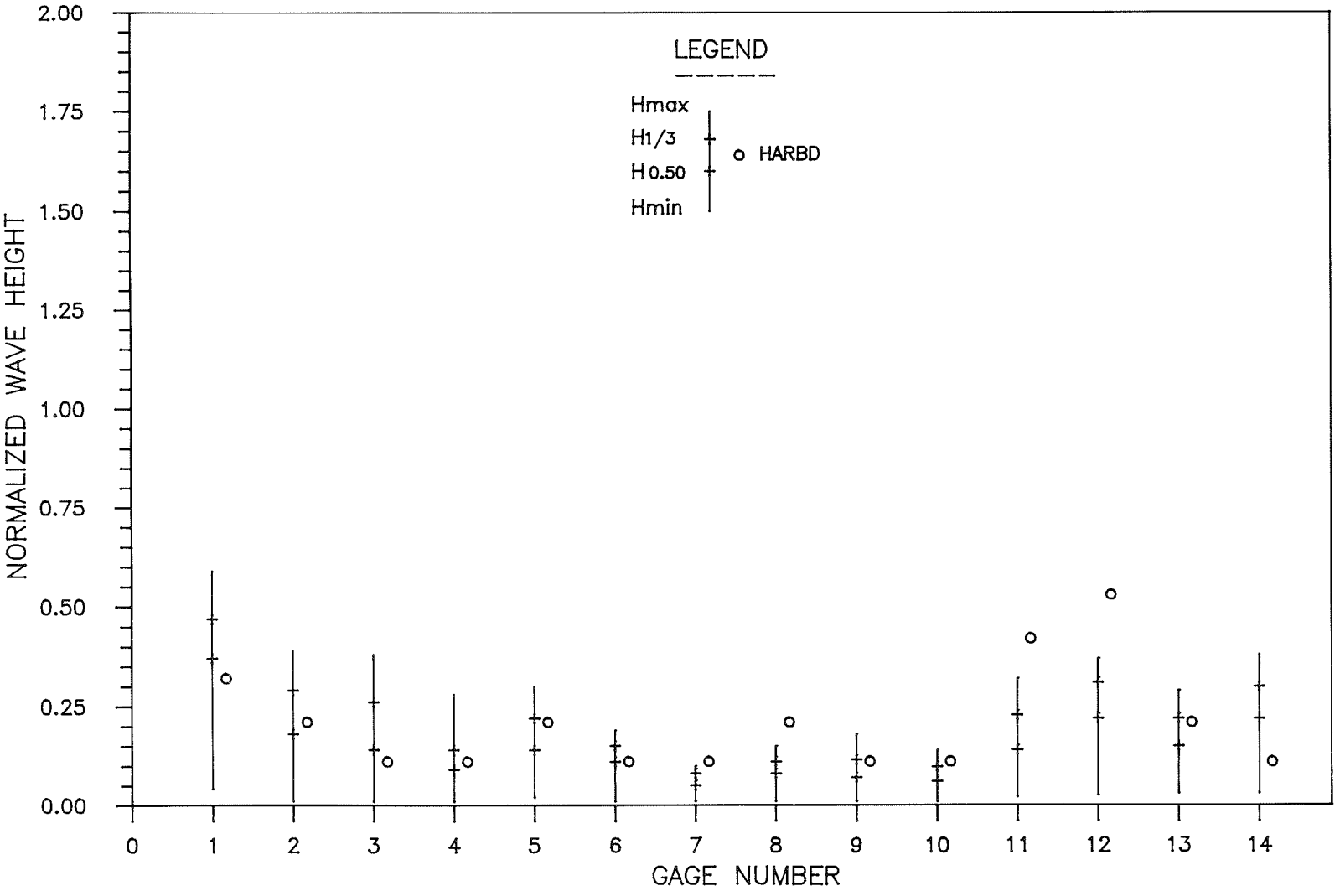

COMPARISON OF PHYSICAL AND HARBD WAVE HEIGHTS FOR RUN NO. 13

PLATE 13

PLATE 14

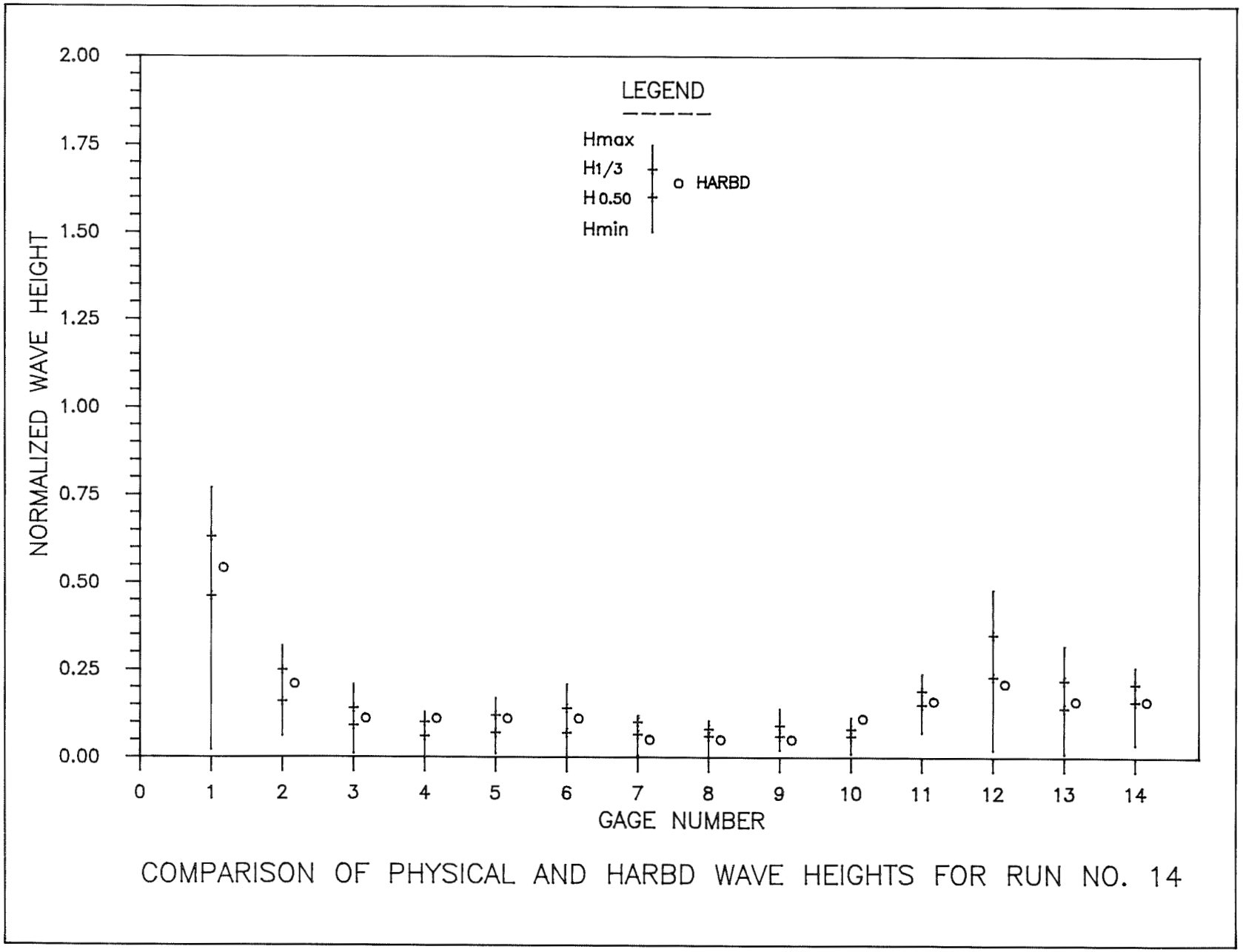

COMPARISON OF PHYSICAL AND HARBD WAVE HEIGHTS FOR RUN NO. 14

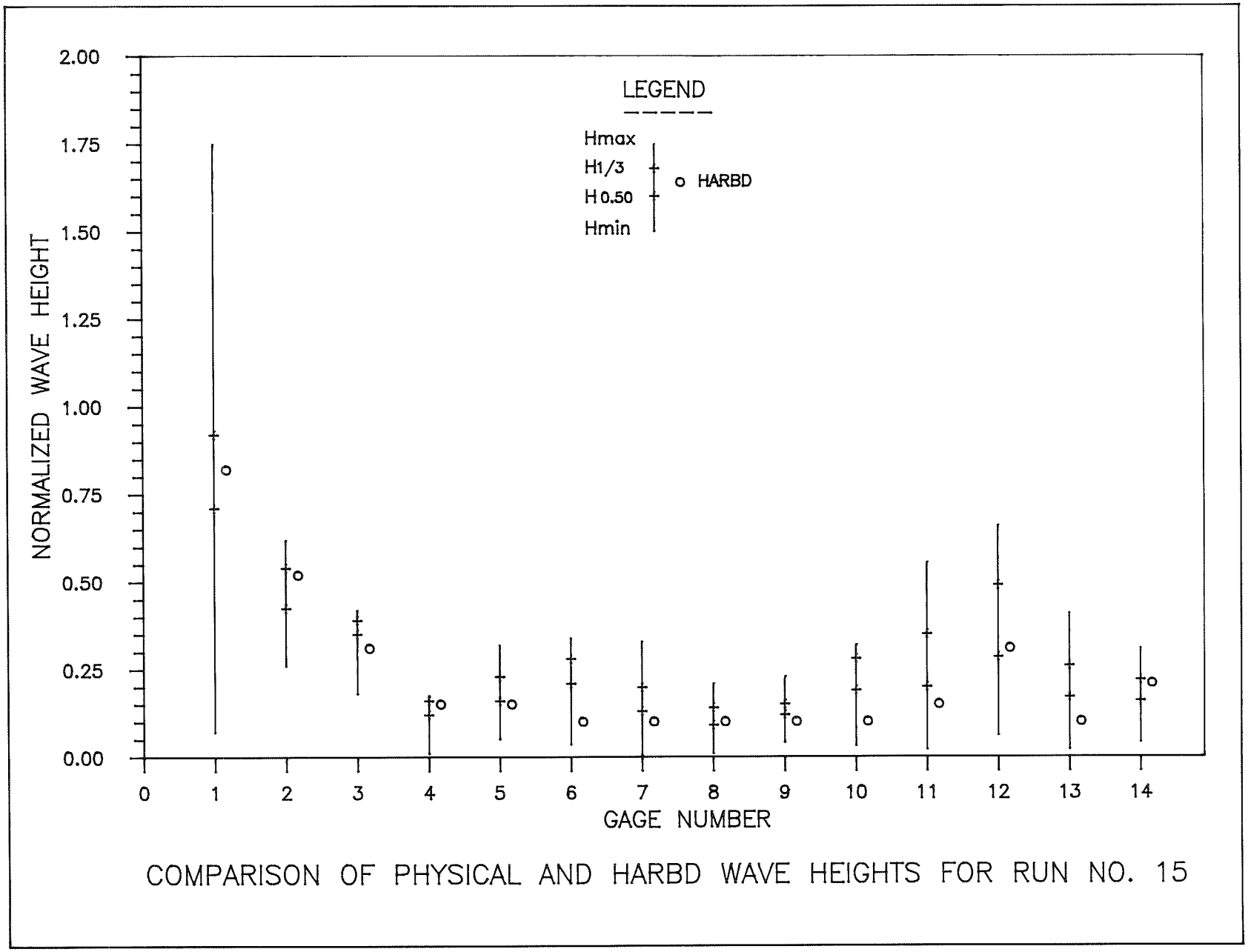

COMPARISON OF PHYSICAL AND HARBD WAVE HEIGHTS FOR RUN NO. 15

PLATE 15

PLATE 16

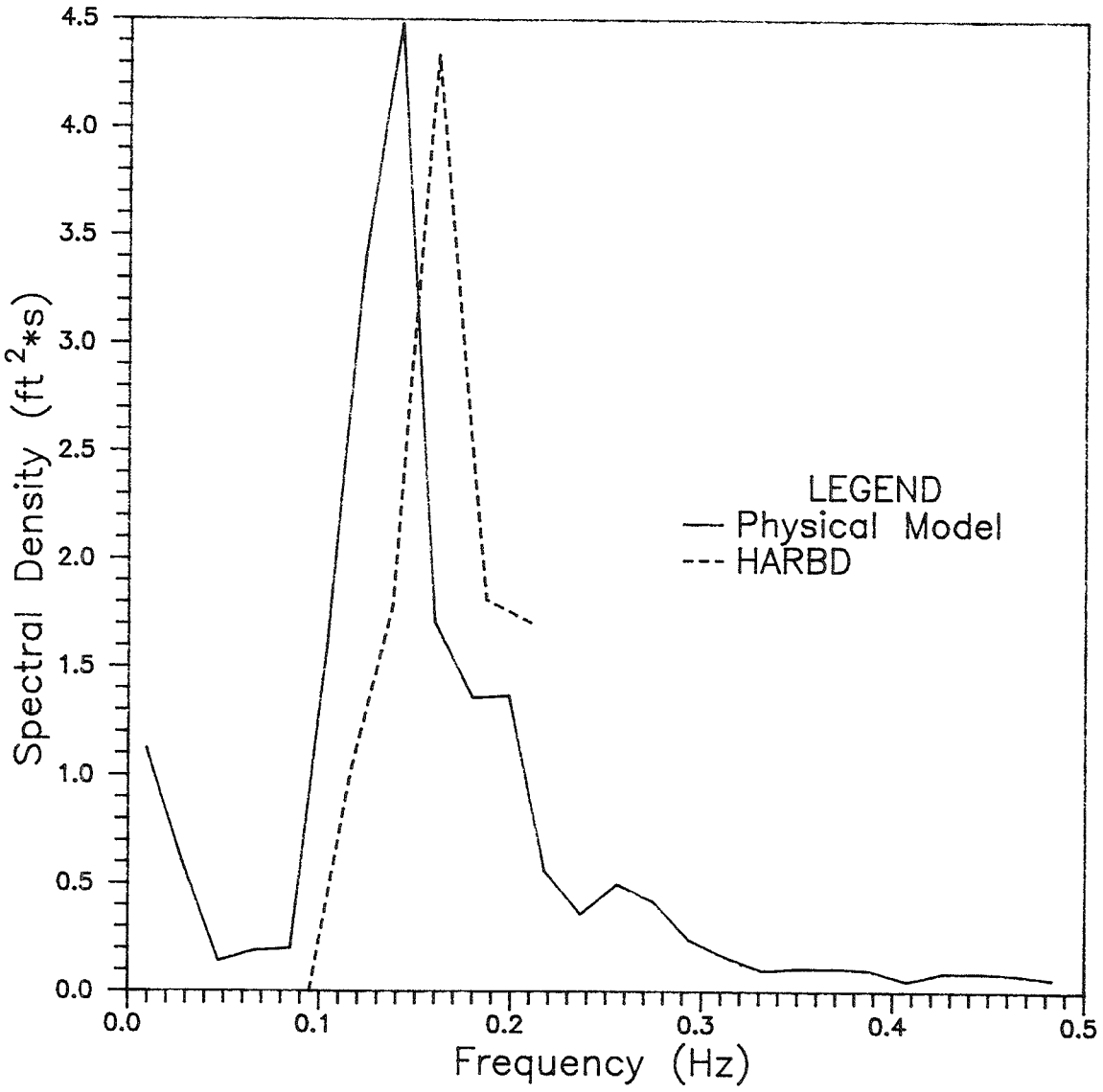

Frequency Spectrum at Gage 1

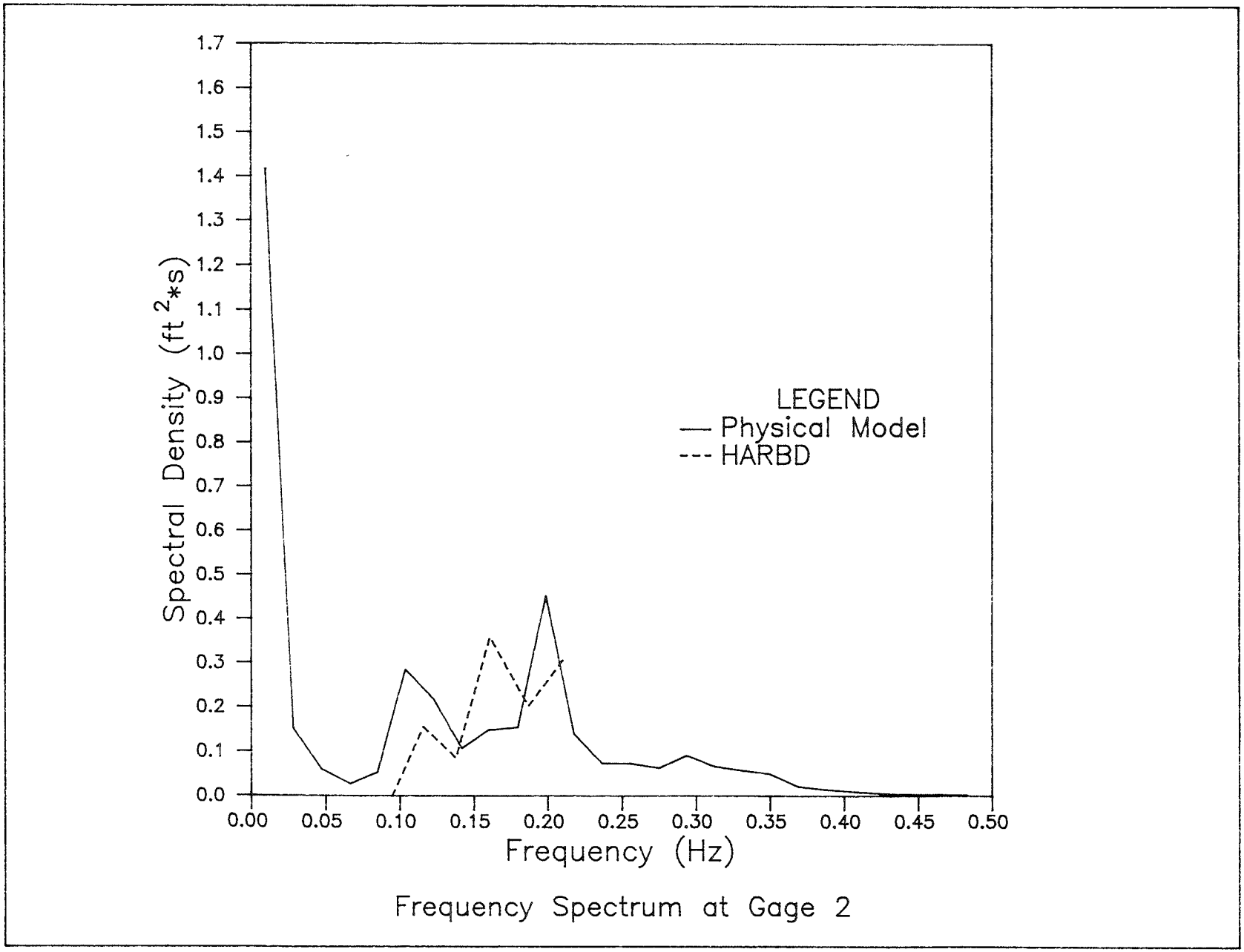

Frequency Spectrum at Gage 2

PLATE 17

PLATE 18

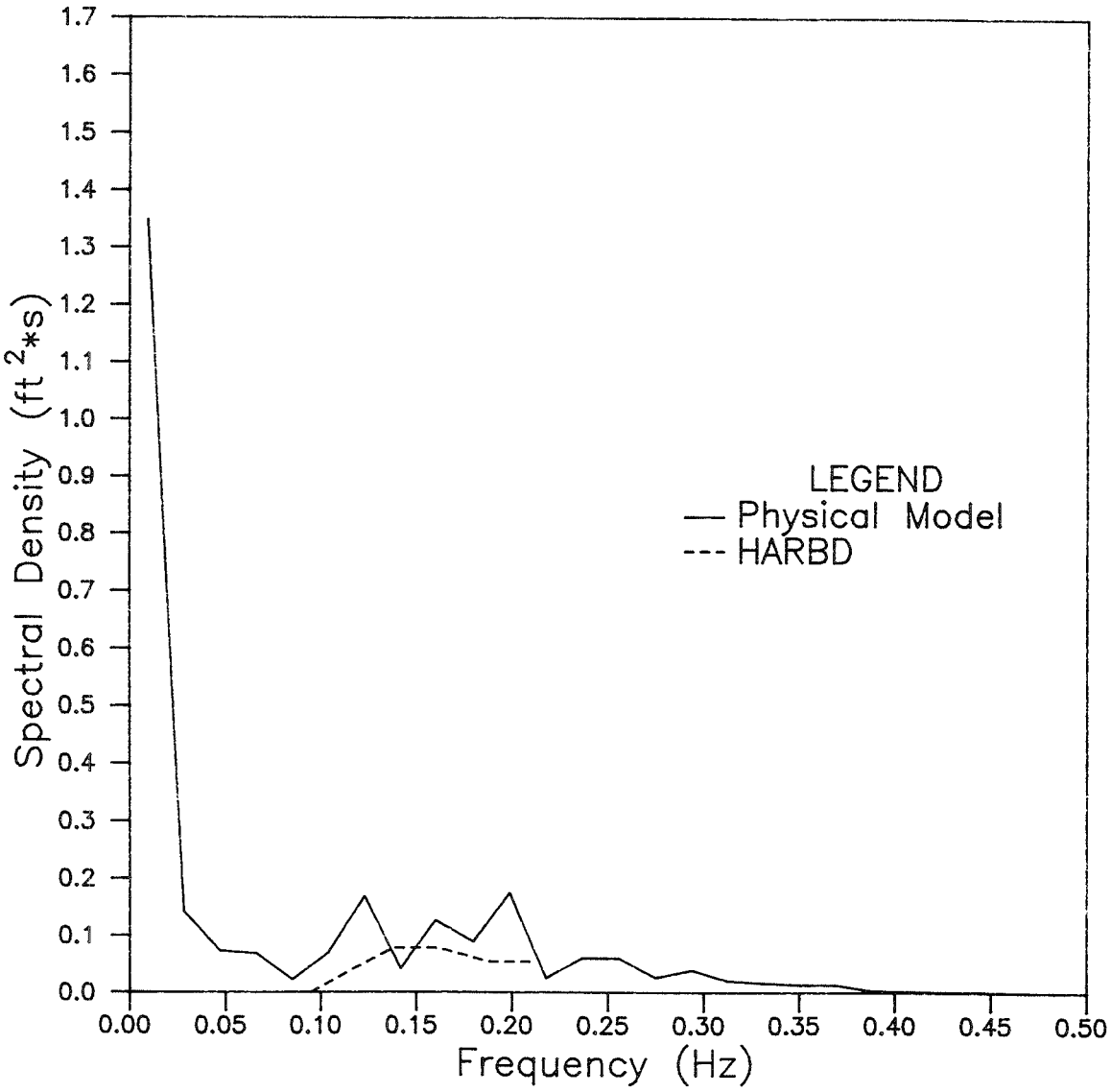

Frequency Spectrum at Gage 3

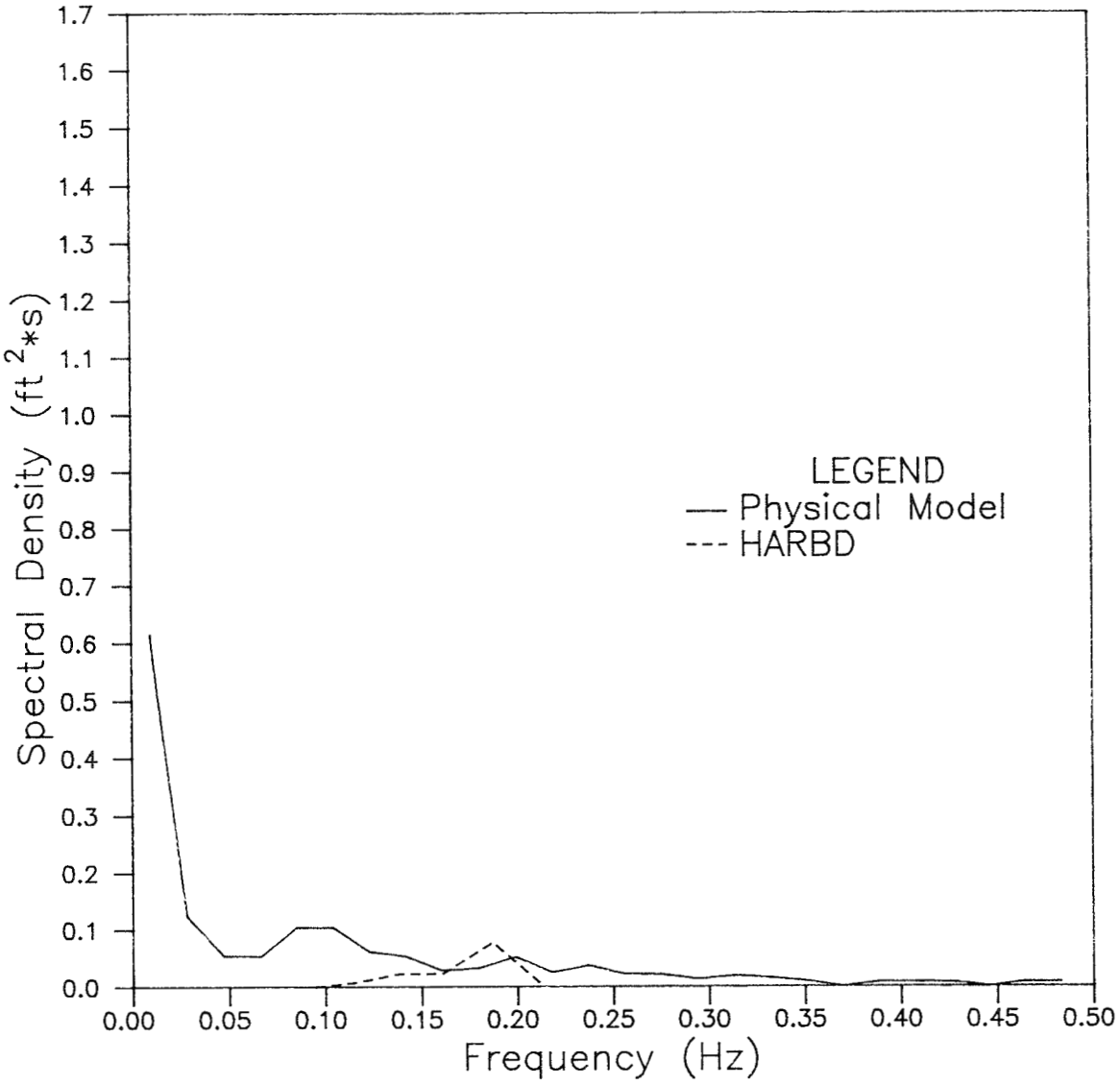

Frequency Spectrum at Gage 4

PLATE 19

PLATE 20

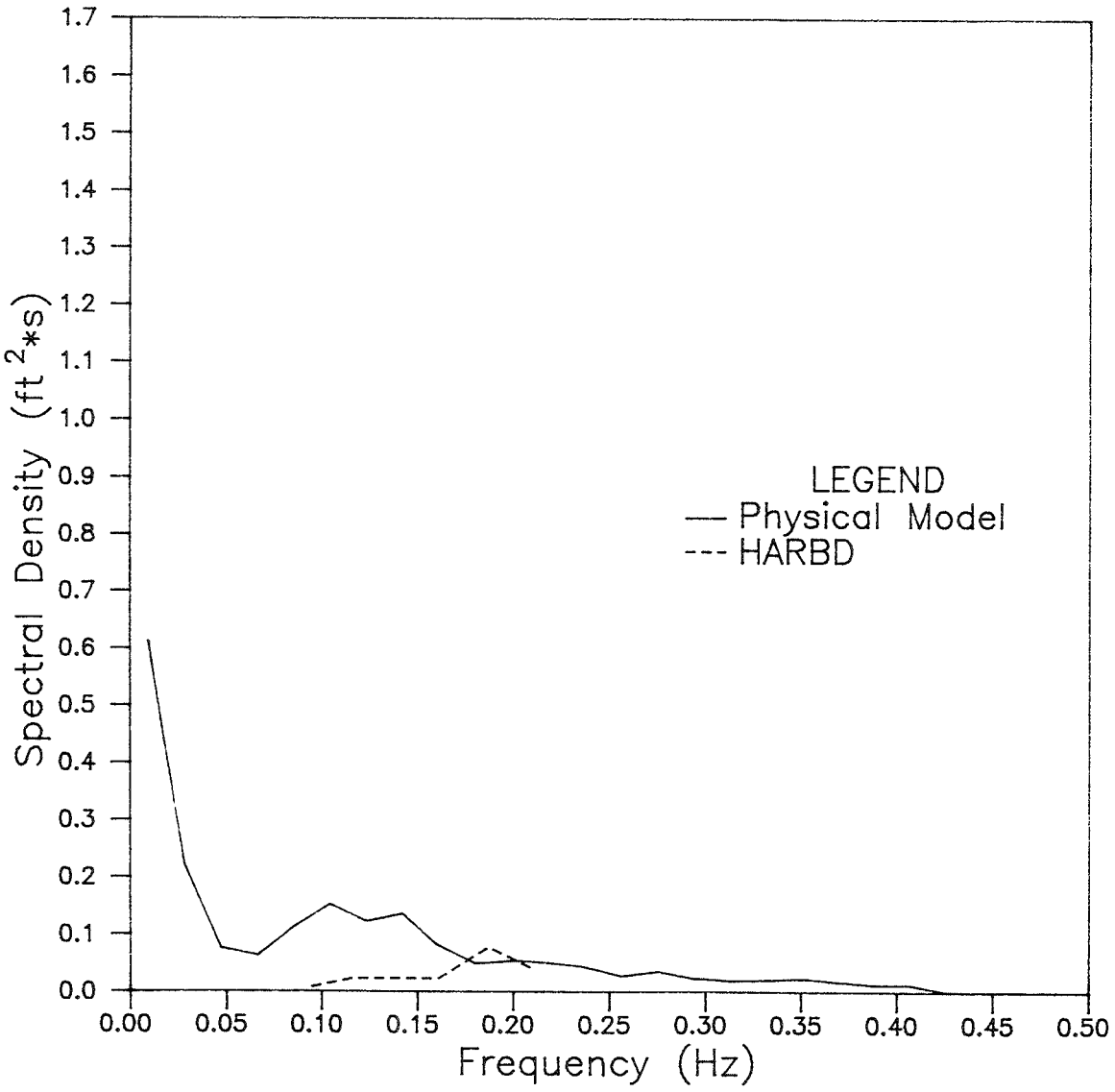

Frequency Spectrum at Gage 5

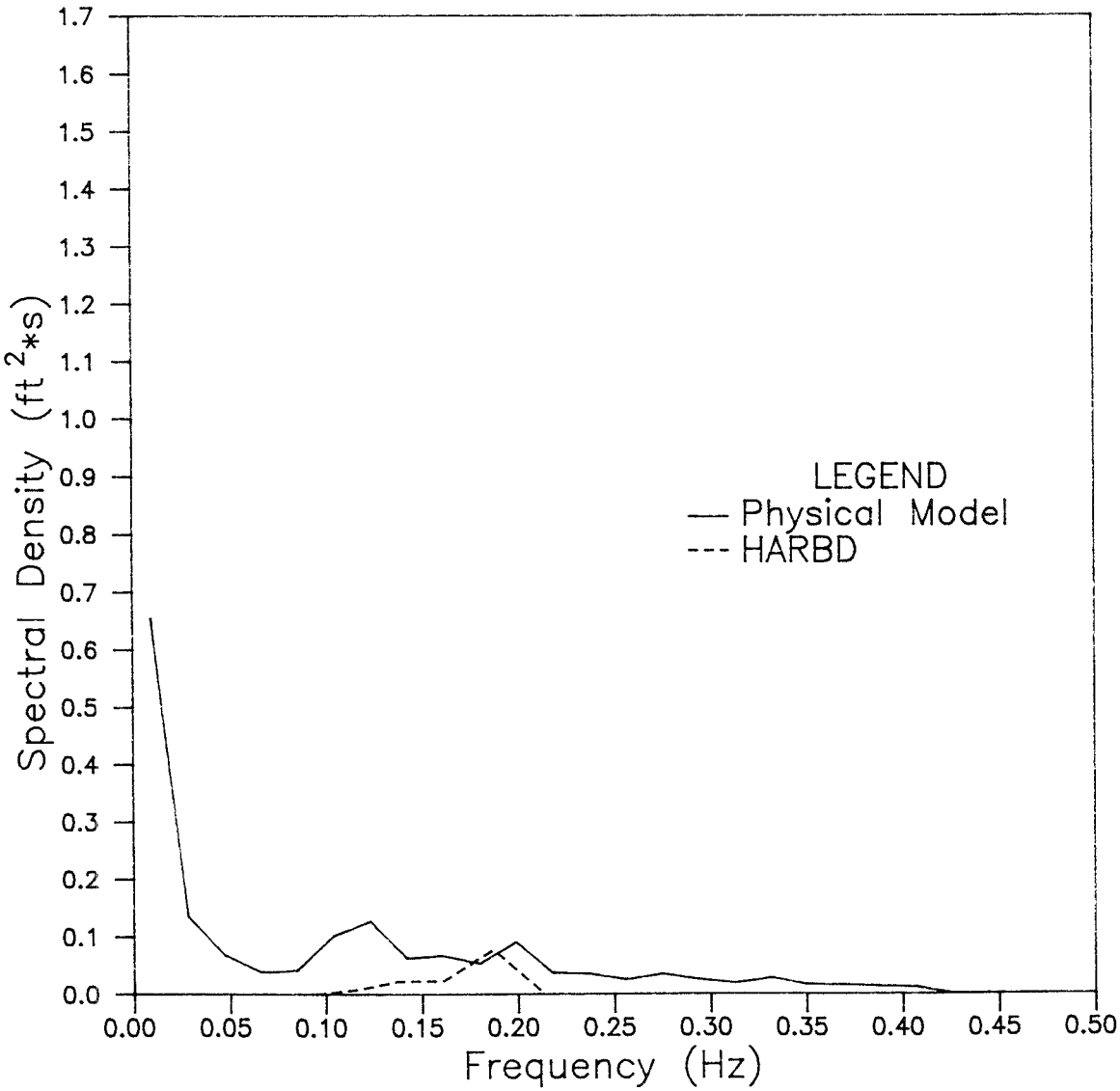

Frequency Spectrum at Gage 6

PLATE 21

PLATE 22

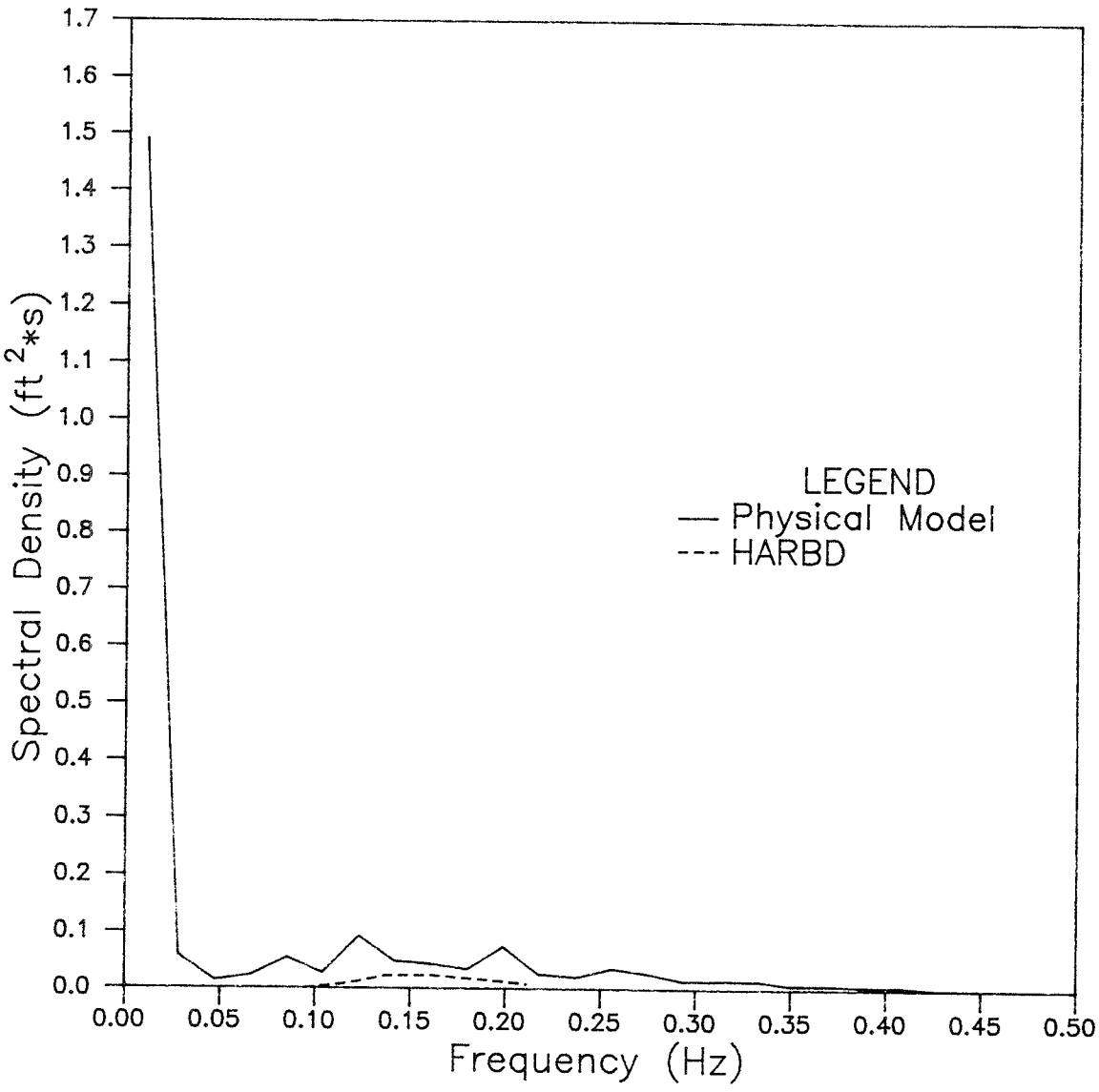

Frequency Spectrum at Gage 7

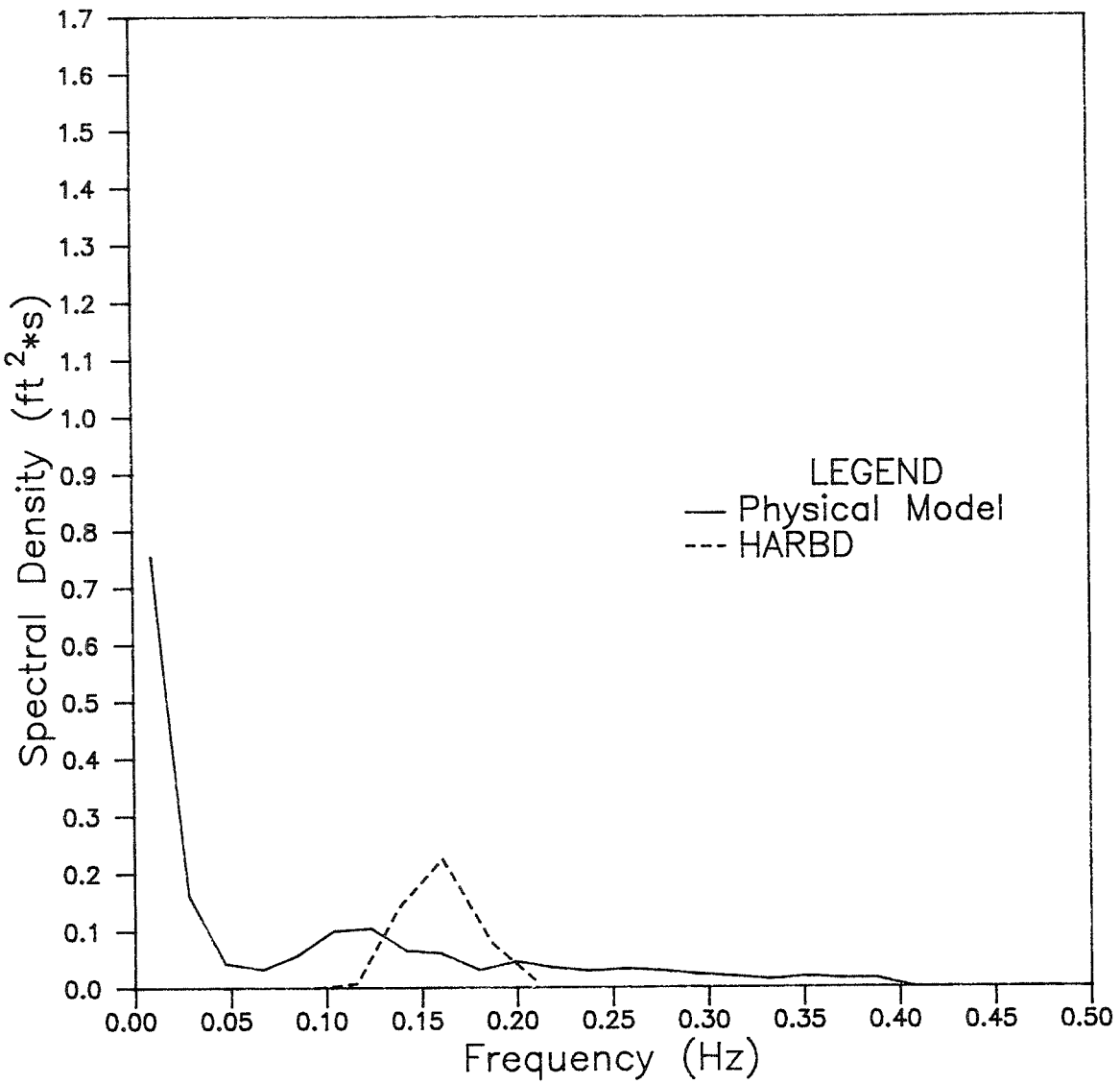

Frequency Spectrum at Gage 8

PLATE 23

PLATE 24

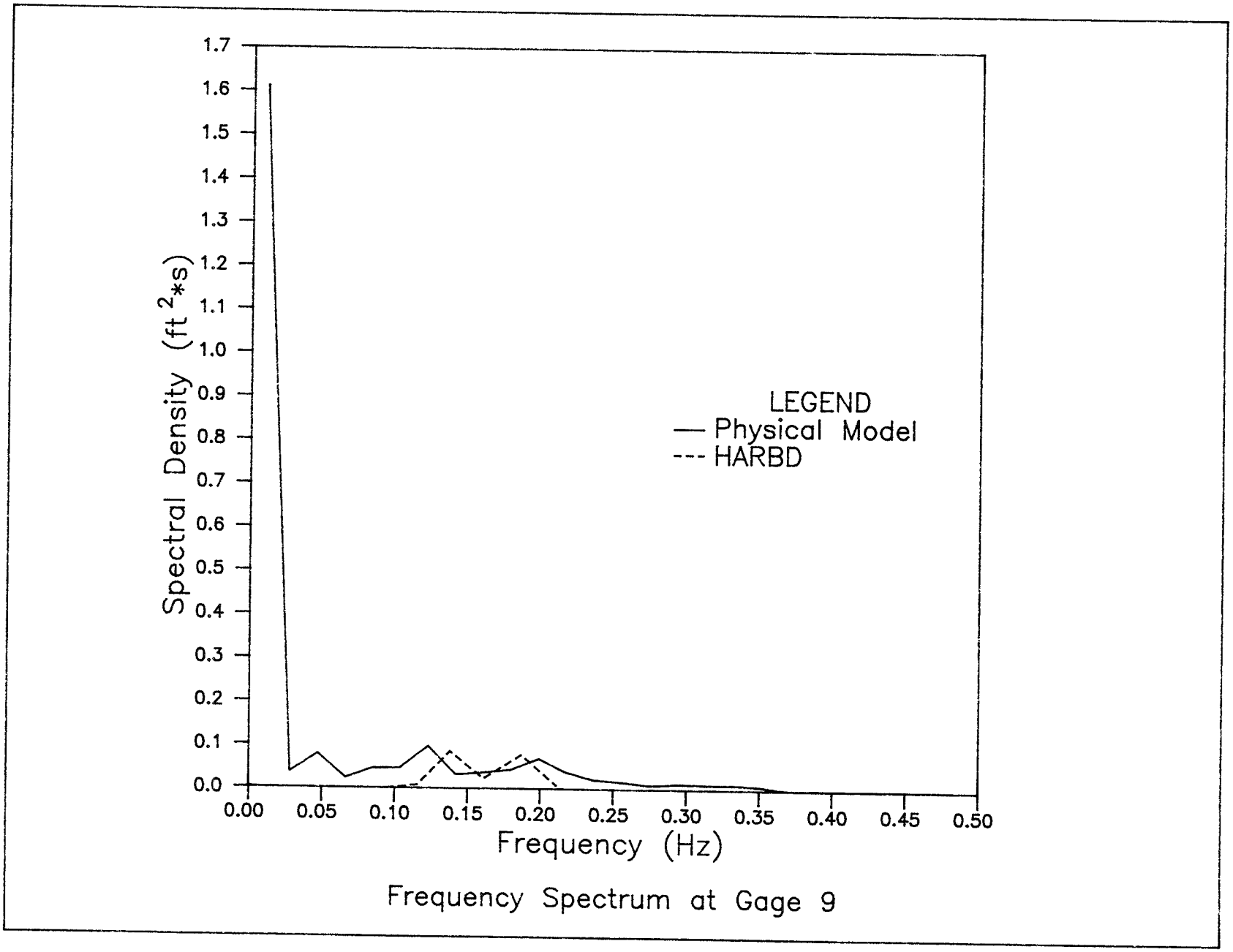

Frequency Spectrum at Gage 9

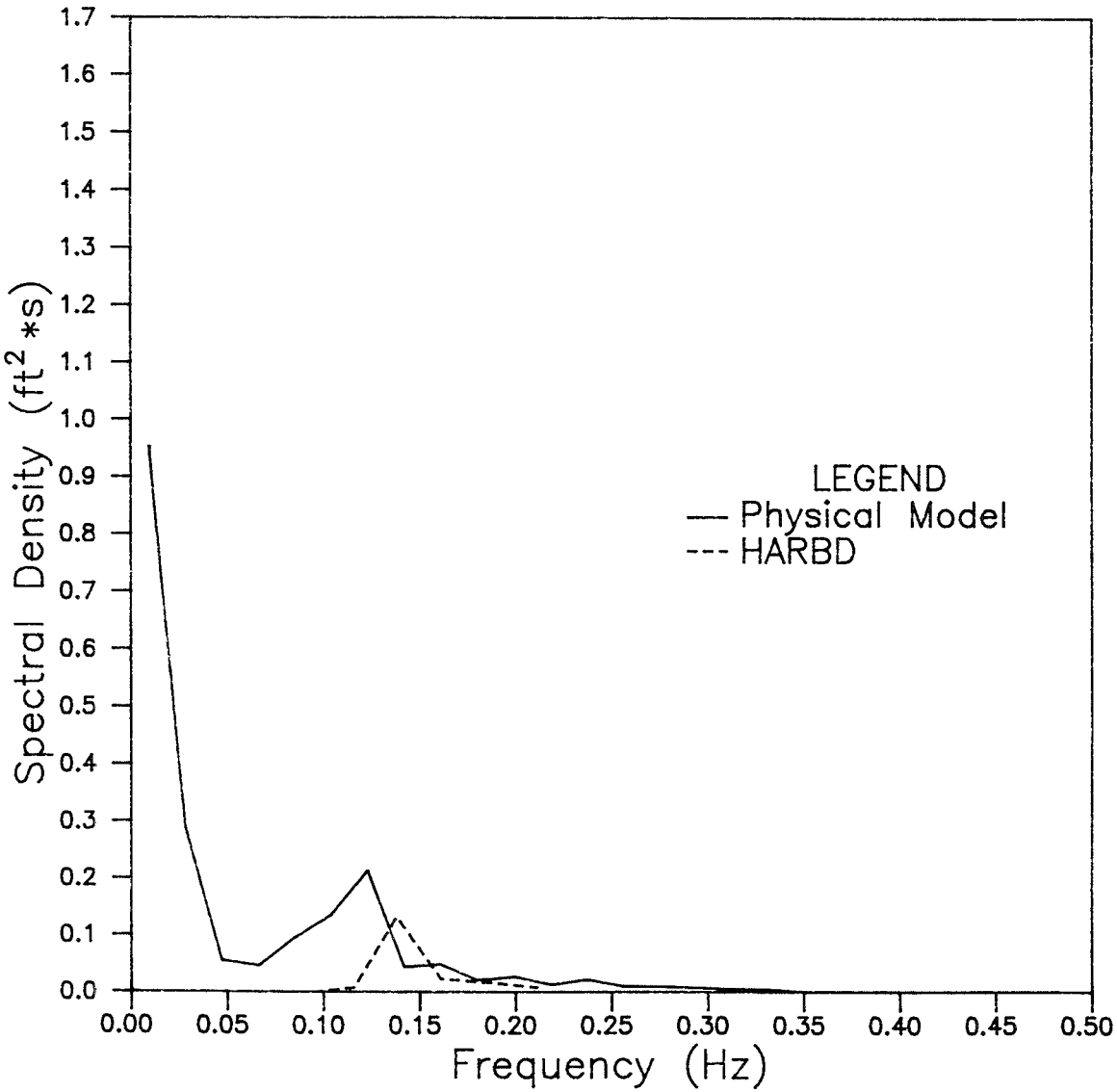

Frequency Spectrum at Gage 10

PLATE 25

PLATE 26

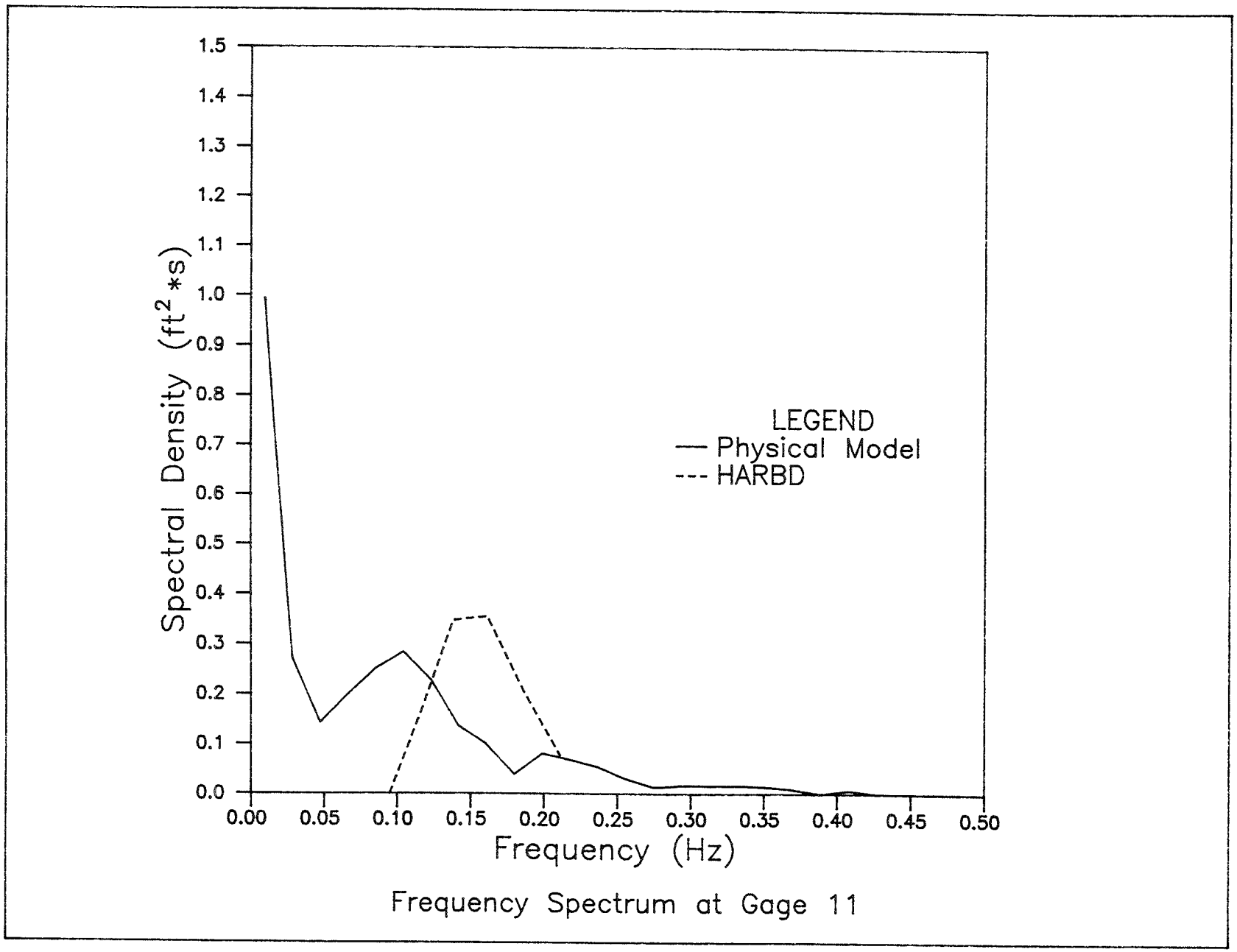

Frequency Spectrum at Gage 11

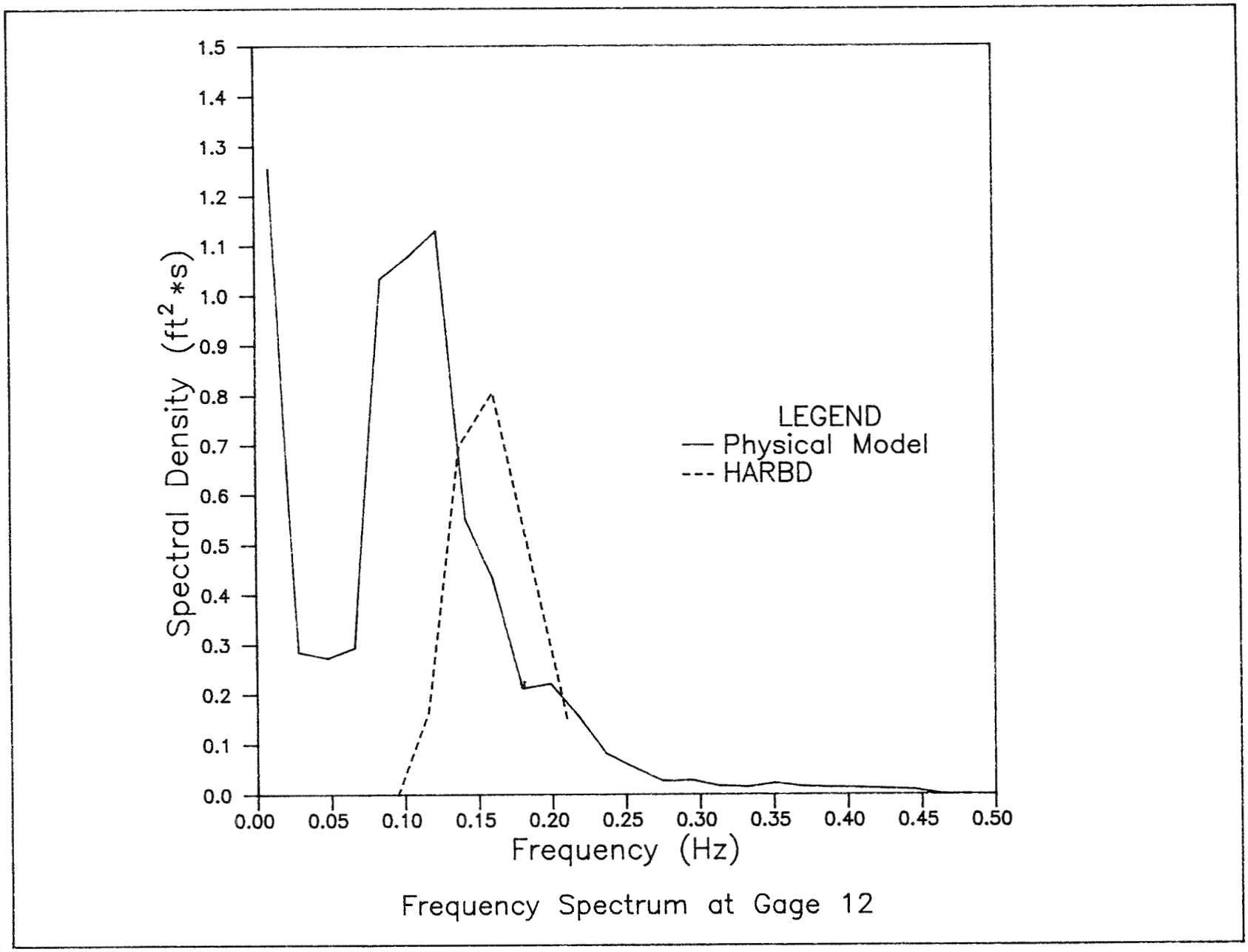

Frequency Spectrum at Gage 12

PLATE 27

PLATE 28

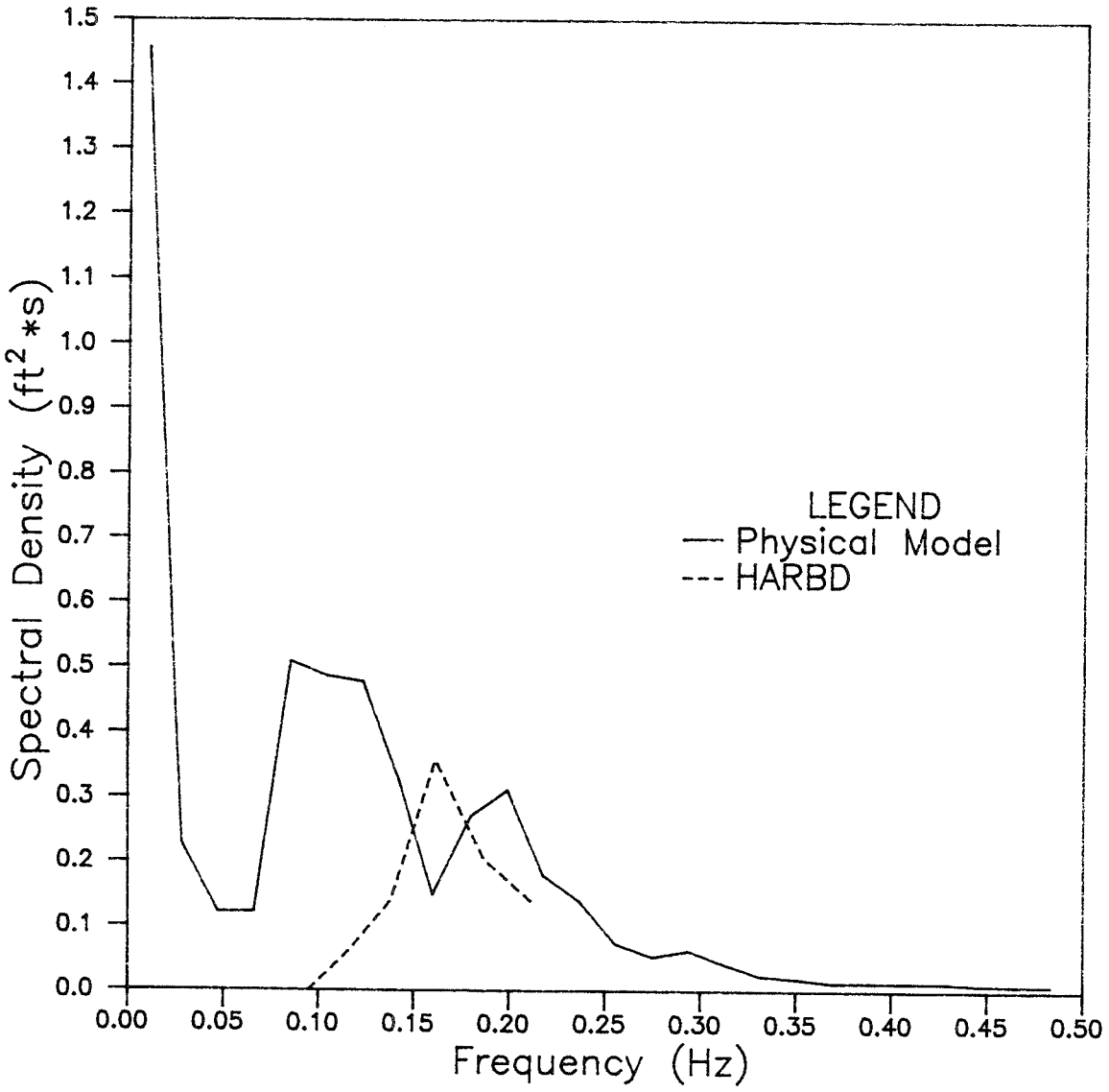

Frequency Spectrum at Gage 13

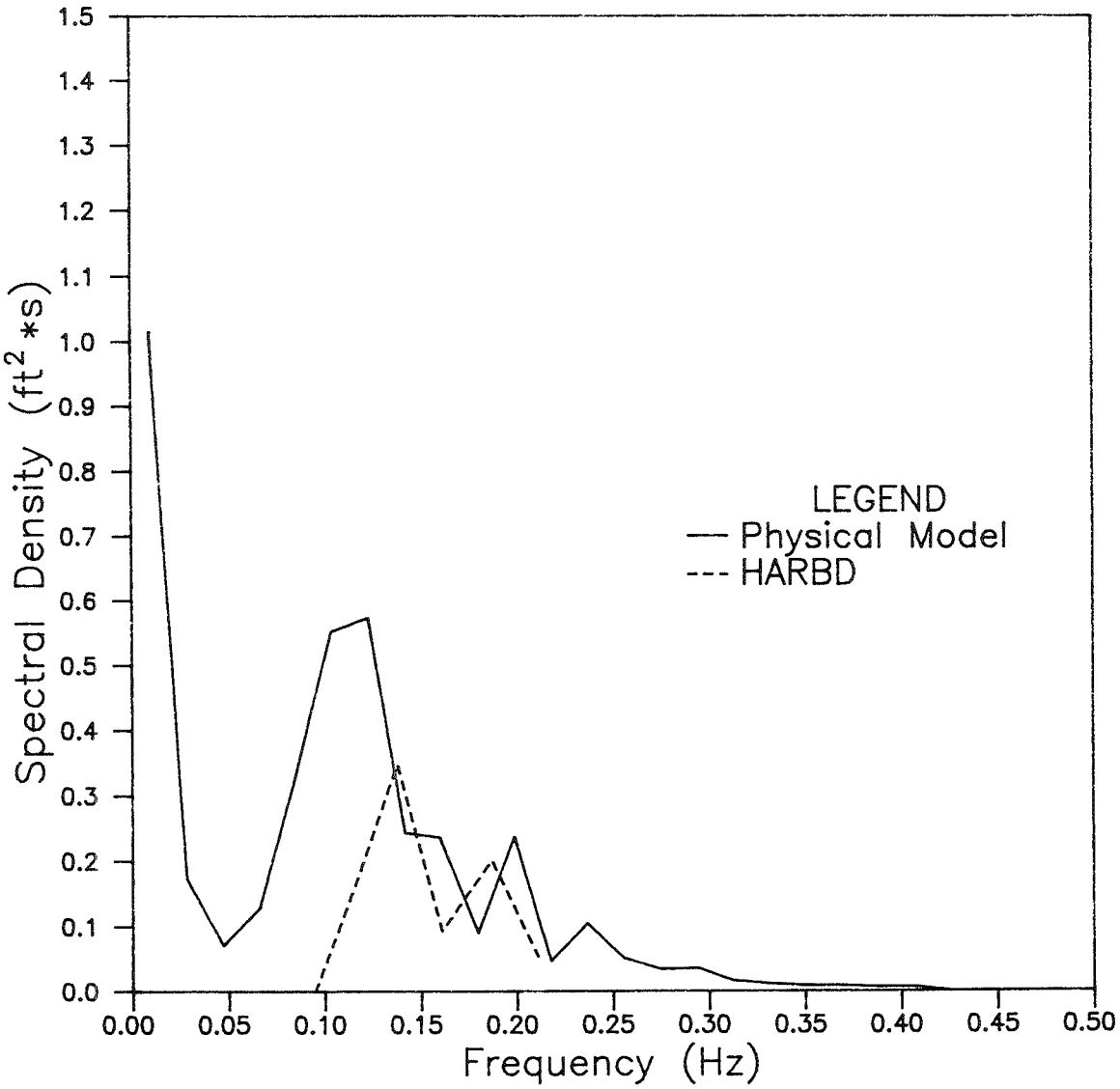

Frequency Spectrum at Gage 14

PLATE 29

APPENDIX A: ESTIMATION OF WAVE CONDITIONS IN BARCELONA HARBOR USING DIFFRACTION DIAGRAMS

1. Diffraction diagrams presented in the Shore Protection Manual* (SPM) (1984) were used to estimate wave conditions in Barcelona Harbor for Runs 1, 3, and 5. (See Table 1 (main text) for characteristics of the generated waves of these runs.) The harbor configuration for all these runs was the base Test 2 harbor configuration. Navigation entrances of the Plan 42 and Plan 58 harbor configurations deviated so much from the simple gap entrances for which the diffraction diagrams were developed that it was impossible to even attempt to use diffraction diagrams to estimate wave conditions for these harbor configurations. It was realized that the methods in the SPM (1984) were not applicable even for the Base Test 2 harbor configuration because most of the assumptions upon which the methods are based were not satisfied in the prototype. Nevertheless, it was deemed worthwhile to try to make crude estimates and to compare the results with results from the numerical and physical models.

2. The method used to determine wave heights inside the harbor using diffraction diagrams follows. First, a cartesian coordinate system, at the prototype scale, was established for the harbor, the origin of which was located at the center of the breakwater gap. The y-axis was established colinear with the bisector of the angle formed by the two breakwaters with y increasing toward shore. The orientation of the x-axis is immaterial since the diffraction diagrams are symmetric about the y-axis. Next, the coordinates of Gages 2 through 14 were determined (Gage 1 was not considered since it is outside the harbor), in prototype units, for the stated coordinate system. Then for Runs 1, 3, and 5, the following steps were used to determine the wave height at Gages 2 through 14:

a. The linear theory dispersion relation was used to calculate the wavelength using the period of the generated wave and the depth at the breakwater gap.

b. The coordinates of the gages were nondimensionalized by dividing by the wavelength from a.

---

* References cited in the Appendix can be found in the References at the end of the main text.

c. The ratio of gap width to wavelength B/L was determined, and this value, along with the direction of the generated wave, was used to select the appropriate diffraction diagram in the SPM (1984).

d. The selected diffraction diagram along with the dimensionless gage coordinates were used to determine the diffraction coefficient for each gage.

e. The wave height at each gage was calculated as the product of the diffraction coefficient for that gage times the incident wave height times a shoaling coefficient (see paragraph 33, main text); the latter accounted for shoaling between the wave generator and breakwater gap. Shoaling coefficients ranged from 1.03 to 1.14.

3. Wave heights thus determined are listed, along with values found from the physical and numerical models, in Tables A1, A2, and A3 for Runs 1, 3, and 5, respectively. The SPM method includes no reflection and hence significantly underestimates wave heights in some areas, particularly at the city dock (Gages 11 and 12).

Table A1

Comparison of Wave Heights for Run 1 Using Diffraction Diagram, Numerical Model, and Physical Model*

Gage Number	Wave Height		
	Diffraction Diagram	Numerical Model	Physical Model
2	1.14	0.91	0.82
3	0.23	0.23	0.27
4	0.17	0.23	0.25
5	0.21	0.23	0.27
6	0.18	0.23	0.22
7	0.16	0.34	0.25
8	0.14	0.34	0.23
9	0.14	0.23	0.22
10	0.12	0.11	0.34
11	0.12	0.34	0.47
12	0.17	0.91	0.80
13	0.21	0.46	0.57
14	0.22	0.68	0.99

* Values given are predicted wave height ($H_{1/3}$ for the physical model) normalized by the generated wave height from Table 1 (main text).

Table A2

Comparison of Wave Heights for Run 2 Using Diffraction Diagram, Numerical Model, and Physical Model

Gage Number	Wave Height		
	Diffraction Diagram	Numerical Model	Physical Model
2	1.07	1.18	1.09
3	0.72	0.64	0.70
4	0.36	0.43	0.45
5	0.57	0.43	0.53
6	0.51	0.32	0.45
7	0.36	0.21	0.34
8	0.50	0.21	0.40
9	0.37	0.21	0.34
10	0.42	0.21	0.56
11	0.45	0.96	1.22
12	0.35	0.54	0.51
13	0.30	0.54	0.42
14	0.56	0.75	0.49

Table A3

Comparison of Wave Heights for Run 3 Using Diffraction Diagram, Numerical Model, and Physical Model

Gage Number	Wave Height		
	Diffraction Diagram	Numerical Model	Physical Model
2	1.03	1.34	1.76
3	0.37	0.21	0.98
4	0.35	0.72	0.91
5	0.18	0.10	0.60
6	0.25	0.10	0.51
7	0.26	0.00	0.56
8	0.16	0.21	0.35
9	0.22	0.00	0.34
10	0.12	0.10	0.30
11	0.10	0.10	0.67
12	0.05	0.52	1.20
13	0.05	0.52	0.78
14	0.10	0.31	1.34